eCAM Evidence-Based Complementary and Alternative Medicine

New Developments in Primo Vascular System: Imaging and Functions with regard to Acupuncture

Guest Editors: Kwang-Sup Soh, Kyung A. Kang, John H. Barker, He Sheng Luo, Moriya Ohkuma, and Richard C. Niemtzow

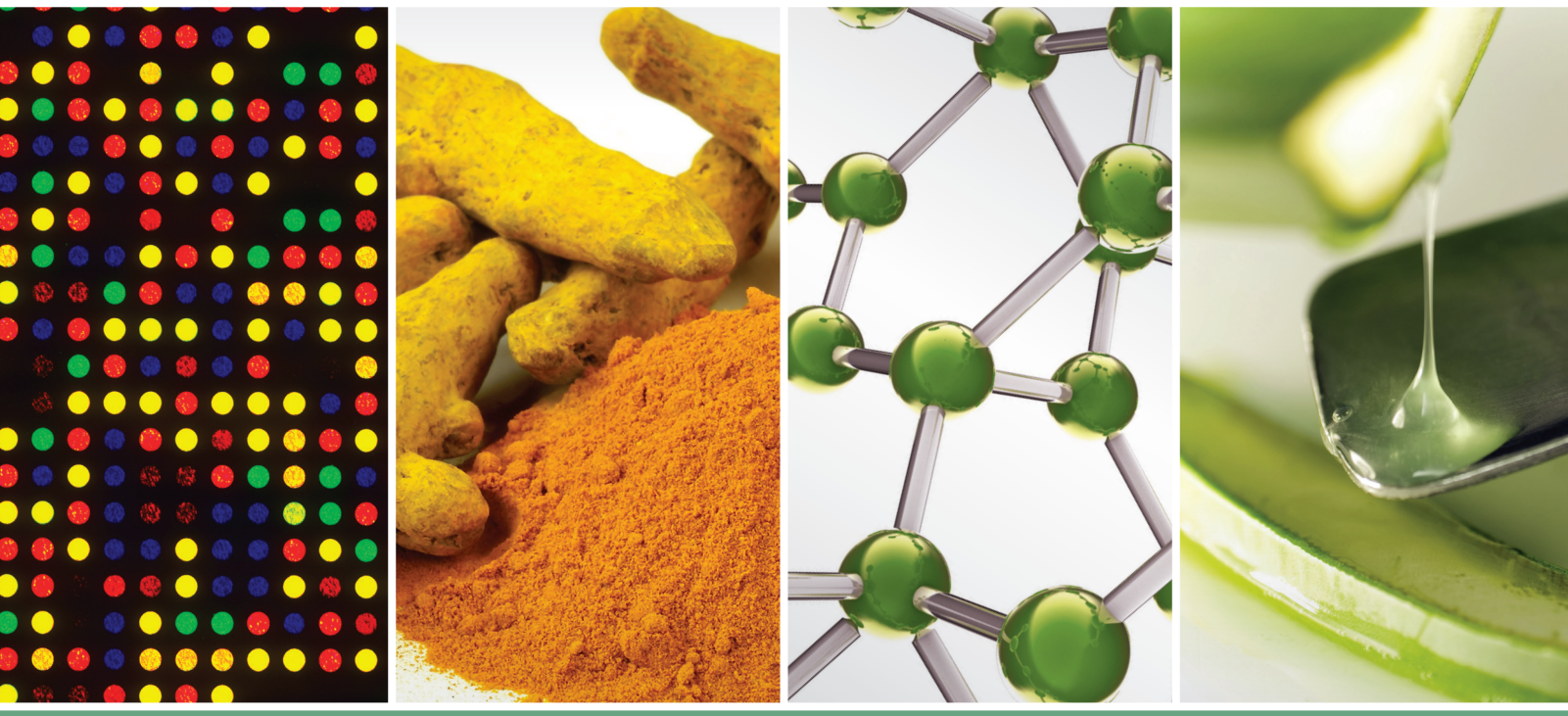

New Developments in Primo Vascular System: Imaging and Functions with regard to Acupuncture

Evidence-Based Complementary and Alternative Medicine

New Developments in Primo Vascular System: Imaging and Functions with regard to Acupuncture

Guest Editors: Kwang-Sup Soh, Kyung A. Kang, John H. Barker, He Sheng Luo, Moriya Ohkuma, and Richard C. Niemtzow

Editorial Board

Contents

Hindawi Publishing Corporation
Evidence-Based Complementary and Alternative Medicine
Volume 2015, Article ID 142705, 2 pages
http://dx.doi.org/10.1155/2015/142705

Editorial

New Developments in the Primo Vascular System: Imaging and Functions with regard to Acupuncture

Richard C. Niemtzow,[1] Kwang-Sup Soh,[2] Kyung A. Kang,[3] John H. Barker,[4] He Sheng Luo,[5] and Moriya Ohkuma[6]

[1] *United States Air Force Acupuncture Center, Malcolm Grow Medical Clinics and Surgery Center, 1050 W. Perimeter Road, Joint Base Andrews, Prince George's County, MD 20762, USA*
[2] *Nano Primo Research Center, Advanced Institute of Convergence Technology, Seoul National University, Suwon 443-270, Republic of Korea*
[3] *Department of Chemical Engineering, University of Louisville, Louisville, KY 40292, USA*
[4] *Frankfurt Initiative for Regenerative Medicine (FIRM), Experimental Orthopedics and Trauma Surgery, JW Goethe University Hospital, 60528 Frankfurt am Main, Germany*
[5] *Department of Gastroenterology and Hepatology, Renmin Hospital of Wuhan University and Wuhan University Institute of Digestive and Liver Diseases, Wuhan 430-060, China*
[6] *Department of Dermatology, Sakai Hospital, Kinki University, Sakai, Osaka 590-0132, Japan*

Correspondence should be addressed to Richard C. Niemtzow; n5evmd@gmail.com

Received 12 March 2015; Accepted 12 March 2015

The Primo Vascular System (PVS) is an enigma. Does it exist or not? But Richard C. Niemtzow has seen it at the Nano Primo Research Center, Advanced Institute of Convergence Technology under the Direction of Dr. Kwang-Sup Soh in Seoul, South Korea.

Superficial primo-vessels, also known as Bonghan ducts and Bonghan channels, were first reported in 1962 by the North Korean scientist, Kim [1]. His work is shrouded in a cloak of mystery. Scientists are not able to reproduce all of his data, or at least for the moment without substantial difficulties.

The PVS appears to be distributed throughout the entire body. Some scientists may say it is an illusion; others say it is a "new" anatomical system, while still others are convinced that these infinitesimal channels may act like optical fiber cables and transmit DNA related information continuously throughout the body using biophotons. As a comparison, we cannot see the millions of transistors on a CPU, but they are part of a manmade system that we use every day. Similarly many biological systems are indeed very minuscule. We need electronic microscopes to visualize some of their structures; otherwise, we would not know they exist.

This special issue, focused on the Primo Vascular System, contains several unique articles that challenge its understanding: in the article "Primo Vascular System: An Endothelial-to-Mesenchymal Potential Transitional Tissue Involved in Gastric Cancer Metastasis," P. An and colleagues investigate the exciting area of gastric carcinoma and the possible role of PVS vessels as precursors of blood vessels. As such they claim that PVS may facilitate the metastatic spread of gastric cancer in the endothelial to mesenchyme tissues. The association of the PVS with cancer is one of the important discoveries by modern PVS researchers that Kim did not investigate [2].

The article "Identification of Primo-Vascular System in Abdominal Subcutaneous Tissue Layer of Rats" by C. J. Lim and colleagues describes a methodology employing Hemacolor staining to identify the PVS in rat abdominal subcutaneous tissues. The authors substantiate it by providing images. Staining methods have been critical for revealing the hard-to-observe PVS. The first effective dye used to visualize the PVS was Trypan blue [3] followed by Hemacolor [4]. Additionally, the authors present a newly developed method using Hemacolor staining to identify the PVS in the subcutaneous tissue. They explain that the importance

of this observation is that these skin-PVS could be the Conception Vessels in the skin of the rats. And this may provide substantial evidence that the PVS is located at acupuncture meridians. This article provides the incentive for further research into the relationship between the PVS and anatomy [5].

The article "Fascia and Primo Vascular System" by C. Yang and colleagues reviews fascia research and its relationship with acupuncture points, meridians, and PVS. The fascia bands together the tissues in the body and is receiving attention as the basis for clinical effectors. This article provides a timely review on the relationship between basic anatomy and clinical strategies.

The article "Primo-Vascular System as Presented by Bong Han Kim" by V. Vodyanoy and colleagues discusses staining methods used by Kim [1] in his original work, which with the aid of a high-resolution microscope have subsequently been confirmed. This article provides valuable information on effective histological methods for investigating the PVS.

The article "Comparison of Alcian Blue, Trypan Blue, and Toluidine Blue for Visualization of the Primo Vascular System Floating in Lymph Ducts" by R. Cha and colleagues describes the different characteristics of these dyes that may elucidate the mechanism of preferential PVS staining.

Finally, we are evoked by the words of Konrad Lorenz, "Truth in science can be defined as the working hypothesis best suited to open the way to the next better one."

Acknowledgment

On behalf of the Guest Editors of this special issue Richard C. Niemtzow acknowledges their kind and wise counsel in writing this editorial.

Richard C. Niemtzow
Kwang-Sup Soh
Kyung A. Kang
John H. Barker
He Sheng Luo
Moriya Ohkuma

References

[1] B. H. Kim, "The Kyungrak system," *Journal of Jo Sun Medicine*, vol. 108, pp. 1–38, 1965 (Korean).

[2] K. S. Soh, K. A. Kang, and D. Harrison, Eds., *The Primo Vascular System: Its Role in Cancer and Regeneration*, Springer, New York, NY, USA, 2011.

[3] B.-C. Lee, K. W. Kim, and K.-S. Soh, "Visualizing the network of bonghan ducts in the omentum and peritoneum by using trypan blue," *Journal of Acupuncture and Meridian Studies*, vol. 2, no. 1, pp. 66–70, 2009.

[4] C. J. Lim, J.-H. Yoo, Y. Kim, S. Y. Lee, and P. D. Ryu, "Gross morphological features of the organ surface primo-vascular system revealed by hemacolor staining," *Evidence-Based Complementary and Alternative Medicine*, vol. 2013, Article ID 350815, 12 pages, 2013.

[5] M. J. McDonald, "Will the primo vascular system finally solve the mystery of acupuncture?" *Medical Acupuncture*, vol. 27, no. 1, pp. 33–37, 2015.

Hindawi Publishing Corporation
Evidence-Based Complementary and Alternative Medicine
Volume 2015, Article ID 751937, 13 pages
http://dx.doi.org/10.1155/2015/751937

Research Article

Identification of Primo-Vascular System in Abdominal Subcutaneous Tissue Layer of Rats

Chae Jeong Lim, So Yeong Lee, and Pan Dong Ryu

Laboratory of Veterinary Pharmacology, College of Veterinary Medicine and Research Institute for Veterinary Science, Seoul National University, Seoul 151-742, Republic of Korea

Correspondence should be addressed to Pan Dong Ryu; pdryu@snu.ac.kr

Received 3 October 2014; Revised 22 December 2014; Accepted 26 December 2014

Academic Editor: Kwang-Sup Soh

The primo-vascular system (PVS) is a novel network identified in various animal tissues. However, the PVS in subcutaneous tissue has not been well identified. Here, we examined the putative PVS on the surface of abdominal subcutaneous tissue in rats. Hemacolor staining revealed dark blue threadlike structures consisting of nodes and vessels, which were frequently observed bundled with blood vessels. The structure was filled with various immune cells including mast cells and WBCs. In the structure, there were inner spaces (20–60 μm) with low cellularity. Electron microscopy revealed a bundle structure and typical cytology common with the well-established organ surface PVS, which were different from those of the lymphatic vessel. Among several subcutaneous (sc) PVS tissues identified on the rat abdominal space, the most outstanding was the scPVS aligned along the ventral midline. The distribution pattern of nodes and vessels in the scPVS closely resembled that of the conception vessel meridian and its acupoints. In conclusion, our results newly revealed that the PVS is present in the abdominal subcutaneous tissue layer and indicate that the scPVS tissues are closely correlated with acupuncture meridians. Our findings will help to characterize the PVS in the other superficial tissues and its physiological roles.

1. Introduction

The primo-vascular system (PVS) is a novel vascular network that was first reported in the 1960s by Kim, who claimed that the tissue corresponded with the acupuncture meridians [1]. This tissue was therefore named "Bonghan tissue" after its discoverer. More recently, the tissue has been reidentified by Dr. Soh and colleagues [2]; it was subsequently renamed the "primo-vascular system" at an international conference in Jecheon, South Korea [3]. The PVS is composed of primo vessels (PVs, or Bonghan ducts) that connect primo nodes (PNs, or Bonghan corpuscles), which are relatively thicker than the PVs [2]. The PVS tissue has been identified in various sites, such as internal organs [4–7], brain ventricles [8], and blood and lymphatic vessels [9–11] in several animal species [12]. Various techniques have been used to visualize the PVS, including trypan blue, through which many important anatomical features of the PVS have been elucidated [2], and Hemacolor utilized in recent research [6].

PVS studies in the past 10 years have identified the following hallmarks of PVS. First, the PVS primarily consists of vessel parts (PVs) and node parts (PNs), and the vessels are often subbranched from each node [2, 4, 5]. Second, rod-shaped nuclei (revealed by DNA-specific staining) are linearly aligned along the longitudinal axis of the PVS [5, 9, 11]. Third, the PVS contains various immune cells, including mast cells (MCs) and white blood cells (WBCs), such as eosinophils, neutrophils, and lymphocytes, and it has a unique cellular composition [6, 13, 14] and a high number of MCs and WBCs. Fourth, the PVS is composed of a bundle of several small subducts or ductules (10–50 μm) containing immune cells [6, 13, 14]. This bundle structure is morphologically different from that of a lymphatic vessel, which only has a single lumen [5, 13].

Based on Kim's claim in the 1960s that the PVS is a reality of acupuncture meridians [1], more recent research has sought to identify the PVS in the skin or hypodermis, where the putative acupoints are located. For example, in

2009, Ogay et al. [15] showed a series of blood plexuses at the putative acupoints along the left and right kidney meridian lines in the abdominal skin of rats using a diffusive light illumination technique. In 2010, Lee and Soh [16] reported a trypan blue-stained structure along the skin skeletal muscles in the hypodermal layer of a rat. In these studies, the locations of the putative PVS tissue appeared to correspond to the acupuncture meridians in the subcutaneous area. However, clear evidence that these putative PVS tissues have the established hallmarks of the existing PVS is missing.

Therefore, in this study, the gross morphological features of putative PVS in rat abdominal subcutaneous tissue were first examined using the Hemacolor reagents, which comprise a rapid staining system that is commonly used in hematological and clinical specimens [17, 18] and has been effectively used to characterize organ surface PVS (osPVS) *in vitro* [6]. Then, we confirmed the putative PVS is distinct from the lymphatic vessel by scanning and transmitting electron microscopy. Finally, we also examined the relationships between the subcutaneous PVS (scPVS) and the acupuncture meridians of the abdominal area.

2. Materials and Methods

2.1. Animal Preparation. Male Sprague-Dawley rats weighing 120–150 g (4-5 week; $n = 23$; Orient Bio, Gyeonggi-do, Korea) were used for this study. The rats were housed in a temperate (20–26°C), relatively humid (40–70%), light-controlled (12-hour light/dark cycle; with the light coming on at 9:00 AM) environment. They were allowed open access to water and standard rodent chow *ad libitum*. The rats were allowed to adjust to this environment for 3-4 days before the experiments were conducted. All animal experiments were conducted in accordance with the Guide for the Laboratory Animal Care Advisory Committee of Seoul National University and were approved by the Institute of Laboratory Animal Resources of Seoul National University (SNU-140926-2). All surgical procedures were performed under general anesthesia.

2.2. Identification of osPVS and scPVS In Vivo. Under deep anesthesia induced with an anesthetic cocktail (Zoletil, 25 mg/kg; xylazine, 10 mg/kg) administered intramuscularly into the right femoral regions, two types of PVS samples were collected according to the following procedures. For the first procedure, the osPVS was identified on the surface of the abdominal organs using the trypan blue or Hemacolor staining method. The Hemacolor dyes were comprised of a three-solution system (Solution 1, absolute methyl alcohol for primary fixation; Solution 2, buffered eosin with sodium for eosin staining; Solution 3, phosphate-buffered thiazine for methylene blue staining) [17, 18]. These solutions (1 mL each) were applied to the surface of the internal organs, such as the intestines and the liver, in the cut abdominal cavity for 5 s. After application of Solution 3, the dye solutions were washed out using the Krebs solution (NaCl, 120.35 mM; $NaHCO_3$, 15.5 mM; glucose, 11.5 mM; KCl, 5.9 mM; $CaCl_2$, 2.5 mM; NaH_2PO_4, 1.2 mM; and $MgSO_4$, 1.2 mM) [7]. After the Hemacolor staining, the revealed osPVS tissues were immediately sampled for additional staining under a stereomicroscope. For the second procedure, scPVS tissue was identified in the subcutaneous tissue layer using Hemacolor staining. Solution 1 (1 mL) was first applied to the hypodermis region of interest for 5 s, and then Solutions 2 and 3 (1 mL each) were applied to the same region one by one. Then, Solution 3 had been applied for 5 s; the region was washed out with a 0.9% saline solution and observed under a stereomicroscope (~1,000x).

2.3. Staining Methods for the Identification of scPVS In Vitro. For the characterization of gross morphology, the identified scPVS was isolated from the abdominal hypodermis region using a microscissor (blade 5 mm) and transferred into a drop of Hank's balanced salt solution (Sigma, St. Louis, MO, USA) on a slide glass. After the sample was completely air-dried at room temperature for 1–3 min, the slide glass was immersed 10 times in and taken out of dye Solution 1 for 10 s (~1/s). Additional staining with Solutions 2 and 3 was repeated using the same process. The sample was then placed in a drop of phosphate buffer solution (pH 7.2) for 20 s, washed by shaking it 10 times in distilled water for 20 s, air-dried for 3–5 min, and finally mounted with Canada balsam (Sigma). The PVS slice preparation was performed according to the previous method [6]. To confirm the DNA and RNA contents of the scPVS, the sample was kept immersed in a 0.1% acridine orange solution for 15 min, and a digital photograph was then taken using a confocal laser-scanning microscope at the wavelength of the acridine orange [19]. To verify the MCs in the scPVS, the sample was immersed in a 1% toluidine blue solution for 3 min [20].

2.4. Electron Microscopy of scPVS and the Lymphatic Vessel. For the scanning electron microscopy (SEM), scPVS and lymphatic vessels were collected from the rats. The procedure for harvesting the scPVS tissue was the same as that used in the sampling by Hemacolor staining. The harvesting procedure for the lymphatic vessel was as follows: under deep anesthesia, the abdomen of the rat was incised, and the lymphatic vessel was sampled under a stereomicroscope around the kidney by reference to the previous report [21]. The scPVS attached hypodermis layer (Figure 3(a)) was isolated from the area of umbilicus on the rat abdominal middle line (Figures 2(a) and 11(a)). The sampled scPVS and lymphatic vessels were kept in 2% paraformaldehyde for 24 hr and primary fixed by Karnovsky's fixation for 2 hr. After washing them with 0.05 M sodium cacodylate buffer 3 times for a total of 10 min, the samples were postfixed by 2% osmium tetroxide (1 mL) and 0.1 M cacodylate buffer (1 mL) and washed twice using distilled water for 5 s each. Dehydration was conducted using a series of ethanol of 30%, 50%, 70%, 90%, and 100% for 10 min each, and then the samples were dried using a critical point dryer (CPD 030, BAL-TEC) for 1 hr, coated by a sputter coater (EM ACE200, Leica), and observed under a field-emission SEM (SIGMA, Carl Zeiss, UK). For transmission electron microscopy (TEM), several procedures were added to those of SEM. (1) After washing the samples with distilled water, en bloc staining was conducted with 0.5% uranyl acetate for 30 min; (2) after dehydration with ethanols, a transition procedure using propylene oxide was conducted

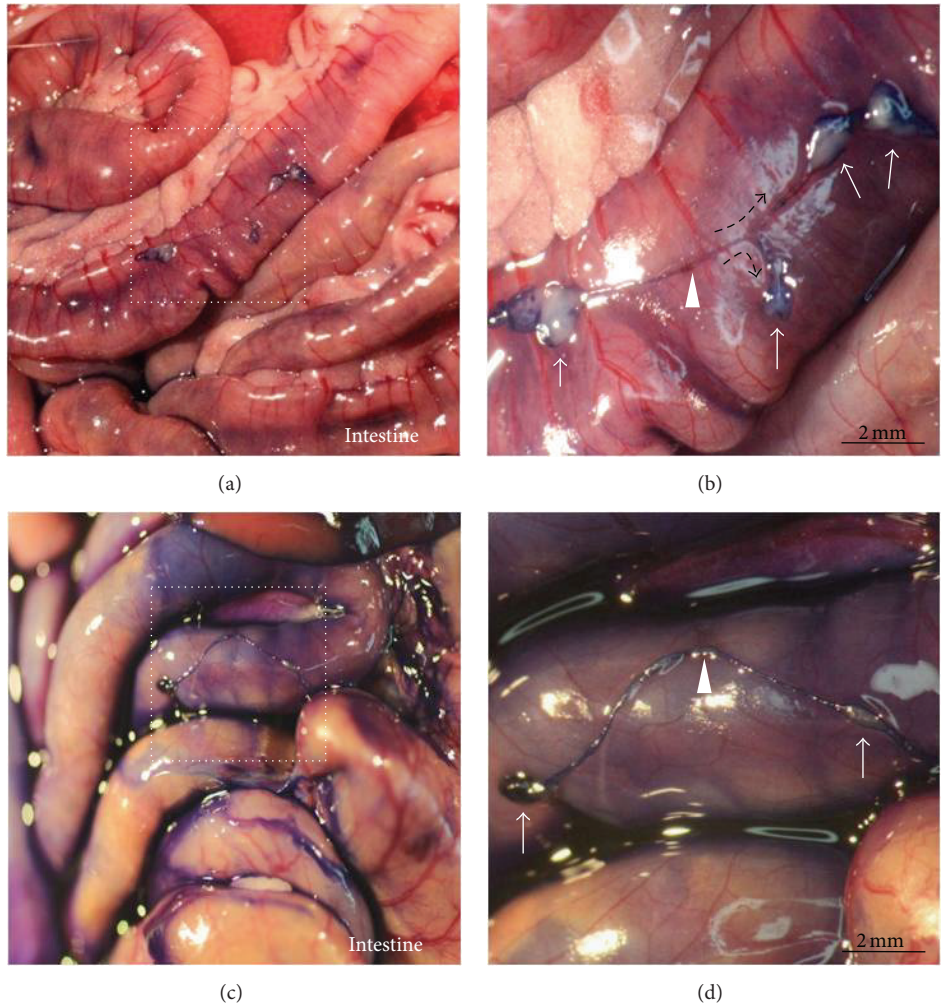

Figure 1: Identification of intact PVS tissue on the surface of abdominal organs in rats using Hemacolor and trypan blue staining. (a) PVS tissue on the surface of the small intestine stained by Hemacolor. (b) Magnified view of the organ surface PVS structure (square in (a)) composed of multiple-PNs (arrows), a PV (arrowhead), and a subbranching point (dotted arrows). (c) PVS tissue on the surface of the large intestine stained by trypan blue. (d) Magnified view of the organ surface PVS structure (square in (c)) composed of two PNs (arrows) and a PV (arrowhead).

twice for 10 min each; (3) then the samples were embedded into Spurr's resin (2 mL), sectioned, and observed under a TEM (JEM1010, JEOL, Japan).

2.5. PVS Cell Counting and Data Analysis. The PVS cells were counted from 21 fields ($100 \times 100\,\mu$m) in an image of the Hemacolor staining of the PVS tissues ($n = 7$) at magnifications of 400 and 1,000x. The sizes of the PNs, PVs, and resident cells were measured using image J software (developed at the US National Institute of Health). All results are shown as mean ± standard errors, and the number of samples or cells was represented by n.

3. Results

3.1. Gross Morphology of the scPVS In Vivo. The results of the present study were obtained from the examinations of subcutaneous PVS (scPVS) tissues in 14 rats and organ-surface PVS (osPVS) tissues in 7 rats. The osPVS tissues ($n = 17$) were sampled mainly from the surfaces of the abdominal organs, including the large intestine (32%), the small intestine (38%), and the liver (17%). The scPVS tissues ($n = 24$) were sampled exclusively from the abdominal subcutaneous area. The osPVS tissues were identified without staining, whereas the scPVS tissues were identified with Hemacolor staining.

Previously, it has been shown that Hemacolor staining is effective in characterizing the gross morphology of the osPVS in isolation [6]. In this study, Hemacolor dyes were directly applied to the PVS tissues on the surfaces of the abdominal organs to determine whether the osPVS could be stained *in vivo* as it is stained by trypan blue, which is a well-known dye that is used to identify PVS *in situ* [2]. The Hemacolor staining revealed that the PVS was attached to the surface of the abdominal organ. Figures 1(a) and 1(b) show representative osPVS tissue composed of primo-nodes (PNs) and primo-vessels (PVs) on the surface of the small intestines revealed

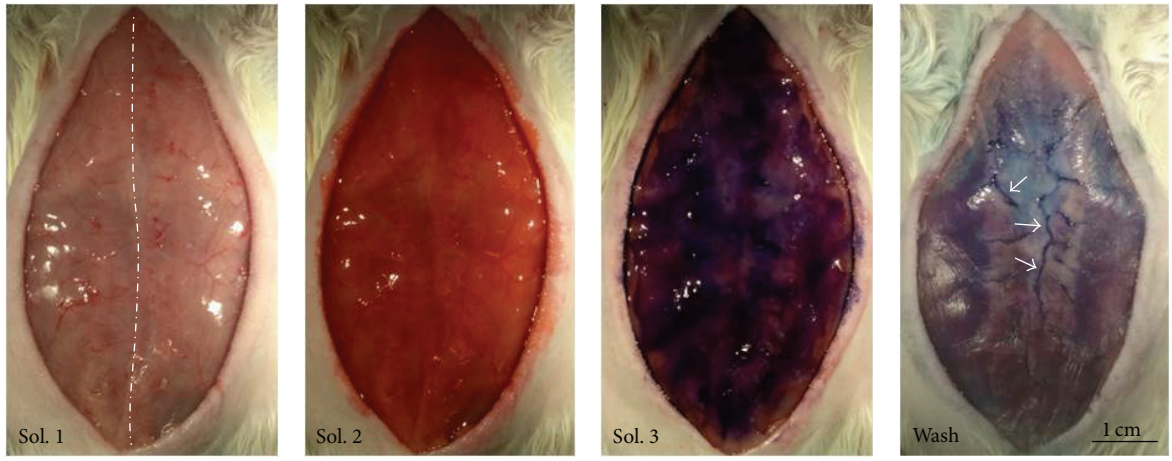

Figure 2: Identification of the threadlike structures in the rat abdominal subcutaneous tissue using Hemacolor staining. ((a), (b), and (c)) Appearance of the subcutaneous area after serial applications of three Hemacolor solutions: Solution 1 (methanol fixative, (a)), Solution 2 (eosin stain, (b)), and Solution 3 (methylene blue stain, (c)). Dotted line is the abdominal middle line. (d) Appearance of the subcutaneous area after wash-out of Hemacolor solutions. Note the dark blue threadlike structures (arrows). See the *Materials and Methods* sections for a description of the protocol.

by Hemacolor staining. The Hemacolor staining of the osPVS was comparable to the trypan blue staining (Figures 1(c) and 1(d)).

Figure 2 shows the appearance of the abdominal subcutaneous region after the applications of Solutions 1, 2, and 3 for the Hemacolor staining *in vivo*. After completion of the Hemacolor staining, dark blue threadlike structure was observed through the fascia in the stained area of the abdominal subcutaneous tissue layer (Figure 2(d)). Figure 3 shows the anatomical location of the Hemacolor stained-dark blue threadlike structure on the surface of the subcutaneous tissue layer identified by scanning electron microscopy (SEM). This threadlike structure was comprised of a bundle of subducts or small tubes; this morphology was characteristically different from that of the lymphatic and blood vessels, which consisted of a single tube.

Figure 4 shows a representative example of a dark blue-colored threadlike structure revealed by Hemacolor staining in the abdominal subcutaneous area. The vessels were divided into a vertically elongated type (yellow vertical arrow) along the abdominal middle line and a horizontally elongated type (yellow horizontal arrow) branched from each node form (Figure 4(b)). As shown in Figures 4(b) and 4(c), the dark blue-colored multiple-branched threadlike structures (white arrows) were distributed across the surface of the subcutaneous tissue. In addition, some vessels were also distributed beneath the surface of the subcutaneous tissue (Figures 4(b) and 4(c), two-way dotted white arrows and open arrowheads). The dark blue threadlike structures appeared to be interrupted where the structures were buried underneath the surface of the subcutaneous tissue layer. In addition, blood vessels were observed around the threadlike structures (Figures 4(b) and 4(c), asterisks). The blood vessels were not stained dark blue like the threadlike structures by Hemacolor staining; rather, they maintained their original red colors. The average size of the nodes of the threadlike structures was 0.94 ± 0.14 mm ($n = 12$), and the average thickness of the vessels was 0.21 ± 0.05 mm ($n = 15$).

3.2. Cytomorphology of the scPVS In Vitro. The threadlike structure was isolated and the tissue was restained *in vitro* to identify the cellular properties of the threadlike structure stained by Hemacolor. Figure 5(a) shows a sample on the slide glass of a threadlike structure composed of nodes and vessels connected by these nodes. Figure 5(b) is a representative stereoscopic image of the threadlike structure stained by Hemacolor. The Hemacolor-stained cells of the threadlike structure were mainly classified into two groups based on their morphologies: small round cells (~10 μm) and large granular cells (10–20 μm). The cells in the vessels and nodes differed in shape and distribution. The cells within a node were mostly round in shape and were dispersed unsystematically (Figure 5(c)). In contrast, the cells within a vessel were elliptical and linearly aligned along the longitudinal axis of the vessel (Figure 5(d)). Figure 5(e) shows the image of the cells of the threadlike structure revealed by toluidine blue staining, which is widely used to stain selectively MCs [20]. In previous studies, the PVS has been found to contain a variety of immune cells, including MCs and WBCs [6, 17]; therefore, in this study, toluidine blue staining was performed. The granules within large granular cells showed the typical metachromatic staining property of toluidine blue staining, indicating that the large granular cells in the threadlike structure were MCs (Figure 5(e)) [20]. The threadlike structure was also stained with acridine orange staining to determine DNA (revealed green) and RNA (revealed red) components for the further characterization of the cellular properties of the threadlike structure [19]. Figure 6(a) illustrates the threadlike structure consisting of one node and connecting vessel stained with acridine orange. The majority of cells in

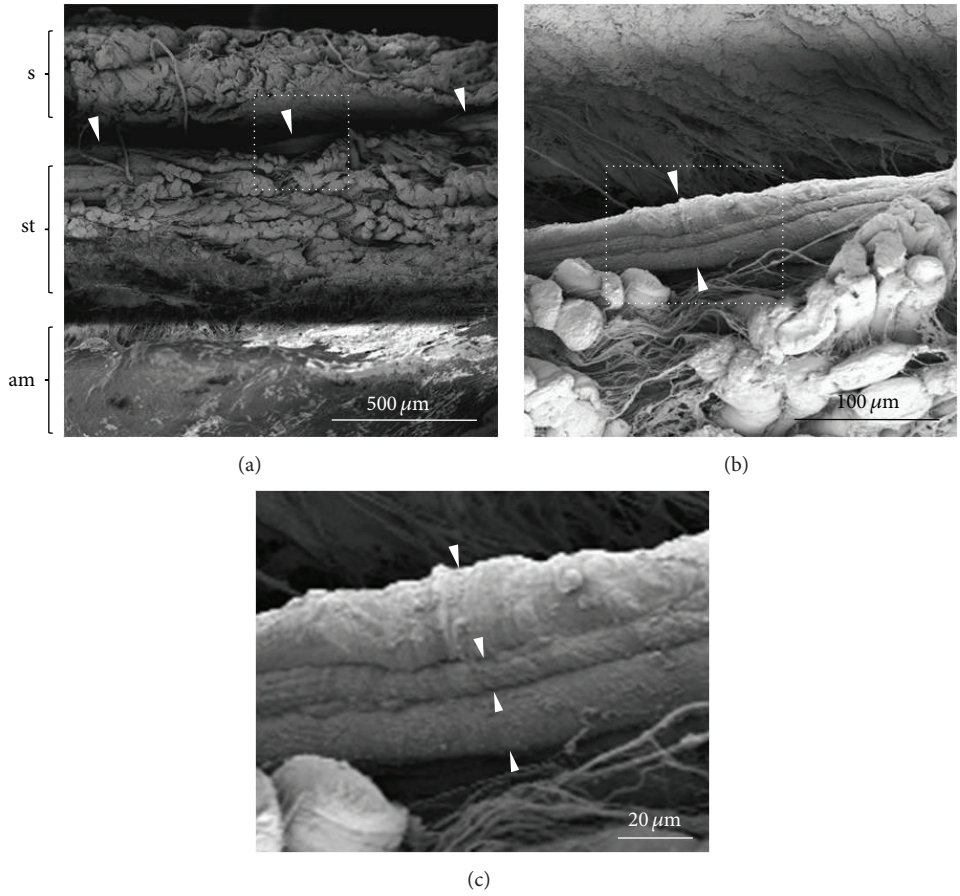

Figure 3: The location of the threadlike structure in the rat abdominal tissue layer revealed by scanning electron microscopy. (a) Cross-section of tissue explant including the skin (s), subcutaneous tissue layer (st), and abdominal wall muscle (am). The explant is isolated from the near area of umbilicus on the abdominal middle line. Note that the threadlike structure (arrowheads) is located between the skin and subcutaneous tissue layer. (b) Magnified view of the threadlike structure (square in (a), arrowheads) on the surface of subcutaneous tissue layer. (c) Magnified view of the threadlike structure (square in (b)) showing a bundle structure of three subducts (arrowheads). Note the rough surface of threadlike structure.

the threadlike structure were stained a green color, as shown in Figure 6. The nuclei of the small round cells were stained green (Figures 6(b) and 6(c), arrowheads), whereas the large granular cells were stained green and red in the nuclei and surrounding granules, respectively (Figures 6(b) and 6(c), arrows). The shape and distribution of the acridine orange-stained cells were similar to those of the Hemacolor staining, as shown in Figure 5. Most cells in the vessel were aligned along the long axis of the vessel (Figures 6(a), arrowheads in the bottom inset, and 6(c)). In contrast, the cells in the node were randomly distributed without any clear direction (Figure 6(b)).

3.3. Structural Properties of the scPVS In Vitro. The inner regions of the vessel of the threadlike structure revealed by Hemacolor staining appeared as white space, indicating a lower cellularity (Figure 7). The inner space was linearly continuous along the longitudinal axis of the vessel (Figures 7(a) and 7(b)). The diameters of the inner space were 20–60 μm. The inner space structures contained various cells, such as large granular cells (Figure 7(b), arrowheads), granules (Figure 7(b), dotted circle), and small round cells (Figure 7(d), arrowheads). Figure 7(c) shows a bundle-like structure revealed by Hemacolor staining as shown in Figure 3 by scanning electron microscopy. In addition, a cross-sectioned slice (200 μm) of the threadlike structure was stained, and the small and large granular cells were observed in the whole threadlike structures. As shown in Figures 7(e) and 7(f), there was a sinus (~60 μm) that contained granules (~1 μm).

3.4. Comparison of the Ultrastructural Features between the scPVS and Lymphatic Vessel. Electron microscopy was used to show differences between the threadlike structure and the lymphatic vessel in isolation (Figure 8). The threadlike structure was comprised of a bundle structure of several subducts (Figure 8(a)), whereas the lymphatic vessel did not appear to have bundle structure (Figure 8(c)). At a higher magnification view, we observed the round cells (Figure 8(b), asterisks) and fine fiber structures on the surface of the threadlike structure. In contrast, in the lymphatic vessel,

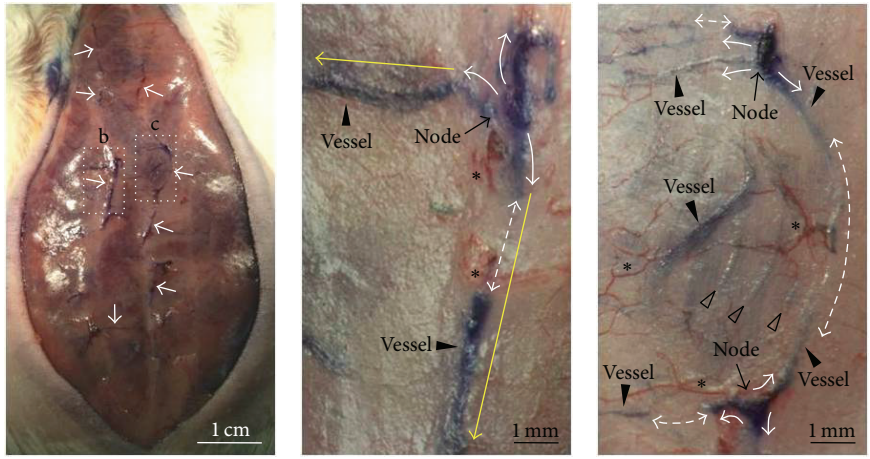

(a) (b) (c)

Figure 4: Hemacolor-stained threadlike structures in the rat abdominal subcutaneous tissue. (a) Typical example of the distribution of threadlike structures (white arrows) on the subcutaneous area stained by Hemacolor. ((b) and (c)) Threadlike structures (dotted squares marked as "b" and "c" in (a)) composed of the vessels (arrowheads) that connect the nodes (arrows). Note that the node structures are multibranched (white arrows) from the nodes, and the vessel structures are distributed either on or beneath the subcutaneous surface (two-way dotted white arrows and open arrowheads). Note that the blood vessels (BVs, asterisks) maintain their red color and that threadlike structures are aligned in either a vertical or horizontal direction (yellow arrows). Note the blood vessels around the branching points of the threadlike structures (asterisks).

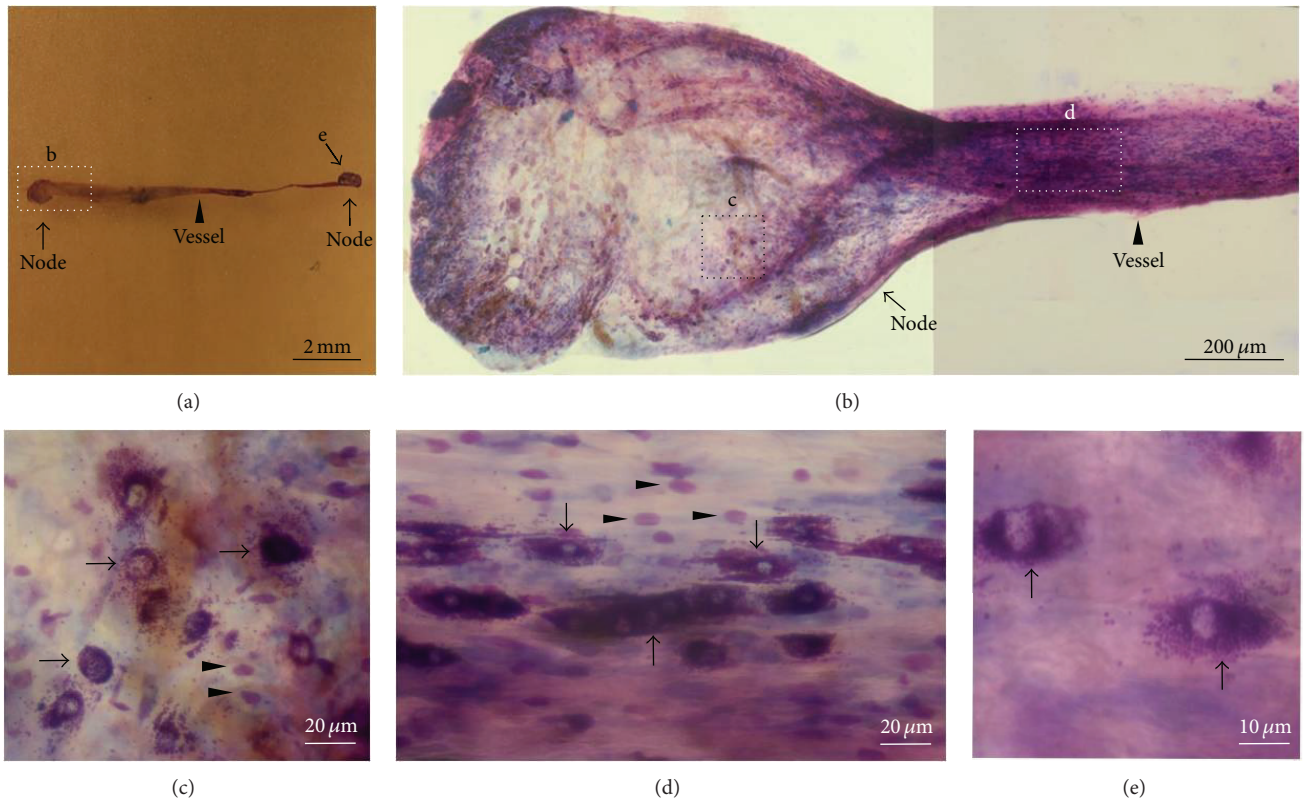

(a) (b)

(c) (d) (e)

Figure 5: Hemacolor staining of the threadlike structure isolated from the rat abdominal subcutaneous tissue. (a) Threadlike structure isolated from the Hemacolor-stained layer of the subcutaneous tissue. (b) Typical longitudinal image of a whole threadlike structure (marked as "b" in (a)). ((c) and (d)) Two major types of cells in the threadlike structure: large granular (arrows) or small round cells (arrowheads). Note that the cells in the node (c) and in the vessel (d) are aligned differently. (e) Toluidine blue staining of the large granular cells (arrows).

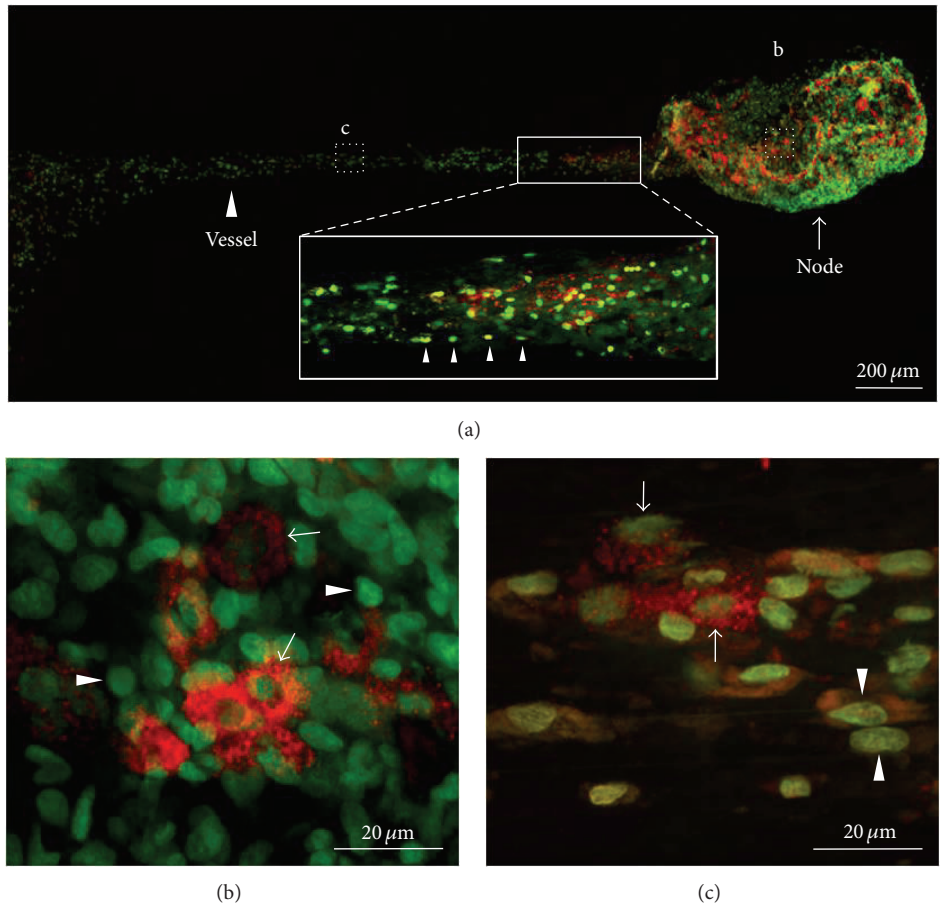

Figure 6: Confocal laser-scanning microscopic image of the cells in the threadlike structure stained with acridine orange. (a) Typical longitudinal image of the whole threadlike structure. Note that the cells (arrowheads in bottom inset) in the vessel are linearly aligned along the longitudinal axis of the vessel. (b) Acridine orange-stained cells in the node (marked as "b" in (a)) showing the small round cells with green nuclei (arrowheads) and large cells with green nuclei and red granules (arrows). (c) Acridine orange-stained cells in the vessel (marked as "c" in (a)). Note that the density and alignment of resident cells are different in the node (b) and in the vessel (c).

such cells were not found and the fiber structures were more extensive than those of threadlike structure (Figures 8(b) and 8(d)). Figure 9 shows the major resident cells of the threadlike structure and the lymphatic vessel revealed by transmission electron microscopy. As can be seen, the threadlike structure contains various immune cells, including MCs, eosinophil, and granules (Figure 9(a)), whereas the lymphatic vessel is mostly comprised of lymphocytes (Figure 9(b)). Thus, there are clear differences between the threadlike structure and lymphatic vessel in terms of the presence or absence of the bundle structures and the types of resident cells.

3.5. Comparison of the MC Density between the scPVS and the osPVS. The above results regarding gross morphology, cytomorphology, and structural properties have many features in common with the well-established PVS [2, 5, 6]; thus, the subcutaneous threadlike structure, vessel, and node part were identified as the scPVS, the PV, and the PN, respectively. In addition, the large granular cells and small round cells of the threadlike structure were also identified as the MCs and WBCs of the PVS reported previously in the osPVS [6]. Figure 10 shows a comparison of the density and degranulation ratios of the MCs in the scPVS and osPVS tissues stained by Hemacolor. The cell densities of the MCs in the scPVS were lower than that of the osPVS (Figures 10(a) and 10(b)), and the degranulation ratio of the MCs in the scPVS was higher than the ratio in the osPVS (Figures 10(c) and 10(d)), which indicates that the scPVS is different from the osPVS in MC activation.

3.6. Relationship between the scPVS and Acupuncture Meridians. Hemacolor staining of the abdominal subcutaneous tissue revealed that there were multiple scPVS tissues over the whole abdominal space, as shown in Figures 2 and 4. Among these, the most consistently observed tissue was the scPVS tissue, which was located on the abdominal middle area (Figure 11). Since the conception vessel (CV) meridian is also known to be located at the ventral midline connecting the umbilicus to the sternum [22], the correlation between the positions of the scPVS present in the ventral midline and the CV meridian was also examined. The CV meridian and acupoints are illustrated in Figures 11(a) and 11(b).

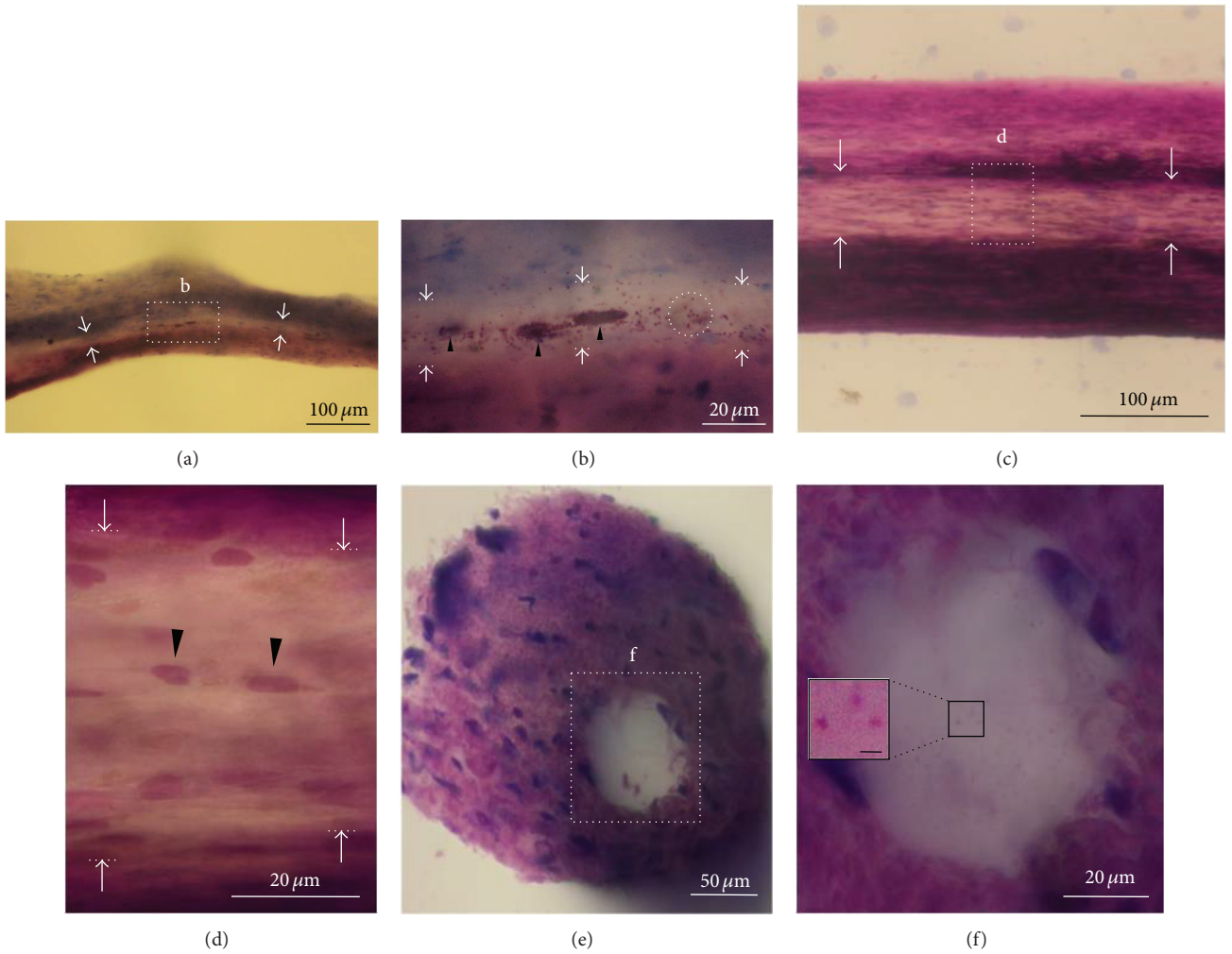

Figure 7: The inner space structure containing cells along the inside of the subcutaneous threadlike structure. (a) Continuous inner space (arrows) along the longitudinal axis of a threadlike structure revealed by Hemacolor staining. (b) Distribution of the cells (large granular cells, arrowheads; granules, dotted circle) in the inner space (marked as "b" in (a), 20–30 μm) of the vessel. (c) Large inner space structure (> 50 μm) inside the subcutaneous threadlike structure showing low cellularity revealed by Hemacolor staining. (d) Distribution of the cells (small round cells, arrowheads) in the inner space (marked as "d" in (c)) of the vessel. (e) Cross-sectional image (200 μm) showing an inner space (dotted square, > 50 μm) of a threadlike structure revealed by Hemacolor staining. (f) Inner space (marked as "f" in (e)) within a vessel slice containing granules (about 1 μm, inset). Note that the inner space contains the resident cells of the threadlike structure.

Figure 11(c) shows a typical example of scPVS tissue in the abdominal subcutaneous tissue visualized by Hemacolor staining. The most notable observation is that the scPVS is mainly distributed along the ventral midline, which consists of the vessels connected by nodes. The nodes appear to correspond to the CV acupoints (i.e., CV13, CV10, and CV8). For example, the node corresponding to CV13 appears to be enlarged and located near the blood vessel (Figure 11(d)). The node corresponding to CV10 appears to be subbranched and connected another node of the scPVS (Figure 11(e), open arrow) located in the right lateral area. A dark blue structure, scPVS, was also noted that it appeared to be mixed with bloods/plexus (Figure 11(e), arrow). Collectively, these observations indicate that the scPVS in the middle of the abdominal subcutaneous tissue layer is likely to correspond to the CV acupuncture meridian. In addition to scPVS in the ventral midline, scPVS tissue was also located laterally, at about 6 mm (Figure 11(c), dotted circles) and 9 mm from the midline (Figure 11(c), white arrows). A connection between each scPVS was also noted (Figure 11(e), dotted arrows).

4. Discussion

In this study, we identified the PVS in the abdominal subcutaneous tissues in rats using various staining techniques. The scPVS consisted of vessels that connect the node parts and that the vessels were frequently subbranched. In the Hemacolor-stained whole scPVS tissue in isolation, the cells of the scPVS were found to be composed of WBC-like small round cells and MC-like large granular cells. The cell distributions differed among the nodes (showing a random distribution of round-shaped cells) and the vessels (showing

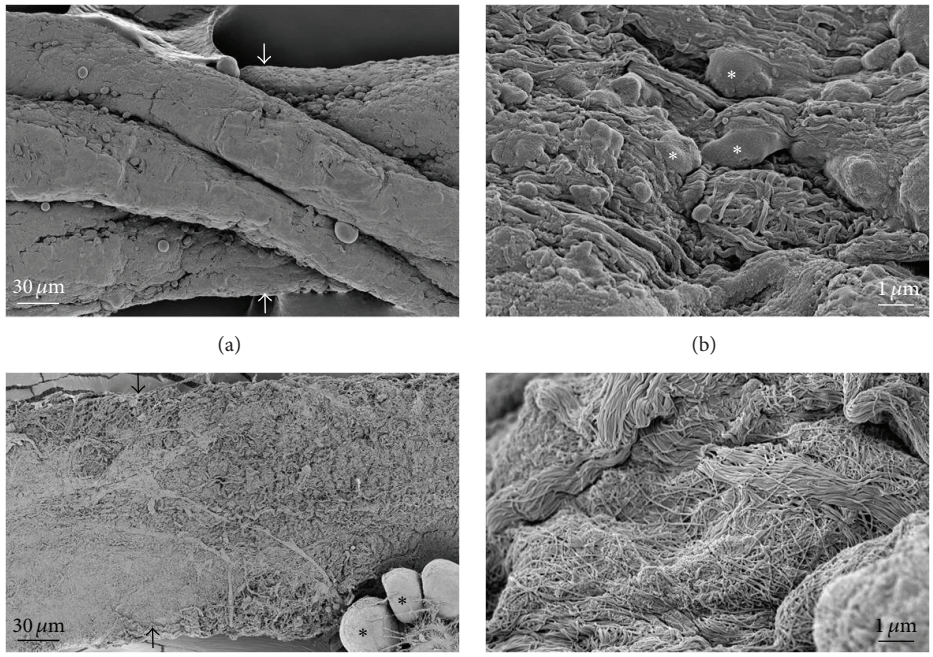

Figure 8: Comparison of the subcutaneous threadlike structure and lymphatic vessel using scanning electron microscopy. ((a) and (c)) Typical longitudinal images of the threadlike structure and lymphatic vessel. Asterisks are an adipocyte attached to the lymphatic vessel. ((b) and (d)) The surfaces of the threadlike structure and lymphatic vessel at higher magnification. Asterisks are the cells on the surface of the threadlike structure. Note that the threadlike structure and lymphatic vessel are different in terms of the presence or absence of the bundle structure of several subducts and cells.

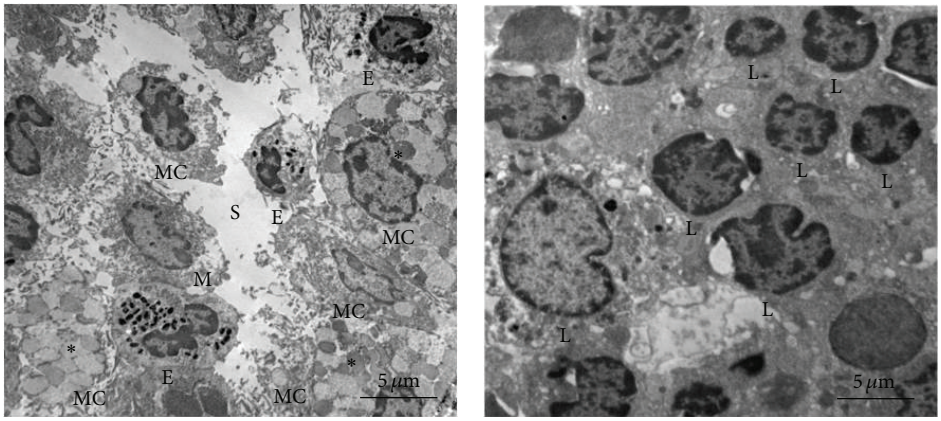

Figure 9: Comparison of the subcutaneous threadlike structure and lymphatic vessel using transmission electron microscopy. (a) Threadlike structure containing a sinus structure (S), mast cell (MC) and its granules (asterisks), monocyte (M), and eosinophil (E). (b) Lymphatic vessel containing mostly lymphocytes (L). Note that there is a difference in the major resident cells between the threadlike structure and the lymphatic vessel.

a linear arrangement of elliptical-shaped cells along the long axis of the vessel). Acridine orange staining showed green-stained WBC nuclei (denoting DNA) and green-stained MC nuclei with red-stained granules (denoting RNA). In addition, the inner space-channel (20–60 μm) structure containing WBCs and MCs along the inside of a vessel of the scPVS was identified. Electron microcopy revealed that the threadlike structure has a bundle structure of subducts and round cells on the surface and that these were not found in the lymphatic vessel. The distribution pattern of scPVS tissues in the ventral midline was similar to the route of the CV meridian. Collectively, these findings indicate that the PVS

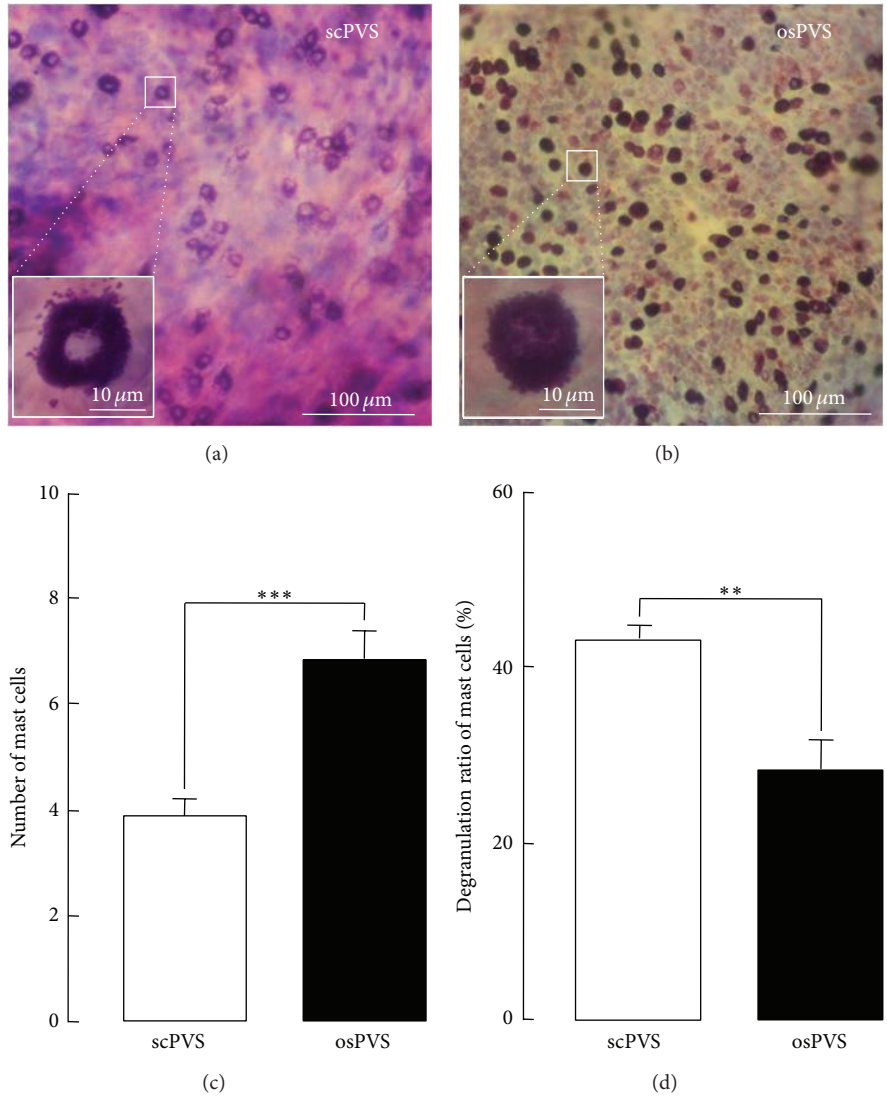

FIGURE 10: Comparison of the density and degranulation ratio of MCs identified in Hemacolor-stained scPVS and osPVS tissue. ((a) and (b)) Representative photomicrographs showing the distribution of MCs in the PNs of scPVS and osPVS stained with Hemacolor. ((c) and (d)) Summary bar graphs showing the number of MCs (c) and the degranulation ratio of these MCs in the scPVS and osPVS tissue (d). PVS cells counted from 21 fields (100 × 100 μm) in an image of the Hemacolor staining of the PVS tissue ($n = 7$) at magnifications of 400 and 1,000x.

is also present on the subcutaneous layer and that the scPVS is likely to be closely related to the acupuncture meridians in the subcutaneous tissue layer.

Compared with the unique characteristics of well-established PVS tissue, the putative scPVS of the present study had several features in common with the existing PVS, which is primarily composed of PVs and PNs that are often branched into multiple vessels [2, 4, 5]. As shown in Figure 4, the scPVS also has vessels that connect the nodes, and there are well-developed branches that form each node. The rod-shaped nuclei (10–20 μm) of the existing PVS were revealed by DNA-specific fluorescent staining, including acridine orange, 4′,6-diamidino-2-phenylindole (DAPI), and the Feulgen reaction [5, 10, 11]. The scPVS revealed that the rod-shaped nuclei were aligned along the longitudinal axis of the vessel stained by acridine orange (Figure 6). The PVS is also known to contain various immune cells [6, 13, 14], and in this study, the scPVS showed many WBCs and MCs (Figures 5 and 9). In terms of the internal structure of the PVS, a bundle structure and diverse subducts (~10 or 20–50 μm) that pass through a vessel or node containing the WBCs, MCs, and granules of about 1 μm in diameter were noted [5, 6, 13]. Figures 7, 8, and 9 demonstrate a bundle structure, subducts, and sinus within the vessels of the long axis or a cross-section of the scPVS, including WBCs, MCs, and granules. These findings indicate that the newly identified scPVS belongs to the existing PVS group. However, there were a few different characteristics between the scPVS and the existing PVS. For example, one can differentiate the osPVS tissue from the surrounding organ tissue because it is semitransparent, freely movable, and present on the surfaces of the internal organs [4–7]. That is, it is possible to identify the osPVS without any

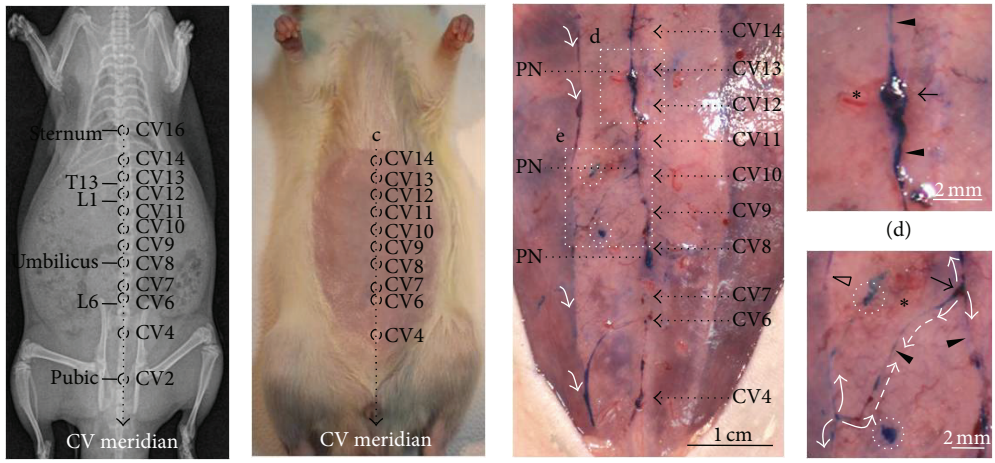

Figure 11: The distribution of scPVS in the abdominal subcutaneous tissue in a rat. ((a) and (b)) Locations of the conception vessel (CV) acupuncture meridian in a rat (L1, L6, and T13; lumbar 1, lumbar 6, and thoracic 13 vertebrae, resp.). (c) Typical example of the scPVS tissue (dotted square marked as "c" in (b)) on the abdominal subcutaneous tissue layer in relation to the CV meridian and the acupoints. Note other abdominal scPVS tissues away from the CV meridian line (white arrows and dotted circles). (d) scPVS corresponding to putative CV 12 and 13 (dotted square marked as "d" in (c)) comprised of a PN (arrow) and a PV (arrowheads). (e) scPVS corresponding to putative CV 9 and 10 (dotted square marked as "e" in (c)) comprised of a PN (arrow) and PVs (arrowheads). Note that there are three direction-branched PVs (white arrows) from a branching point of a PN, and two branches are connected to one vessel (dotted arrows); there is another vessel away from the vessel located at the ventral midline (open arrow). Note the blood vessels around the scPVS tissue (asterisks in (d) and (c)).

staining. In contrast, the scPVS tissue, which is located in the interior regions as well as on the surface of the hypodermis, is not easily identified in adjacent subcutaneous tissues; thus, it is necessary to stain the hypodermis region to distinguish the scPVS from the surrounding tissue. In addition, the vessels of the scPVS are more elastic than of the osPVS, and they are often bent during the process of scPVS sampling.

The presence of enriched MCs in osPVS has been confirmed in previous studies, and they have been considered to be the major resident cells of osPVS [6, 14]. MCs have primarily been viewed as effectors of allergic/inflammatory reactions [23]. The results of the present study indicate that the scPVS also contains MCs, but they are different from those in osPVS in terms of density and their degranulation ratio, which are significant parameters that are widely used in studies on MCs. In this study, the MC density was higher in the osPVS than in the scPVS; however, the granulation ratio was higher in the scPVS than in the osPVS (Figure 10), indicating that the MCs in the scPVS are preferentially activated compared to the MCs in the osPVS. Thus, the scPVS could be more exposed to immune disorders, including physical agents, products of diverse pathogens, and many innate danger signals than osPVS. This idea is consistent with a recent hypothesis on the PVS by Stefanov et al. (2013) [24]. In the hypothesis, the external PVS such as scPVS functions as a receiving PVS that transforms the external stimuli into a type of PVS signals, whereas the internal PVS such as a osPVS functions as communicating PVS that transmits the PVS signals among different PVSs. This may explain the higher level of MC activation in the scPVS. It is well-known that MC degranulation is remarkably increased by acupuncture on the acupoints of skin tissue [25]. Thus, it is conceivable that, in this study, the MCs were more activated when being associated with the position of the CV meridian and its acupoints in the scPVS than in the osPVS.

One of the primary objectives of this work was to correlate the scPVS and acupuncture meridians, which are known to be present in the skin [22, 24]. The present study provides experimental evidences supporting the close correlation between the scPVS and meridians in the abdominal subcutaneous tissue. Firstly, the PNs revealed by Hemacolor staining showed key features of the Bonghan corpuscle. In the early 1960s, Kim reported that the Bonghan corpuscle (denoting PN) corresponding to acupuncture meridians/acupoints was present in the subcutaneous tissue layer and was connected by a bundle of blood vessels and Bonghan ducts (denoting PVs) [1, 2]. Recently, in 2009, Ogay et al. observed a series of blood vessel plexuses at the putative acupuncture points along the left and right kidney meridians in the abdominal subcutaneous tissue layer of rats by using a diffusive light illumination of the region of skin [15]. This report elucidated the morphometric scales of the blood vessel plexus at the kidney and stomach meridians, which are 4-5 mm and 2 cm from the conception vessel meridian in rats by 6–12 weeks. However, they were not able to conclude that the blood plexuses are the anatomical structures of subcutaneous Bonghan corpuscles because the PNs or PVs were not found with the bundle of the blood vessels. The findings in the present study are consistent with the Kim's claim that the scPVSs composed of PNs and PVs are frequently bundled with the blood vessels (Figures 4 and 11). This study also found that the PVS tissue in the subcutaneous layer contains MCs (Figures 5 and 9). This observation is consistent with previous studies that MCs are rich at the various acupuncture

points [25, 26]. The scPVS located on the ventral midline of the abdominal space appears similar to the CV meridian. As shown in Figure 11, the distribution of the nodes, vessels, and subbranches of the scPVS is in good agreement with the known features of the CV meridian.

The Hemacolor staining mainly used in this experiment is a commercially available tool for rapid blood smears that permits good morphological judgment of cells, such as lymphocytes, monocytes, and neutrophilic granulocytes. The total process takes less than 10 min and can be done with prepared dyes without technical assistance [27]. In this study, Hemacolor staining was used as a major diagnostic tool for the PVS because it was possible to identify the PVS *in situ* as well as its cellular properties and structures. In the case of trypan blue, which is a well-known dye that is widely used to identify PVS *in situ*, its use for elucidating detailed information about the cytology and anatomical structure of PVS is somewhat limited although it is easy and simple to use [6].

One of the limitation of this study is that scPVS was not always detected as a uniform pattern or continuous threadlike structure after Hemacolor staining (Figures 4 and 11). This could have been due to differences in the depth of the scPVS from the surface of the abdominal subcutaneous tissue layer (Figures 4(b) and 4(c), two-way dotted white arrows and open arrows). Alternatively, it could also have been be due to variations in the individual rat's genetic or health states. In addition, the sinus structure (Figures 7(e) and 7(f)) in the cross sectioned slice of the scPVS vessel was confirmed twice during the 11th attempt. This could have been due to differences in the vessel structures and the morphological denaturalization during the tissue sectioning and staining. Further studies are needed to fully understand these variations and detailed experimental conditions.

In this study, we showed that the PVS is present on the subcutaneous tissue layer, which is likely to be target sites or area of acupuncture stimulations. It is first to show that the scPVS can be identified in a specific region of the body, namely, the abdominal midline in the subcutaneous tissue layer, and will help further study on the function of PVS in the body. For example, a selected part of a specific PVS could be damaged and then monitored for changes in physiological functions, and changes in the PVS in relation to changes in body states could be investigated [28], or the effect of specific acupuncture stimulation in relation to the changes in the selected PVS tissues could be monitored. In addition, this study will also provide a base for the study on the role of PVS in innate immunity since MCs, rich in the PVS, are important in innate immune system phenotypic and function [29].

5. Conclusion

In this study, the presence of scPVS in abdominal subcutaneous tissue has been identified for the first time using the Hemacolor staining technique. The scPVS has major features in common with the well-established PVS tissue (i.e., osPVS) in terms of gross morphology and cellular/structural characteristics. The scPVS present on the midline of the abdominal subcutaneous tissue layer was also found to overlap with the CV meridian and its acupoints. This study is the first to show the presence of the PVS on the superficial tissues of the body. These findings may help to identify other scPVS tissues in the body and further elucidate their pathophysiological roles in healthy and disease states.

Conflict of Interests

The authors declare that there is no conflict of interests regarding the publication of this paper.

Acknowledgments

This study was supported by the Basic Science Research Program through the National Research Foundation of Korea (NRF) funded by the Ministry of Education, Science and Technology (2012-0007247). The authors thank Dr. Min Cheol Choi for the X-ray imaging of the rat skeleton.

References

[1] B. H. Kim, "On the kyungrak system," *Journal of the Academy of Medical Sciences of the Democratic People's Republic of Korea*, vol. 90, pp. 1–41, 1963.

[2] K.-S. Soh, "Bonghan circulatory system as an extension ofacupuncture meridians," *Journal of Acupuncture and Meridian Studies*, vol. 2, no. 2, pp. 93–106, 2009.

[3] K. A. Kang, "Historical observations on the half-century freeze in research between the bonghan system and the primo vascular system," *Journal of Acupuncture and Meridian Studies*, vol. 6, no. 6, pp. 285–292, 2013.

[4] B.-C. Lee, S.-U. Jhang, J.-H. Choi, S.-Y. Lee, P.-D. Ryu, and K.-S. Soh, "DiI staining of fine branches ofbonghan ducts on surfaceof rat abdominal organs," *Journal of Acupuncture and Meridian Studies*, vol. 2, no. 4, pp. 301–305, 2009.

[5] H.-S. Shin, H.-M. Johng, B.-C. Lee et al., "Feulgen reaction study of novel threadlike structures (bonghan ducts) on the surfaces of mammalian organs," *The Anatomical Record B: The New Anatomist*, vol. 284, no. 1, pp. 35–40, 2005.

[6] C. J. Lim, J.-H. Yoo, Y. Kim, S. Y. Lee, and P. D. Ryu, "Gross morphological features of the organ surface primo-vascular system revealed by hemacolor staining," *Evidence-Based Complementary and Alternative Medicine*, vol. 2013, Article ID 350815, 12 pages, 2013.

[7] J.-H. Choi, C. J. Lim, T. H. Han, S. K. Lee, S. Y. Lee, and P. D. Ryu, "TEA-sensitive currents contribute to membrane potential of organ surface primo-node cells in rats," *The Journal of Membrane Biology*, vol. 239, no. 3, pp. 167–175, 2011.

[8] B.-C. Lee, S. Kim, and K.-S. Soh, "Novel anatomic structures in the brain and spinal cord of rabbit that may belong to the Bonghan system of potential acupuncture meridians," *Journal of Acupuncture and Meridian Studies*, vol. 1, no. 1, pp. 29–35, 2008.

[9] J. S. Yoo, M. S. Kim, V. Ogay, and K.-S. Soh, "In vivo visualization of Bonghan ducts inside blood vessels of mice by using an Alcian blue staining method," *Indian Journal of Experimental Biology*, vol. 46, no. 5, pp. 336–339, 2008.

[10] B.-C. Lee, K. Y. Baik, H.-M. Johng et al., "Acridine orange staining method to reveal the characteristic features of an intravascular threadlike structure," *The Anatomical Record B: The New Anatomist*, vol. 278, no. 1, pp. 27–30, 2004.

[11] C. Lee, S.-K. Seol, B.-C. Lee, Y.-K. Hong, J.-H. Je, and K.-S. Soh, "Alcian blue staining method to visualize Bonghan threads

inside large caliber lymphatic vessels and X-ray microtomography to reveal their microchannels," *Lymphatic Research and Biology*, vol. 4, no. 4, pp. 181–189, 2006.

[12] Z.-F. Jia, K.-S. Soh, Q. Zhou, B. Dong, and W.-H. Yu, "Study of novel threadlike structures on the intestinal fascia of dogs," *Journal of Acupuncture and Meridian Studies*, vol. 4, no. 2, pp. 98–101, 2011.

[13] B.-C. Lee, J. S. Yoo, V. Ogay et al., "Electron microscopic study of novel threadlike structures on the surfaces of mammalian organs," *Microscopy Research and Technique*, vol. 70, no. 1, pp. 34–43, 2007.

[14] B. S. Kwon, C. M. Ha, S. Yu, B.-C. Lee, J. Y. Ro, and S. Hwang, "Microscopic nodes and ducts inside lymphatics and on the surface of internal organs are rich in granulocytes and secretory granules," *Cytokine*, vol. 60, no. 2, pp. 587–592, 2012.

[15] V. Ogay, F. Min, K. Kim et al., "Observation of coiled blood plexus in rat skin with diffusive light illumination," *Journal of Acupuncture and Meridian Studies*, vol. 2, no. 1, pp. 56–65, 2009.

[16] B.-C. Lee and K.-S. Soh, "Visualization of acupuncture meridians in the hypodermis of rat using trypan blue," *Journal of Acupuncture and Meridian Studies*, vol. 3, no. 1, pp. 49–52, 2010.

[17] J. Walter, C. Klein, and A. Wehrend, "Comparison of eosin-thiazin and Papanicolaou-Shorr staining for endometrial cytologies of broodmares: technical note," *Tierärztliche Praxis Großtiere*, vol. 39, no. 6, pp. 358–362, 2011.

[18] Y. Keisari, "A colorimetric microtiter assay for the quantitation of cytokine activity on adherent cells in tissue culture," *Journal of Immunological Methods*, vol. 146, no. 2, pp. 155–161, 1992.

[19] B.-C. Lee, H.-S. Lee, J. E. Yun, and H. A. Kim, "Evidence for the fusion of extracellular vesicles with/without DNA to form specific structures in fertilized chicken eggs, mice and rats," *Micron*, vol. 44, no. 1, pp. 468–474, 2013.

[20] P. S. Cerri, J. A. Pereira-Júnior, N. B. Biselli, and E. Sasso-Cerri, "Mast cells and MMP-9 in the lamina propria during eruption of rat molars: quantitative and immunohistochemical evaluation," *Journal of Anatomy*, vol. 217, no. 2, pp. 116–125, 2010.

[21] S. J. Jung, K.-H. Bae, M.-H. Nam, H. M. Kwon, Y.-K. Song, and K.-S. Soh, "Primo vascular system floating in lymph ducts of rats," *Journal of Acupuncture and Meridian Studies*, vol. 6, no. 6, pp. 306–318, 2013.

[22] C. S. Yin, H.-S. Jeong, H.-J. Park et al., "A proposed transpositional acupoint system in a mouse and rat model," *Research in Veterinary Science*, vol. 84, no. 2, pp. 159–165, 2008.

[23] P. Ma, T. G. Villanueva, D. Kaufman, and J. F. Gillooley, "Respiratory cryptosporidiosis in the acquired immune deficiency syndrome. Use of modified cold kinyoun and hemacolor stains for rapid diagnoses," *The Journal of the American Medical Association*, vol. 252, no. 10, pp. 1298–1301, 1984.

[24] M. Stefanov, M. Potroz, J. Kim, J. Lim, R. Cha, and M.-H. Nam, "The primo vascular system as a new anatomical system," *Journal of Acupuncture and Meridian Studies*, vol. 6, no. 6, pp. 331–338, 2013.

[25] D. Zhang, G. Ding, X. Shen et al., "Role of mast cells in acupuncture effect: a pilot study," *The Journal of Science and Healing*, vol. 4, no. 3, pp. 170–177, 2008.

[26] H.-N. Chen, J.-G. Lin, A. D. Yang, and S.-K. Chang, "Safe depth of abdominal acupoints in pediatric patients," *Complementary Therapies in Medicine*, vol. 16, no. 6, pp. 331–335, 2008.

[27] T.-F. He and Y.-F. Chen, "Advances in studies on the correlation between acupuncture-moxibustion treatment and mast cells," *Zhongguo Zhen Jiu*, vol. 30, no. 1, pp. 84–87, 2010.

[28] X. Wang, H. Shi, J. Cui et al., "Preliminary research of relationship between acute peritonitis and celiac primo vessels," *Evidence-Based Complementary and Alternative Medicine*, vol. 2013, Article ID 569161, 8 pages, 2013.

[29] S. J. Galli, N. Borregaard, and T. A. Wynn, "Phenotypic and functional plasticity of cells of innate immunity: macrophages, mast cells and neutrophils," *Nature Immunology*, vol. 12, no. 11, pp. 1035–1044, 2011.

Hindawi Publishing Corporation
Evidence-Based Complementary and Alternative Medicine
Volume 2015, Article ID 361974, 17 pages
http://dx.doi.org/10.1155/2015/361974

Review Article

Primo-Vascular System as Presented by Bong Han Kim

Vitaly Vodyanoy,[1,2,3] Oleg Pustovyy,[1] Ludmila Globa,[1] and Iryna Sorokulova[1,2,3]

[1]*Department of Anatomy, Physiology and Pharmacology, College of Veterinary Medicine, Auburn, AL 36849, USA*
[2]*School of Kinesiology, Auburn University, Auburn, AL 36849, USA*
[3]*Edward Via College of Osteopathic Medicine, Auburn, AL 36849, USA*

Correspondence should be addressed to Vitaly Vodyanoy; vodyavi@auburn.edu

Received 29 September 2014; Revised 1 January 2015; Accepted 5 January 2015

Academic Editor: John H. Barker

In the 1960s Bong Han Kim discovered and characterized a new vascular system. He was able to differentiate it clearly from vascular blood and lymph systems by the use of a variety of methods, which were available to him in the mid-20th century. He gave detailed characterization of the system and created comprehensive diagrams and photographs in his publications. He demonstrated that this system is composed of nodes and vessels, and it was responsible for tissue regeneration. However, he did not disclose in detail his methods. Consequently, his results are relatively obscure from the vantage point of contemporary scientists. The stains that Kim used had been perfected and had been in use for more than 100 years. Therefore, the names of the stains were directed to the explicit protocols for the usage with the particular cells or molecules. Traditionally, it was not normally necessary to describe the method used unless it is significantly deviated from the original method. In this present work, we have been able to disclose staining methods used by Kim.

1. Introduction

In the early 1960s, Bong Han Kim discovered and described a new vast anatomical vascular system that he believed underpins the acupuncture meridian system. During the three years from 1962 to 1965 Kim published five reports [1–5]. Four of Kim's reports were translated into English as two books [6, 7]. He analyzed and described this new anatomical system that he named as Bonghan system. It was obvious from his publications that Kim had far-reaching scientific goals, but, in 1965, his research ceased, and his fate became unknown [8, 9].

Following Dr. Kim's disappearance, his findings remained dormant for many years. In 2002, the scientific group of Dr. Kwang-Sup Soh initiated a series of experiments that validated many of Kim's results. This research has ignited a new interest in this anatomical vascular system that now is termed primo-vascular system (PVS) [10]. Soh and his colleagues have described the major achievements of Bong Han Kim in the understanding of structure and functions of PVS, as well as the experimental and theoretical results obtained by Kim during the relatively short time [10]. Kim offered a comprehensive picture of primo-vascular system. Kim presented the structural architecture that he had observed, which included organ, tissue, cells, and molecules involved in the function of PVS [7]. A short list of his techniques consisted of microsurgery, light and electron microscopies, and time-lapsed photography. Instead of dye-labeled antibodies he used fluorescent and nonfluorescent histochemistry with a large variety of stains, radioactive tracers, microautoradiography, and emission spectral analysis. He also perfected cell analysis, nucleic acid analysis, ultracentrifugation, cell culture, cell development, tissue regeneration, chromatography, electrophoresis, embryology, physiology, and electrophysiology [6, 7]. Kim gave a vivid description of primo-nodes and primo-vessel, which are two major components of primo-vascular system.

In this work, we have recreated structural models of the PVS node and vessels as they were described by Kim and compare these models with our optical experimental data and results found so far in the literature.

2. Terminology

Shortly before the first International Symposium on Primo-Vascular System, which was held in Jecheon, Korea, during September 17-18, 2010, Dr. Kwang-Sup Soh suggested that it would be important to agree upon a single terminology for the Bonghan system. It was agreed that the following terms would be adopted: Bonghan system (BHS) = primo-vascular system (PVS), Bonghan duct (BHD) = primo-vessel (PV), Bonghan corpuscle (BHC) = primo-node (PN), Bonghan ductule = P-subvessel, Bonghan liquor = primo-fluid (P-fluid), and Sanal = p-microcell.

The present work includes detailed presentations of PVS structures that require additional new terms as follows:

periductium= p-vessel external jacket;

wall of the Bonghan ductule + outer membrane of Bonghan ductule = external envelope of p-subvessel;

outer membrane of Bonghan corpuscle = primo-node capsule;

sanalosome= p-microcell nucleosome;

sanaloplasm= p-microcell nucleoplasm;

small nucleus-like structures = small (immature) p-microcell = progenitors of multipotent stem cells;

large nucleus-like structure = large (mature) p-microcell = multipotent stem cell; sanalization = conversion of cell into p-microcell.

3. A Brief Old History

For many, the acupuncture meridian system is nothing more than a network of lines drawn on a body map and labeled with hieroglyphs. For others, the exact positions and locations of acupuncture points and meridians result from a few thousand years' empirical practices of acupuncturists. It seems that no theoretical or anatomical background for the location and morphology of these points is available. On the contrary, there is strong evidence that information on the acupuncture points and meridians is based on the anatomical knowledge used in ancient Chinese surgical practices [11–13]. Anatomical dissections are mentioned in the Huang-Di Nei-Jing Ling-Shu, one of the oldest traditional books relating to Chinese medicine that describes anatomical structures of acupuncture points [14]. The most important source of information and exact anatomical description of acupuncture points is the classic Tong Ren, the Copper Man by Wang Wei-Yi published around 1027 A.D. (cited by Schnorrenberger [11]).

Due to the considerable difference between ancient and modern anatomical nomenclature, it is difficult to comprehend the full extent of the morphological properties of acupuncture points described by ancient scholars. It seems that detailed descriptions of anatomical structures given in the ancient Chinese sources would require microscopic histological examination. It is not known if ancient Chinese medical doctors used any magnifying tools in their anatomical work. The first recorded use of a microscope can be traced 4,000 years back to the Chow-Foo Dynasty. Ancient Chinese text refers to the construction of a magnifying tube filled with water with a refractive single lens in the lower end of this tube. By filling the tube with water at different level, they attained different level of magnification [15]. The highest magnification possible, 150x, would be powerful enough to see many morphological features that can be observed in modern microsurgery. Therefore, it would be very exciting to find a correspondence between ancient and modern anatomical nomenclature to comprehend the vast morphological knowledge that might have been available 2000 years ago. Additionally, there is evidence that acupuncture was practiced in Central Europe over 5200 years ago [16, 17].

Based upon the ancient literature, it is not clear whether ancient Chinese doctors knew the specific morphology of an acupuncture point. However, it is clear that the ancient knowledge of acupuncture meridians was more detailed and explicit. In contrast to the western view of meridians as mere lines on the skin, the classical Chinese text indicates that the meridians, in fact, possess a three-dimensional topology. They run deep inside the human body connecting with internal organs. In ancient Chinese text they are referred to as "Jing Mai" (pulsing vessels) [13] that carry Qi, nutrition, defensive factors, and liquid [18, 19]. The Qi is known to have many different meanings. In most cases, it is interpreted as a special substance or liquid that is in "a constant state of flux and varying states of aggregation" [18]. "Jing" is often translated as "essence." Congenital Jing is a substance that is received from one's parents at conception and which governs the growth and regeneration processes from the conception to death.

Huang-Di determined that Jing Mai also participated at the earliest stages of the human embryo development. He explains the creation of a human being by the combination of the female ovum Jing with a male sperm Jing. It involves Jing Mai (pulsing vessels) at the unfolding of brain and spinal cord tissues that correspond to the ectoderm layer, one of the three germ layers recognized in embryology [13, 14, 20].

Rephrasing the ancient Chinese concept of acupuncture meridians (Jing Mai), one can say that ancient Chinese medical doctors viewed the meridians as a three-dimensional vascular system. The system is carrying a special liquid (Qi) which contains genetic material (Jing) that is initially obtained after conception.

Ironically, putative primo-vessels have been discovered in Europe before the discovery of lymphatic vessels/system. In 1622, Gasparo Aselli, a professor of anatomy and surgery, Pavia, Italy, found vessels in the mesentery of dog that were filled with a white liquid. These white vessel structures ran through the mesentery and along the surface of the intestines and emitted a milky fluid when cut. Because of the milky appearance of the vessels, Aselli named these structures as *lacteis venis or* milky veins. Aselli stated that the liquid in these vessels is transformed in blood. Later, this statement was rejected by the researchers working with lymphatic vessels [21, 22], but Aselli is still credited as the discoverer of the lymphatic system. It is interesting to note that Aselli may have, in fact, described the existence of primo-vessels because the hematopoiesis that he described was also documented to be in the internal primo-node. It was later demonstrated by Kim [5, 7].

In 1874, Louis-Antoine Ranvier, who discovered nodes of Ranvier, also described unusual structures in the omentum of new born animals. He described these structures as being elongated or round, occasionally branched elements, containing red and white corpuscles [23]. About a quarter of the century later, Marchand [24] also found and described similar structures in the animal omentum. He described them as elongated elements, accompanied by blood vessels and associated with the production of all types of blood cells. In 1909, analyzing the interaction of various vital stains and colloidal metals with these structures, Goldman [25] reported that this type of "reticular-endothelial" system can be identified by trypan blue stain. Trypan blue belongs to the group of benzidine dyes containing trypan red and pyrrhol blue. He indicated that the pyrrhol blue particles create granular inclusion in the cells of these systems, which he named as "pyrrhol cells."

Maximow, the scientist who coined the name "stem cell" [26], also described structures and functions of hematopoietic systems as scaffolds or niches for stem cell maturation and subsequent development of blood cells: "*. . . they appear as sharply outlined, polymorphous, flat, spindle shaped or branched elements, often containing inclusions and are then easily distinguishable from the fibroblasts. They may also assume a flat shape and line blood or lymph channels. More than by a peculiar histological structure all these elements are characterized by a series of very important functional properties. Being endowed with ample prospective potencies they can produce, provided external conditions are favorable for hemocytoblasts* (hematopoietic stem cells) *and different types of blood cells. It is difficult to choose a suitable general name for these elements of the connective tissue, remaining throughout the whole life in an undifferentiated embryonic condition. They represent a vast cell system, distributed all over the body, over various organs and assuming, according to their position, manifold histological aspects. As we have seen, single parts of this cell system have been described by various investigators under different names. However, the idea of the close interrelation or even identity of all these cells, the fact that they form one entity, one vast group of elements with a very prominent function in the body, has made headway slowly*" [27]. In this relatively short paragraph, Maximow described the essence of the primo-vascular system that was independently discovered by Bong Han Kim, which he subsequently named as Bonghan system [1–7, 28, 29].

4. Summary of Kim's Findings on Primo-Vascular System

In the 1960s, Bong Han Kim, a North Korean scientist and professor of Pyongyang Medical College, suggested that the superficial acupuncture meridian system represented a fundamental vascular system. He injected radioactive phosphorus (P^{32}) into a rabbit primo-node and documented that the P^{32} tracked or followed the acupuncture meridians [6]. Kim revealed that he separated DNA granules (p-microcells) from the primo-vessels and stimulated their proliferation under artificial conditions [7].

Importantly, radioactive visualization of the acupuncture meridians was reported again [30–32]. The research teams injected the radioisotope technetium (Tc^{99}) at acupoints and described that the effective radiotracer pathways coincided with acupuncture meridians. A physical reality of acupuncture meridians was also confirmed by the increase in electroconductivity, hydraulic conductance, and propagation of acoustic waves [32–34]. Furthermore, infrared light delivered at acupoints was shown to travel in tracks detectible on the skin and these tracks correspond to traditional acupuncture meridians [35].

Three uniquely critical anatomical structures were reported as having both distinctive functions and structures. These are (1) superficial nodes positioned at the acupuncture points; (2) profound nodes in deep tissues located in and around blood and lymphatic vessels and internal organs; and (3) primo-vessels that connect all nodes which comprises the primo-vascular system. Kim proposed that p-microcells, DNA-containing granules, mature in the Bonghan system and produce small cells that are transported through ducts to replace aged and dying cells. These small cells, as described by Kim, behaved like multipotent stem cells [7].

5. Primo-Vascular Node and Vessels

According to Kim, a primo-vessel connects primo-nodes, and a primo-node is linked with primo-vessels.

5.1. Primo-Vessels. Kim recognized four different types of primo-vessels as follows. (1) The primo-vessels floating in the blood and lymphatic vessels were named as the internal (*intravascular*) primo-vessels. (2) The primo-vessels distributed on the surface of the organs, independent of the blood and lymphatic vessels and neuronal axons, were named as the *intraexternal* primo-vessels. (3) The primo-vessels running along the outer surface of the walls of blood and lymphatic vessels were named as the external (*extravascular*) primo-vessels. The external primo-vessels sometimes run, either independently of blood vessels or along neuronal axons. (4) The primo-vessels distributed in the internal and the peripheral nervous system, running inside the central canal of the spinal cord and the cerebral ventricles, were named as the *neural* primo-vessels [7].

The anatomical structure of different types of primo-vessels varies, but all of them share some common features. The primo-vessel is composed of 1–20 p-subvessels of 3–25 μm in diameter (Figure 1(a)) [7]. The bundle of p-subvessel of the primo-vessel is laid into an external jacket composed of endothelial cells with 6–12 μm round or oval nuclei.

The intraexternal primo-vessels, the simplest for microscopic observations, run openly on the surface of the internal organs in the thoracic and abdominal cavities and create a network, giving branches to various internal organs. Analyzed under a microscope, the nonfixed sample of intraexternal primo-vessel is revealed as a translucent, milk-white structure, which is covered with a very thin, transparent membrane [7].

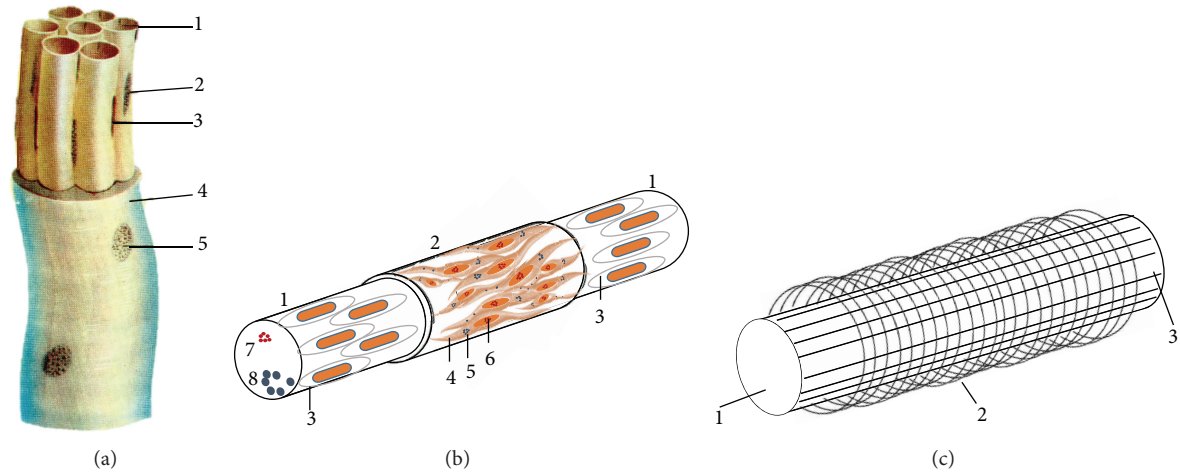

Figure 1: Illustration of the primo-vessel and p-subvessel. (a) Primo-vessel. 1: primo-subvessel; 2: cell nucleus of the outer membrane; 3: nucleus of endothelial cell; 4: external jacket of primo-vessel; 5: nucleus of jacket endothelial cell [7]. (b) Diagram of primo-subvessel. 1: wall of subvessel formed by endothelial cells; 2: outer membrane of subvessel; 3: endothelial cell with rod-shaped nucleus; 4: spindle-shaped cell with ellipsoidal nucleus; 5: fine basophil granules in the cytoplasm; 6: fine chromatin granules inside nucleus; 7: basophil granules inside the subvessel; 8: p-microcells. (c) Diagram of subvessel fibers. 1: primo-subvessel; 2: fine transversal fiber; 3: longitudinal fiber.

5.2. P-Subvessels. The external envelope of the p-subvessel is composed of two layers (Figure 1(b)): the wall of endothelial cells with a rod-shaped nucleus of 15–20 μm and the outer membrane containing spindle-shaped cells with ellipsoidal nucleus of 13–27 μm long and 4-5 μm thick that are similar to smooth muscle cells. These cells are characterized by fine basophil granules in the cytoplasm and fine chromatin granules inside the nuclei. The thickness of the internal wall, when observed by an electron microscope, is only 0.1–0.2 μ. The p-subvessels are surrounded by fine, longitudinal, and circular fibers crossing each other (Figure 1(c)). A high magnification of a primo-vessel was imaged by Kim using transmission electron microscopy [7] and presented in Figure 2(a). It clearly shows that the external envelope of p-subvessel is a two-layer structure. The micrograph also shows that the endothelial nucleus (ENBD) of the p-subvessel belongs to the internal layer. So it is safe to speculate that the external layer is the outer membrane of p-subvessel that contains muscle-like cells.

5.3. Primo-Nodes. Kim classified the primo-nodes into two categories: the superficial and the profound primo-nodes. The profound primo-nodes again were further categorized into the internal (intravascular), external (extravascular), intraexternal, neural, and intraorganic primo-nodes. The primo-vessel departs the intraorganic primo-node branches and extends to several small intraorganic nodes (called the terminal primo-nodes). The fine p-subvessels running out of the terminal primo-nodes (terminal p-subvessels) are directly linked to the cell nuclei. The internal primo-node is linked by internal primo-vessels, the external node by external vessels, and the superficial node by superficial vessels. The intraexternal and the neural nodes are also linked by the vessels of relevant names, respectively [7].

The primo-nodes have various shapes (round, oval, or multifaceted). One to a few p-vessels enter and exit the node. The most typical primo-nodes have oval shape of 0.1–0.5 mm over the short and 0.5–1 mm over the long axis. Both node's ends are linked to primo-vessels of 3–6 cm long and 40–100 μm in diameter (Figure 2(b)). The primo-node is the anastomosis of widened and branched p-subvessels covered with a 5–40 μm thick capsule. A p-vessel bundle of the incoming (afferent) vessel enters into the node, branches into additional bundles, and fills the node interior with tightly twisted and bent bundles. P-subvessels converge, narrow, and come out from the node as a single efferent primo-vessel. An enlarged p-subvessel which is called the sinus of the node harbors basophil granules and p-microcells.

Reticular fibers composed of collagen secreted by reticular cells are part of the primo-node. Reticular fibers intersect to form a fine network that functions as a supporting lattice in the primo-nodes and vessels [7].

5.4. Primo-Fluid inside PVS. Kim found that p-fluid contains large concentration of nucleic acids, 3.12–3.40% of total nitrogen, 10–0.17% of nonprotein nitrogen, 0.57–1.00% of lipids, 0.10–0.12% of reduced sugars, 170.4 mg% of total hyaluronic acid, 0.22–0.4 μg/g of epinephrine (adrenaline), and 0.6–1.5 μg/g. It also contains norepinephrine (noradrenaline) and gonadal hormone, estrogen, more than 19 free amino acids including several essential amino acids, and more than 16 free mononucleotides. The p-subvessel in the node contains basophile granules, small p-microcell, and somewhat large, round p-microcells. Cells with pale cytoplasm are also found, and the cytoplasm often contains many chromaffin granules. Kim also reported the presence of copper, magnesium, calcium, iron, manganese, zinc, and cobalt [7].

6. Primo-Vascular Systems

Kim recognized five different primo-vascular systems comprised primo-nodes and vessels as follows. (1) Internal PVS

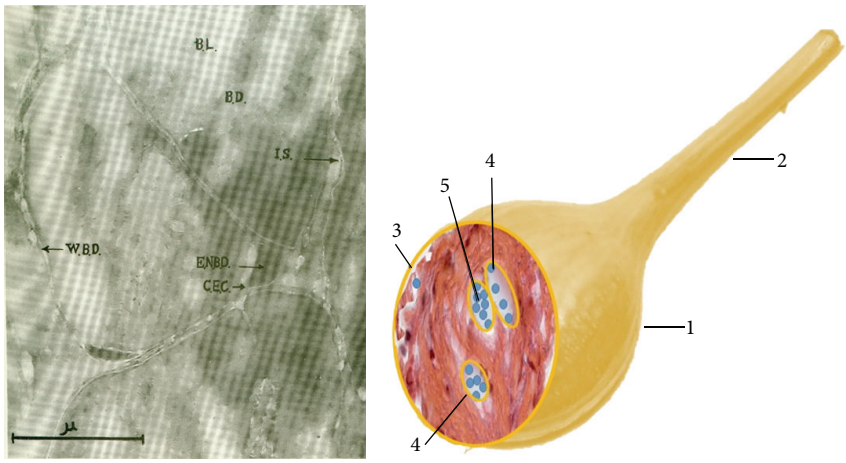

(a) (b)

Figure 2: Primo-vessel and node. (a) Electron micrograph of the internal primo-vessel (cross section) (×42,000). BL: primo-fluid, BD: p-subvessel, IS: interstitial substance, WBD: external envelope of p-subvessel, ENBD: endothelial nucleus of the p-subvessel, and CEC: cytoplasm of endothelial cell [7]. (b) Diagram of the transversal section of a primo-node. 1: Primo-node; 2: primo-vessel; 3: node capsule; 4: lumens; 5: p-microcells.

contains internal primo-vessel and internal primo-nodes, which is distributed in all the blood vessels, lymphatic vessels, and the cardiac cavity. The internal primo-vessel is very fragile, and its external jacket and connective tissue are weakly developed. The internal primo-node has a structure particularly similar to that of the hematopoietic organ, and myeloid and lymphoid cells are present in the network of the reticular tissues. Cells similar to those found in parenchymal organs are also occasionally identified. (2) The intraexternal PVS includes intraexternal primo-vessel and intraexternal primo-node and extends separately of the neighboring organs, the blood, lymphatic vessels, and nerves. In the intraexternal primo-vessel, the connective tissue and the external jacket are, usually, more developed as compared to the internal primo-vessel. The primo-vessel sinus of the intraexternal primo-node includes cells with a light cytoplasm and also basophile structures. (3) The external PVS contains external primo-vessels and external primo-nodes and primarily passes around vessels and nerves. A thick connective tissue membrane covers the external primo-vessel. The primo-vessel sinus of the external primo-node includes a large number of chromaffin granules. (4) The neural PVS comprises neural primo-vessels and neural primo-node, and it is immersed in the cerebrospinal fluid of the central nervous system. Its branches are dispersed not only in the parenchyma of the central nervous system but also in the peripheral nerves. (5) The intraorgan PVS is located inside the organs. They include intraorgan primo-nodes, terminal primo-nodes, and terminal p-subvessels. They are the intraorgan elements of the internal primo-nodes, external primo-vessels, and neural primo-vessels. Many primo-vessels are joined in the intraorgan primo-node to the terminal p-subvessels, which are connected directly with cell nuclei.

Different primo-vascular systems are connected with one another. The internal PVS connects with the intraexternal PVS through the blood vessel wall and with the external PVS via the external primo-node. The intraexternal PVS communicates with the external PVS through the external primo-node and it is connected with the neural PVS. All the systems are totally interrelated to each other [7].

6.1. Histochemistry of PVS. In order to characterize the cellular and molecular composition of PVS, Kim used various staining techniques, which were largely practiced at his time as immunohistochemistry is practiced today. Kim did not describe the stains that he used in his research. Rather he only mentioned the stain names, because their use and properties were well known and did not require special explanations. Most of the stains that Kim employed in his experiments are still in use today and are commercially available. For example, Kim used Feulgen stain to visualize nucleic acids in PVS [6, 7]. The Feulgen staining remains the standard for precise imaging of DNA [37].

6.2. Nucleic Acids. Kim used Feulgen, Unna-Pappenheim, Brachet, acridine orange, and hematoxylin-eosin stains to characterize nucleic acid distribution in PVS (Table 1). The Feulgen stain was used to visualize cell nuclei, basophile granules, and other structures containing DNA inside p-subvessels by virtue of its capacity to penetrate the cellular membrane. He also imaged basophile particles and p-microcells in the sinuses of primo-nodes (Figure 3(a)). As a result of acid hydrolysis of DNAs [38], it stains them red as showed in many images of endothelial cell nuclei in walls of p-subvessels. The elongated, rod-like nuclei of p-subvessel endothelial cells work as a unique marker of PVS. In Kim's studies, the DNA of p-microcell nucleosome was stained by Feulgen reaction while DNA in p-microcell nucleoplasm was revealed by the Brachet stain [7].

Kim used acridine orange in his earlier experiments to visualize nucleic acids in nonfixed PVS samples. "*Corpuscles*

Table 1: Stains used by Bong Han Kim.

Stain	Target	Color	Mechanism	Reference
Feulgen	Cell nuclei, basophile granules, and other structures containing DNA inside p-subvessels. Basophile particles and p-microcells in sinuses of primo-node. Endothelial cell nuclei in walls of p-subvessels. DNA of p-microcell nucleosome.	DNA is stained red 570 nm. The background, if counterstained, is green.	Acid hydrolysis of DNA.	[6, 7, 37, 38]
Hillarp-Hokfelt	Chromaffin cells, epinephrine (adrenaline), and norepinephrine (noradrenaline). Small granules inside p-subvessels.	Yellow.	Oxidation of adrenaline and noradrenaline with potassium iodate gives a pigment formation. The method is based on the formation of iodochromes of the hormones.	[7, 39]
Sevki	Chromaffin cells, epinephrine, and norepinephrine.	Chromaffin cells: bluish-red; inside primo-node: red to bluish-red; red blood cells: brown; mast cell granules: red.	Sevki stain (~6% water dilution of Giemsa stain).	[7, 40–42]
Giemsa	Adrenal medullary cells, chromaffin cells, epinephrine (adrenaline), norepinephrine (noradrenaline), collagen, erythrocytes, platelets, lymphocytes, monocytes, megakaryocytes, and hemocytoblasts.	Chromaffin: brown; collagen: blue; erythrocytes: pink; platelets: light pale pink; lymphocyte: sky blue; monocyte: pale blue; leukocyte nuclear chromatin: magenta; megakaryocytes: reddish-blue nuclei and blue cytoplasm; hemocytoblasts: large, vesicular, pink nuclei, and prominent nucleoli. Giemsa, after a dichromate fixation, produced a green color.	Giemsa's solution is a mixture of methylene blue, eosin, and Azure B. Methylene blue is a cationic dye. It binds to tissue anions and stains basophilic substances, including nucleic acids. Eosin is an anionic dye and is attracted to positively charged protein groups (cations), such as amino groups. It is an acidophilic stain. Azure B is formed by the oxidation of methylene blue and is a basic stain.	[7, 40, 43–45]
Gros-Schultze	Nerve fibers and nerve endings.	Dark brown to black.	Silver nitrate bath. The silver nitrate is reduced by the sodium potassium tartrate into a metal silver that is adsorbed by argyrophilic nerve fibers.	[7, 46, 47]
Van Gieson	Neural vessels. Collagen.	Collagen: pink or deep red; cytoplasm: yellow; elastic fibers: blue to black.	Mixture of picric acid and acid fuchsine (picrofuchsin). The method is based on the affinity towards elastic fibers displayed by the dye resulting from a reaction between resorcin and basic fuchsine in the presence of ferric chloride.	[7, 43, 48]
Verhoeff	Elastic fibers, nuclei, and collagen.	Elastic fibers: intense blue-black to black; nuclei: blue to black; collagen: red; other: yellow. Eosin counterstain shows erythrocytes red.	[a]Combination of stains: hematoxylin, iron(III) chloride, Lugol's iodine, Van Gieson's stain (acid fuchsine, picric acid), and sodium thiosulfate. The tissue is stained with a hematoxylin, ferric chloride, and iodine.	[7, 49, 50]
Unna-Pappenheim	RNA and DNA in tissue sections.	RNA: red; DNA: green.	[ab]Methyl green-pyronin combination. Competition between the slow staining, but doubly charged, methyl green and the more rapidly staining, singly charged pyronin Y.	[6, 51, 52]
Brachet	DNA, RNA, and DNA in the nucleus of cells and RNA in the nucleolus. RNA in the cytoplasm of cells. DNA in p-microcell nucleoplasm.	DNA: green; RNA; p-microcell nucleoplasm: Red.	Methyl green-pyronin combination. Similar to that of Unna-Pappenheim method. Brachet introduced control by using RNase solution before staining.	[7, 50, 51]

Table 1: Continued.

Stain	Target	Color	Mechanism	Reference
Acridine-orange	Vital stain for DNA and RNA. Primo-vascular nodes and vessels. Acridine orange also accumulates and emits red light in mast secretory granules and other cellular acidic compartments.	RNA: fluorescent red; DNA: fluorescent green; mast cells: red.	Acridine orange is a basic dye. Basic dyes are cationic and will stain anionic or acidic molecules. Staining is pH sensitive. Acidic substances that stain with basic dyes are termed basophilic.	[6, 51, 53, 54]
Hematoxylin-eosin	The basophilic structures containing nucleic acids, such as the ribosomes and the chromatin-rich cell nucleus, and the cytoplasmic regions rich in RNA. The eosinophilic structures composed of intracellular or extracellular protein. Most of the cytoplasm is eosinophilic.	Hematoxylin colors basophilic structures with blue-purple hue and alcohol-based acidic eosin colors eosinophilic structures as bright pink. Red blood cells, collagen fiber: red.	Oxidized hematoxylin (hematein) has a selective affinity for nuclei when combined with aluminum ion. The mechanism of eosin staining is not fully understood but is believed to be of an electrostatic nature. Negatively charged eosin ions will stain positively charged tissue ions.	[7, 43, 50, 55]
Resorcin-fuchsin	Glycogen, basement membrane, reticulum fibers, collagen, and other structures containing polysaccharides. flexible fibers, and collagen inside primo-nodes.	Elastic fiber: purple; elastic membrane in blood vessel: dark purple; nuclei: pale red; red blood cells: red if counterstained by eosin.	Acetylation, sulfaction, and phosphorylation induce binding of resorcin-fuchsin.	[7, 43, 56]

[a] *Verhoeff mechanism*: the differentiating is accomplished by using excess of ferric chloride to break the tissue-ferric chloride dye complex. The dye will be attracted to the larger amount of ferric chloride in the differentiating solution and will be removed from the tissue. The elastic fibers have the strongest affinity of the iron-hematoxylin complex and will retain the dye longer than the other tissue components. Van Gieson's solution is used as a counterstain. [b] *Unna-Pappenheim mechanism*: methyl green has two cationic charged groups that become linked to the phosphate moieties in the DNA. The pyronin Y displaces the methyl green from all sites of linkage except where its double charge gives it a selective advantage (acidic polymer such as DNA). Consequently the methyl green stains DNA and retains its binding to this substance against the competitive action of pyronin Y. Pyronin Y stains the less polymerized RNA rapidly, and it can displace methyl green from linkages having smaller polymeric acidic substances (RNA).

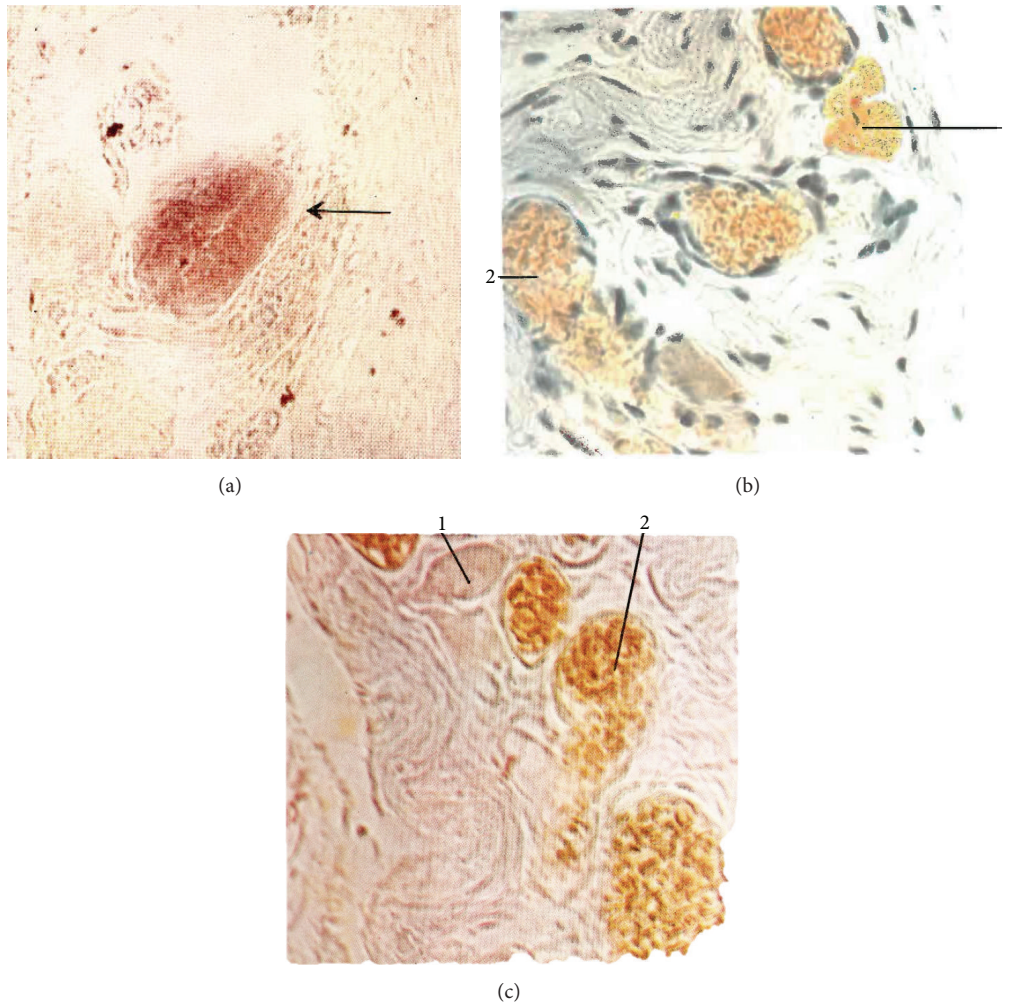

Figure 3: Superficial primo-node. (a) Feulgen stain. Sinus of the superficial primo-node (arrow) (×160). (b) Hillarp-Hokfelt stain. 1: chromaffin cell, 2: blood vessel. (c) Sevki stain; 1: chromaffin cell; 2: blood vessel [7].

and ducts were extracted and stained with acridine orange, and examined under a luminescent microscope. The inner substance of the corpuscle and the duct linked to it selectively fluoresced brilliantly: in blue green or yellowish green. This fact has convinced us that an enormous amount of DNA is contained in the inner substance of the corpuscle and the duct" [6]. Acridine orange is used as a nucleic acid-selective fluorescent cationic dye. Being cell-permeable, it binds with DNA and RNA [51]. A light with a maximum wavelength of 502 nm excites the acridine orange/DNA complex which emits at the maximum wavelength of 525 nm (green). When it interacts with RNA, the excitation shifts to 460 nm and the emission shifts to 650 nm (red) [57]. However, acridine orange also is accumulated in mast secretory granules and other cellular acidic compartments and emits red light [53, 54].

When Kim studied regeneration of injured tissues, he observed newly formed round p-microcells that contain clear chromatin particles. These basophile structures were stained deep violet by hematoxylin and show a strong positive Feulgen reaction [7].

6.3. Chromaffin Cells, Epinephrine, and Norepinephrine. Kim identified chromaffin cells in the internal substance of superficial primo-nodes, primarily in its superior and central parts [7]. Chromaffin cells congregate in small groups close to the sinus around the blood vessels. These cells vary in shape and size, and the location of their nuclei is not well defined. In some instances, chromaffin granules are collected together both within and outside the sinus. These granules are positive in the Hillarp-Hokfelt and Sevki stains (Table 1). They are dispersed around the blood capillaries in the internal substance of the node (Figures 3(b) and 3(c)).

6.4. Fibers. Large amount of fibrous connective tissue was found between sinuses in primo-nodes. The primo-nodes are partly filled with collagen fibers that are produced by reticular cells. Reticular fibers intersect to create a thin net that serves as a supporting mesh in the primo-nodes and vessels. Kim found that this connective tissue contains collagenous, elastic, and argyrophilic fibers. To characterize these materials histologically, Kim used resorcin-fuchsin, Van Gieson, Verhoeff,

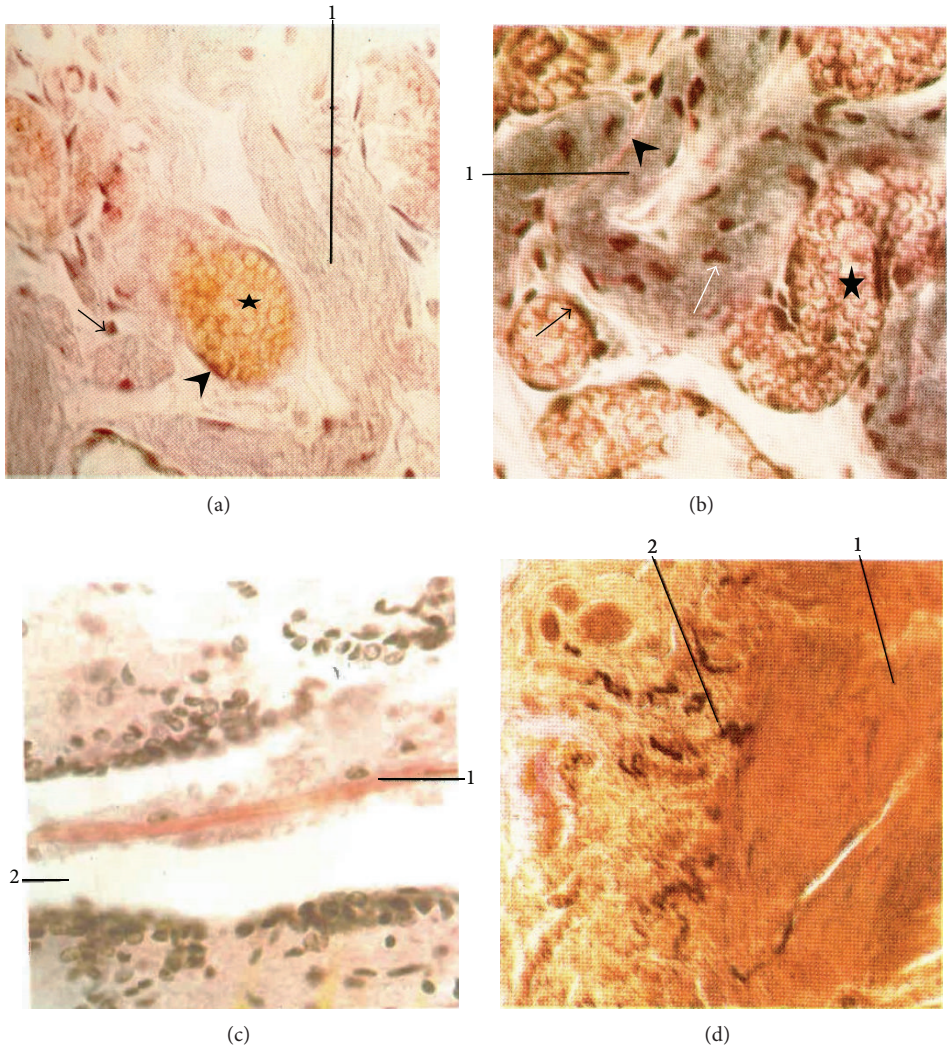

Figure 4: Fibers. (a) Superficial primo-node (resorcin-fuchsin stain) (×400). 1: sinus, arrow: elastic fiber, arrowhead: elastic membrane in blood vessel, and star: erythrocytes. (b) Superficial primo-node (Verhoeff stain) (×400). 1: sinus, white arrow: basophil particle, star: erythrocytes, blood vessel membrane: black arrow, and collagen fiber between sinus folds: arrowhead. (c) Neural Bonghan duct (in the central canal of the spinal cord) (Van Gieson stain) (×400). 1: primo-vessel, 2: central canal of the spinal cord. (d) Nerve-supply at the superficial primo-node (Gros-Schultze reaction) (×160). 1: superficial primo-node, 2: nerve fiber [7].

and Gros-Schultze stains (Table 1) [7]. A large number of fibers were found on the external envelope of the sinus, which were stained by the resorcin-fuchsin (Figure 4(a)). The jacket is folded in a distinctive way and appears light purple in color. The elastic fibers that are perpendicular to the slide and along the outer surface of the sinus together with the outer membrane of blood vessels appear dark purple. Erythrocytes counterstained with eosin appear yellow-red. The details of the sinus in primo-vessels are more pronounced with Verhoeff stain (Figure 4(b)). The elastic fibers of the sinus appear transparent black. The sinus is folded, and the collagen fibers between the folds are stained red. Basophil particles cover the sinus surface. The blood vessels filled with erythrocytes surround the sinus, and a dark purple color distinguishes the outer membranes of blood vessels.

Kim used Van Gieson and Gros-Schultze stains to visualize the neuronal primo-vessels. He described the live neuronal primo-vessels as semitransparent, milk-white, and of a very delicate texture [7]. Figure 4(c) shows the neural primo-vessel in the central canal of the spinal cord stained by Van Gieson stain, showing red collagen fiber. The nerve fibers were imaged in the superficial primo-node by a Gros-Schultze stain (Figure 4(d)).

6.5. Hematopoietic Stem Cells. All cellular blood components are formed from hematopoietic stem cells. In developing embryos, blood formation occurs in aggregates of blood cells in the yolk sac, called blood islands [58]. Maximow was the first who coined the word "stem cell" for the initial cell that gives rise to all blood cells. He used the cell name hemocytoblast for the multipotent hematopoietic stem cell. He also discovered that hemocytoblast generates two independent series of blood cells: myeloid and lymphoid systems. Furthermore, Maximow determined that as the development progresses,

blood formation occurs in the spleen, liver and lymph nodes, and later in the bone marrow [26, 27]. The common myeloid progenitor produced from the hemocytoblast differentiates into four cell classes: erythrocytes, mast cells, megakaryocytes (which form platelets), and myeloblasts. Myeloblasts differentiate into basophils, neutrophils, eosinophils, and monocytes, which later mature into macrophages. Lymphoid progenitors differentiate into natural killer cells and lymphocytes (B cells and T cells). B cells differentiate into plasma cells [59] (Figure 5).

By using a variety of stains and biochemical tests, Kim discovered that internal primo-nodes contain cells that are typical for the hematopoietic organs. "*These are myelopoietic and lymphogenetic cells in different stages of differentiation, that is, granulopoietic, monopoietic, erythrogenic and lymphopoietic elements and megakaryocytes*" [5, 7]. These are the same two major progenitor cell lineages and cell classes shown in Figure 5. Kim gave an example by revealing the cellular composition of the internal primo-node by using the Giemsa stain. Giemsa stain has a remarkable dynamic range of colors capable of visualizing the complex morphological composition of blood cells (Table 1) [43, 60–62]. Figure 6 identifies a multipotent hematopoietic stem cell, hemocytoblast, and an important member of myeloid lineage, megakaryocyte [5, 7]. He described other cells differentiated from both myeloid and lymphoid progenitors. "*This suggests that an active hematopoietic process takes place in the internal Bonghan corpuscles*" [7]. Kim designed and carried out an elegant experiment to prove this last statement. In his experimental design, Kim used the known effects of phenylhydrazine on the hematopoiesis. When the erythrocytes in the bone marrow and peripheral blood are destroyed with phenylhydrazine, erythropoiesis is increased [63, 64]. Kim also challenged rabbits with the phenylhydrazine and observed a striking increase in production of erythrocytes. He explained this effect by activated internal primo-nodes, which were significantly enlarged after the phenylhydrazine treatment. Quite the opposite, anemia happened progressively when the internal PVS was injured. These data provide the evidence that the hematopoiesis is one of the essential functions of the internal primo-vascular system.

It is important to note that the effects of phenylhydrazine on the hematopoiesis have been reported recently in rats and mice [65, 66]. Both research groups observed phenylhydrazine-induced erythropoiesis. However, these researchers could not reconcile the large damage on bone marrow and the increased production of erythrocytes. This phenomenon could be easily explained by the amplified hematopoietic activity arising in the PVS.

6.6. Multipotent Stem Cells. James Till and Ernest McCulloch, while studying the effect of radiation on the bone marrow of mice at the Ontario Cancer Institute, Toronto, demonstrated the presence of self-renewing cells in mouse bone marrow [67, 68]. At the same time, 6500 miles from Toronto, Bong Han Kim reported that he had isolated p-microcells from the newly discovered primo-vascular system and induced their proliferation under artificial conditions. He stated that mature p-microcells had a cell-like structure,

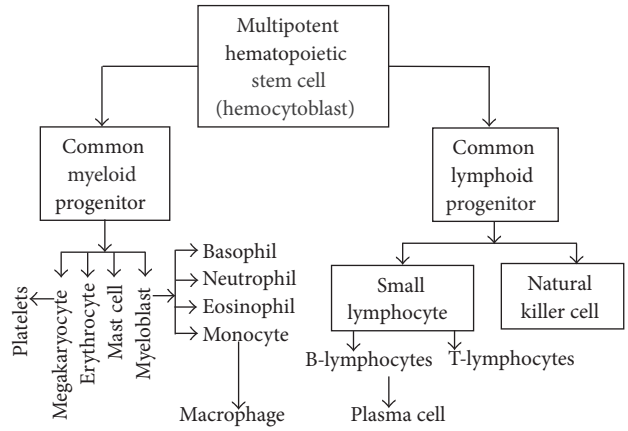

Figure 5: Hemocytoblast cells generate two major progenitor cell lineages, myeloid and lymphoid progenitors.

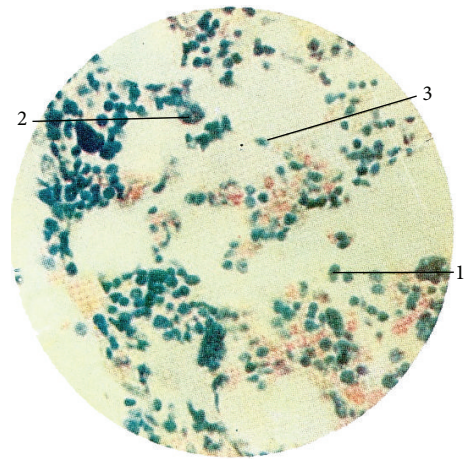

Figure 6: Internal primo-node (Giemsa stain). 1: hemocytoblast, 2: megakaryocyte, and 3: reticular fiber [7].

contained chromosomes, and participated in the tissue regeneration [7]. Each of these properties belongs to stem cells [59, 69]. Kim also demonstrated that p-microcells were harbored in a primo-node, a highly vascular organ that provides physiological conditions favorable for p-microcells [7], as well as a stem cell niche [70]. The role of a primo-node as a stem cells niche was discussed again by PVS researchers [71–73].

6.6.1. Morphology. Kim studied the structure of p-microcell, the electron microscope. Figure 7(a) shows p-microcells inside a small external primo-node. Kim thoroughly described p-microcells found within the node. The p-microcells vary in shape. Some are round and others irregular, and their membranes are smooth. In the cytoplasm of some of the round cells, endoplasmic reticulum is well developed; it is organized around the nucleus and mitochondria. In the cytoplasm of the cells, one nucleus or two nuclei can be found in the middle or periphery of the cell. These nuclei have thin membranes and the abundant chromatin, and the nucleoli are located down in the middle of

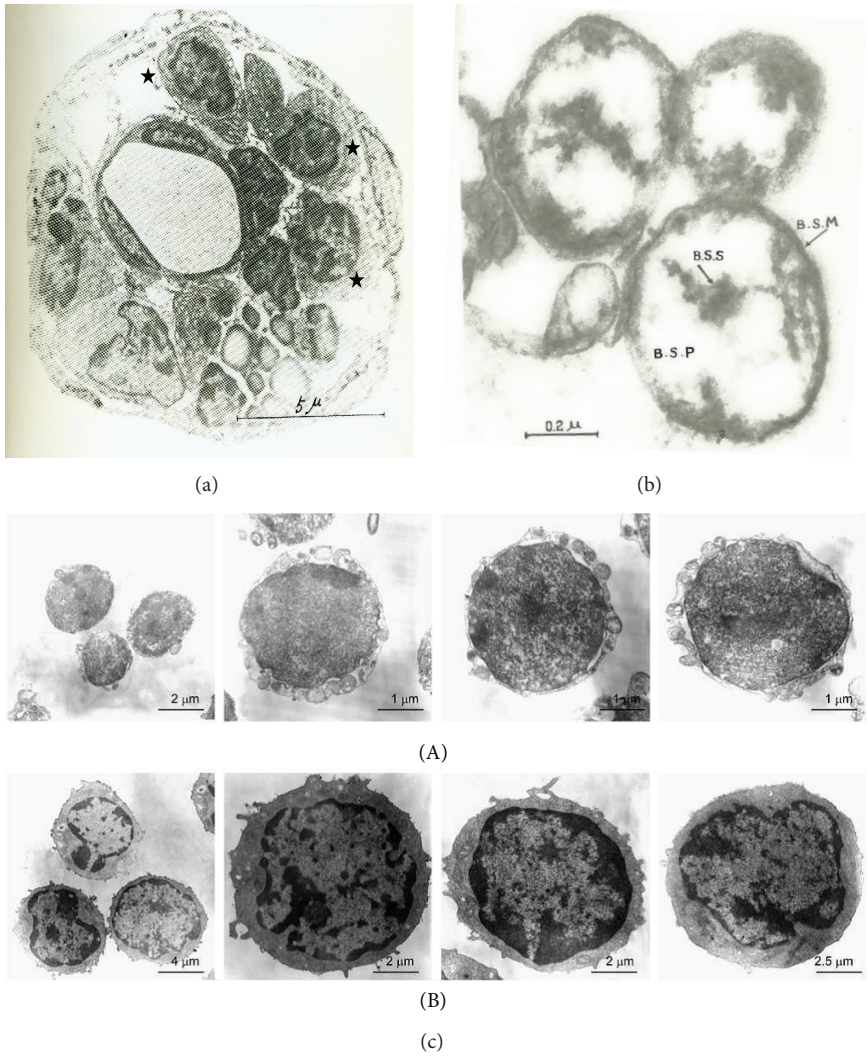

Figure 7: TEM micrographs of p-microcells, very small embryonic-like (VSEL), and hematopoietic stem cells. (a) External primo-node. Star: p-microcells. (b) P-microcells. BSS: p-microcell nucleosome, BSP: p-microcell nucleoplasm, and BSM: p-microcell membrane [7]. (c) TEM of very small embryonic-like (VSEL) cells and hematopoietic stem cells. (A) Small embryonic-like (VSEL) cells are small and measure 2–4 μm in diameter. They possess a relatively large nucleus surrounded by a narrow rim of cytoplasm. The narrow rim of cytoplasm possesses a few mitochondria, scattered ribosomes, small profiles of endoplasmic reticulum, and a few vesicles. The nucleus is contained within a nuclear envelope with nuclear pores. Chromatin is loosely packed and consists of euchromatin. (B) In contrast hematopoietic stem cells display heterogeneous morphology and are larger. They measure on average 8–10 μm in diameter and possess scattered chromatin and prominent nucleoli (reprinted by permission from Macmillan Publishers Ltd. leukemia [36], copyright, 2006).

the nuclei. The nuclear membrane occasionally is wrinkled. The boundary of the cell is smooth or occasionally has processes. In the cytoplasm, there are numerous vacuolar structures. The cytoplasm of some cells includes vesicular endoplasmic reticulum and many small round granules of high electron density. However, such granules cannot be noticed in the vacuoles. Mitochondria of an oblong shape are normally found in a part of the cytoplasm. Adjoining cells come close to each other or are linked to one another via small cytoplasmic processes [7].

Isolated p-microcells at a higher magnification are shown in Figure 7(b). Kim found that the p-microcell was normally round but often oval in shape. A normal p-microcell was 1.2–1.5 microns in size, while the smallest one was 0.8 micron and the largest one, which was not often observed, was 2.4 microns. P-microcell had a thin membrane of high density with very distinct contour. The nucleus took various forms. The p-microcell membrane was very dense and had a distinctive silhouette. Granules of various sizes and relatively high electron density were seen in the cytoplasm next to the p-microcell membrane. Figure 7(c) shows a TEM of very small embryonic-like (VSEL) cells and hematopoietic stem cells obtained by Kucia et al. from murine bone marrow by multiparameter sorting [36]. We noticed (Figure 7(c)) that very small embryonic-like (VSEL) cells as compared to hematopoietic stem cells were smaller in size (2–4 versus

8–10 μm). They contain relatively large nuclei and a narrow rim of cytoplasm. The authors hypothesized that this population of very small embryonic-like (VSEL) stem cells was deposited early during development in bone marrow and could be a source of pluripotent stem cells for tissue/organ regeneration. It should also be noticed that p-microcells are similar by morphology to these cells [36].

6.6.2. Composition. The biochemical properties of p-microcell were carefully analyzed by Kim. The p-microcells were found to contain 2.5×10^{-13} g of DNA, 1.2×10^{-13} g of RNA, and 1.7×10^{-12} g of protein. The molecular weight of DNA in p-microcell was estimated at 1.8×10^{6}–3.0×10^{6} KD. The most of DNA (99.8%) is in p-microcells. Kim suggested that p-microcells mature into cells within primo-vascular system [7].

6.6.3. Cell Culture, Cell Formation from p-Microcells. Kim developed a culture medium that mimics p-fluid by composition, physical, and biochemical properties. He was able to demonstrate the cultivation, proliferation, and fusion of p-microcells leading to the formation of cells in artificial conditions. The entire process was recorded by the time-lapsed photography. The process of the cell formation was described as being composed of the stage of proliferation and the stage of fusion. The p-microcells proliferate by the formation of numerous daughter cells arranged as clusters of cells. Then the p-microcells in the same cluster of cells fuse so that the nuclei of combined p-microcells coalesce into the nucleus of one relatively large cell. Meanwhile, their cytoplasm merges to produce the cytoplasm of a newly created large, mature p-microcell. We speculate that a large mature p-microcell is equivalent to multipotent stem cell. At given conditions, a large, mature p-microcell can be divided back into p-microcells. The number of p-microcells at the time of cell division is similar to the number of chromosomes [3, 7].

6.6.4. In Vitro Proliferation of p-Microcells. In order to observe and quantify *in vitro* proliferation of p-microcells, Kim obtained them from the internal primo-node of a rabbit and were cultivated for various lengths of time. The culture was studied under a phase contrast microscope, and the biochemical analyses of cells were also performed. It had been detected with the phase contrast microscope that initially nearly all the p-microcells were of 1.0–1.5 microns in size. Numerous daughter p-microcells were created from the mother p-microcell within 48 hours. After 72 hours, the multiplied p-microcells were fused into many clusters and, after 144 hours, a large number of cells were in the formation of cytoplasm stage. For the duration of the formation of mature p-microcells from daughter p-microcells, the content of DNA, RNA, and protein increased by factors 16, 9, and 32, respectively. The content of DNA increased rapidly from the start to 72 hours and later the increase was much slower. These data were compared with the morphological transformations detected by the phase contrast microscope. The biosynthesis of DNA occurred primarily within the phase of proliferation of mother p-microcell into daughter p-microcell and the synthesis of DNA barely takes place while p-microcells are fused to form a nucleus and then cytoplasm of mature p-microcells. Contents of protein and RNA, on the other hand, display a gradual increase after 72 hours of cultivation. These results correlate with the morphological findings on the formation of cytoplasm and growth of the mature p-microcell [3, 7]. Accepting the fact that one p-microcell carries one chromosome (see Section 7), we can estimate the frequency of proliferation and formation of new cells from p-microcells. The rabbit has 44 chromosomes and 88 DNA molecules in one adult cell [74]. Because DNA content increased 16 times during 6 days of p-microcell culture [7], the frequency of proliferation and forming of new cells from p-microcells is equal to $16/(88 \times 6) = 0.03$ or 3%. This value agrees well with the frequency of proliferation of the mice CNS progenitor cells into the multipotent CNS neurospheres that are found to be in a range of 1.5–3.3% [75]. The frequency of proliferation and cell forming found by Kim [7] is in a good agreement with the recently reported frequency of forming neurospheres from the p-microcells obtained from the mouse's intravascular primo-nodes and vessels [76]. The authors stated that they produced 176 spheres from 1000 cells per 7 days. These results make the sphere forming the frequency equal to $176/(1000 \times 7) = 0.025$ or 2.5%.

6.6.5. Distribution and Circulation of p-Microcells. P-microcells at different levels of maturity were identified only in the primo-vascular system: in the primo-vessels and primo-nodes. In order to examine distribution and circulation of p-microcells, P32-tagged microcells were utilized and traced by microautoradiography. P-microcells were removed from the superficial nodes, internal primo-vessels, and tissue cells. Tagged p-microcells were injected into the internal primo-vessels of organs and radioautography was used to trace the circulation course of primo-fluid and to the various tissues of internal organs [3, 7].

30 minutes following the injection, a few labelled mature p-microcells of 3-4 microns in size, spherical or oblong, were detected individually or grouped among the lung alveolar epithelial cells. Typically, p-microcells did not mature for up to 12 hours after the injection. However, they were proliferated and grown. In the alveolar epithelial cells, mature p-microcells and basophile, measuring 5-6 microns and which had no visible cytoplasm, were observed labelled in 24 hours following the injection of tagged p-microcells. 48 hours after the injection, alveolar epithelial cells of an almost matured state were found. They were just like the neighboring alveolar epithelial cells; their cytoplasm was quite revealing, and their nuclei were strongly stained with basic dyes. At this time, the tagged p-microcells at various phases of development could be identified [3, 7].

Similar results were obtained with injection of labeled p-microcells into other internal organs: liver, kidney, and ovary. 48 hours after injection, the labeled organ cells could be seen among the endogenous organ cells. These experimental results were completely validated by control experiments. When the suspension incorporating the same quantity of labelled p-microcells as in the PVS tests was injected into blood vessels, the obtained results were very different [3, 7].

In summarizing the labeled p-microcell experiments, Kim made the following conclusions: (1) P-microcells created in the internal organs move into the superficial primo-nodes and after some time return once again to the internal organs. The amount of DNA found in one young p-microcell is nearly equal to that contained in one chromosome. When an adult cell generates p-microcells, the number of p-microcells is equal to the number of chromosomes. (2) P-microcell injected into the superficial primo-node becomes larger and becomes a mature p-microcell on the way to various internal organs via primo-vessels. Then they move through intraorgan primo-vessels and grow into cells within the internal organs. Moreover, p-microcells injected into the superficial primo-node move to the external, intraexternal, and internal primo-nodes. (3) P-microcell of the superficial primo-node, when injected into the primo-vessel, grows into cells in the internal organs. These results mean that p-microcells produced in the organ cells are transported to the superficial primo-nodes through primo-vessels and after that onto the profound primo-nodes and that they form organ cells, passing through different intraorgan nodes [3, 7].

6.6.6. Potency of p-Microcells. It was clear to Kim that mature p-microcells are stem cells and the primo-nodes and vessels collect, harbor, mature, and distribute these cells. He exemplified this point in the description of the hematopoiesis in the internal primo-nodes, where the hemocytoblast, multipotent stem cell, gives rise to myeloid and lymphoid progenitors (see Section 6.5). Kim demonstrated that mixture of p-microcells taken from the superficial nodes, internal primo-vessels, and tissue cells could differentiate into tissue cells of various organs (see Section 6.6.5). However, what is the potency of individual p-microcells removed and cultured from various superficial primo-nodes? In answering this question, Kim was guided by the old and well-established knowledge in acupuncture showing that superficial primo-nodes (acupoints) in different locations possess particular associations with relevant internal organs. Therefore, different cells would be created from p-microcell extracted from different nodes. Kim cultivated 344 samples of the p-microcells taken from the superficial primo-nodes in 79 areas of the human body. As was anticipated, different cells were produced according to the location of those superficial primo-nodes. It means that the p-microcells created in the tissue cells of various organs move through the superficial primo-nodes linked with the internal organs. In PVS, the primo-fluid has many circulating channels, and each channel is linked with a different organ; however some organs may have connections with many circulating channels while some with fewer channels. It means that mature p-microcells taken from adult superficial primo-nodes can differentiate into a few different organ cells [3, 4, 7]. In this sense, they are playing a role of multipotent stem cells.

6.6.7. Regeneration of Injured Tissues. Regeneration of injured tissue was demonstrated with a normal liver of a rabbit that was injured with a glass 2 mm capillary tube, and histological samples were prepared at different time intervals. The regeneration of the injured liver was described to occur in a few phases as follows. (1) At 12 hours following the injury, inflammatory processes (i.e., hemorrhage, accumulation of leukocytes) occurred. The injured liver tissue progressively experienced changes in its stainability and became necrotic at the point of injury. (2) 24 hours after the injury, hemorrhage and buildup of leukocytes began to disappear slowly and karyolysis occurred in the necrosed cells with the injured cells and then disappear entirely. (3) Next, a cluster of mature p-microcells of 3–5 microns in size are detected surrounding the area of the injury. (4) The mature p-microcells assume round-like shapes. (5) Profoundly stainable cytoplasm took shape around the spherical nucleus of the mature p-microcells and (6) the cells developed further and grow to a size resembling normal liver cells [3, 7].

7. Chromosome Recycling

Dr. Kim described cell death as a part of the continuous "cell-*p-microcell* and *p-microcell*-cell" cycle. The steps in the cycle include the following: chromatin condensation and packaging into membrane-bound granules; deformation and rupture of nuclear membrane and granule release into the cytoplasm; and external membrane rupture that releases the granules to the outside. These granules preserve the parent cells' DNA and are subsequently used for generation of mature p-microcells (stem cells) [7]. That process, described by Kim, is almost identical to apoptotic cell death and the generation of apoptotic bodies with a major difference: apoptotic bodies are destroyed by phagocytic cells [77]. Important to note is that it was recently demonstrated that, under specific conditions, DNA can be transferred from one cell to another by phagocytosis of apoptotic bodies [78–80].

Kim's experiments on the adult cell conversion into a stem cell provoke a question of whether differentiated somatic cells can generate stem cells. Recent studies describe the reprogramming of terminally differentiated somatic cells to pluripotent stem cells by transducing adult cells with a limited set of defined transcription factors [81]. What is important and is mentioned a few times in Kim's publication is that the amount of DNA contained in one p-microcell is nearly equal to that contained in one chromosome [3, 7]. It is easy to verify that this statement is true by using experimental data presented in [7]. P-microcells were collected from primo-vessels and nodes of rabbit with a thin glass capillary driven by a micromanipulator. The content of DNA in one p-microcell was found to be $(2.6 \pm 0.6) \times 10^{-13}$ g. The molecular weight of DNA in p-microcells was $(2.4 \pm 0.6) \times 10^{9}$ D. Consequently, the concentration of DNA in one p-microcell is $2.6 \times 10^{-13}/2.4 \times 10^{9} \approx 1.1 \times 10^{-22}$ moles. Therefore, the number of DNA molecules in one p-microcell is $1.1 \times 10^{-22} \times 6 \times 10^{23} = 66 \pm 32$ molecules. The number of chromosomes in rabbit is 44 [74]. The number of DNA molecules per chromosomes is equal to 88. Assuming that Kim used about 10 (or less) samples for his measurements, one can say with 95% confidence that one p-microcell contains one chromosome. It is interesting to note that microcells, cytoplasmic fragments that contain micronuclei composed of one or a few chromosomes, can be generated directly from adult cells [82].

It will take considerable efforts to repeat and validate the "cell-*p-microcell* and *p-microcell*-cell" cycle that has been proven by Kim with very high confidence using a radioactive labeling [3, 7].

8. Future of the Primo-Vascular System

We strongly believe that complete characterization of the PVS will fully confirm the existence of this vast, distinct vascular system, which will soon create a new paradigm in biology and medicine. It will bring together western and eastern medical philosophies, provide an unlimited source of multipotent stem cells, and bring new diagnostic and therapeutic methods. The highest potential impact is expected in acupuncture [83, 84], osteopathic manipulative medicine [85, 86], pain management, developmental biology [87], tissue regeneration, organ reconstruction, diabetes, and cancer prevention and treatment [88].

9. Comment on Terminology

In Section 3 we showed that different parts of the primo-vascular system and the whole system have been described by different scientists under different names. It is very essential that all PVS researchers use the same terminology. It was an important step forward when a new unified terminology for primo-vascular system was proposed [10]. This nomenclature does not include any personal name and allows it to be used internationally without any reservations. This new terminology does not diminish the contribution of Bong Han Kim because his role is acknowledged practically in all PVS publications. Therefore, trying to introduce another new terminology to the same system and its components would only incur the confusion without giving any benefits to this new emerging field.

10. Conclusions

(1) According to Kim, an extensive vascular system, named as primo-vascular system, different from blood and lymphatic vascular system, exists in animals and human. The vascular cell system is distributed throughout the entire body, over and inside of various organs, inside and outside of the blood and lymphatic vessels, in the internal and the peripheral nervous system, and in the corium or in the subcutaneous layers of the skin. It is comprised of two structural elements: vessels and nodes. The vessel is a bundle of 1–20 subvessels of 3–25 μm in diameter laid into an external jacket.

(2) The primo-nodes have various shapes elements (round, oval, or multifaceted). They are of 0.1–1.6 mm in size. A vessel bundle of the incoming (afferent) vessels enter into the node, branch into additional bundles, and fill the node interior by tightly spun and folded bundles. Subvessels converge and exit from the node as efferent primo-vessels. The enlarged p-subvessels inside the node, which are called the sinuses of the node, harbor microcells, the progenitors of multipotent stem cells.

(3) A series of primo-nodes and vessels form a circulatory system that is composed of many circulatory channels. Each channel is linked with a different organ; however some organs may have connections with many circulating channels while some with fewer channels. The individual channel may begin with the superficial node; then, after being successively connected with a few profound nodes, it links with the intraorgan terminal node and then closes by the channel that comes back to the superficial node.

(4) A special fluid moves through the circulating channels and carries progenitors of multipotent stem cells (microcells), hormones, amino acids, lipids, sugars, proteins, and hyaluronic acid. Electrical signals are also shown to travel along these channels. The progenitor stem cells turn into multipotent stem cells within sinuses of the nodes. Being delivered to the internal organ, they differentiate into new organ-specific cells. In turn, the aged (or injured) organ cells are converted into microcells.

(5) Stimulating superficial nodes by acupuncture or osteopathic manipulative techniques results in sending electrical signals, hormones, and multipotent stem cells to a connected organ. These mediators support the organ stimulation and regeneration.

(6) The future characterization of the primo-vascular system will bring better understanding of the mechanisms and underlying techniques of acupuncture and osteopathic manipulative medicine. This knowledge will benefit pain management, developmental biology, tissue regeneration, organ reconstruction, diabetes, and cancer prevention and treatment.

Conflict of Interests

The authors declare that there is no conflict of interests regarding the publication of this paper.

Acknowledgments

The authors thank Mary Rudisill, David Pascoe, and Timothy Moore for critical reading of the paper. They are grateful to Kyung A. Kang and Kwang-Sup Soh for valuable comments. This work was supported by grants from the College of Veterinary Medicine, the School of Kinesiology of Auburn University, and Edward Via College of Osteopathic Medicine.

References

[1] B. H. Kim, "Study on the reality of acupuncture meridian," *Journal of Jo Sun Medicine*, vol. 9, pp. 5–13, 1962.

[2] B. H. Kim, "On the acupuncture meridian system," *Journal of Jo Sun Medicine*, vol. 90, pp. 6–35, 1963.

[3] B. H. Kim, "The Sanal theory," *Journal of Jo Sun Medicine*, vol. 108, pp. 39–62, 1965.

[4] B. H. Kim, "The Kyungrak system," *Journal of Jo Sun Medicine*, vol. 108, pp. 1–38, 1965.

[5] B. H. Kim, "Sanal and hematopoiesis," *Journal of Jo Sun Medicine*, vol. 108, pp. 1–6, 1965.

[6] B. H. Kim, *On the Kyungrak System*, Forein Language Publishing House, Pyongyang, North Korea, 1964, (available at the Duke University Libraries).

[7] B. H. Kim, *Kyungrak System and Sanal Theory*, Medical Literature, Medical Science Press, Pyongyang, North Korea, 1965, English version is availabe in Deutsche STAA, Bibliothen, Berlin.

[8] K. A. Kang, "Historical observations on the half-century freeze in research between the bonghan system and the primo vascular system," *Journal of Acupuncture and Meridian Studies*, vol. 6, no. 6, pp. 285–292, 2013.

[9] H.-G. Kim, "Unscientific judgment on the bong-han theory by an academic authority in the USSR," *Journal of Acupuncture and Meridian Studies*, vol. 6, no. 6, pp. 283–284, 2013.

[10] K.-S. Soh, K. A. Kang, and Y. H. Ryu, "50 years of Bong-Han theory and 10 years of primo vascular system," *Evidence-Based Complementary and Alternative Medicine*, vol. 2013, Article ID 587827, 12 pages, 2013.

[11] C. C. Schnorrenberger, "Morphological foundations of acupuncture: an anatomical nomenclature of acupuncture structures," *Acupuncture in Medicine*, vol. 14, no. 2, pp. 89–103, 1996.

[12] C. C. Schnorrenberger, "An interpretation of fundamental ideographs of Chinese medicine. Erroneous Western translations of basic Chinese medical characters reduce the significance of the German Gerac-studies ('Modellvorhaben')," *Schweizerische Zeitschrift für Ganzheitsmedizin*, vol. 17, no. 3, pp. 150–156, 2005.

[13] C. C. Schnorrenberger, "Anatomical roots of Chinese medicine and acupuncture," *Anatomie—Eine Historische Grundlage der Chinesischen Medizin und Akupunktur*, vol. 20, no. 3, pp. 163–171, 2008.

[14] H. Di, N. Jing, and S. Wen, *Simple Questions of the Inner Classic of the Yellow Emperor*, Publishing House of the People's Hygiene, Beijing, China, 1963.

[15] R. R. Rife, "Presenting a brief history of the evolution of the microscope," The Aerohrcrafter, Chula Vista, Calif, USA, Rohr Aircraft Corp, January 1954.

[16] L. Dorfer, M. Moser, F. Bahr et al., "A medical report from the stone age?" *The Lancet*, vol. 354, no. 9183, pp. 1023–1025, 1999.

[17] L. Dorfer, M. Moser, K. Spindler, F. Bahr, E. Egarter-Vigl, and G. Dohr, "5200-Year-old acupuncture in central Europe?" *Science*, vol. 282, no. 5387, pp. 242–243, 1998.

[18] T. J. Kaptchuk, *The Web That Has No Weaver: Understanding Chinese Medicine*, Congdon & Weed, New York, NY, USA, 1987.

[19] G. Macciocia, *The Foundations of Chinese Medicine*, Churchill Livingstone, London, UK, 1989.

[20] B. M. Carlson, *Human Embriology and Developmental Biology*, Mosby, Philadelphia, Pa, USA, 2004.

[21] I. Rusznyak, M. Foeldi, and G. Szabo, *Lymphatics and Lymph Circulation*, Pergamon Press, Oxford, UK, 1967.

[22] M. Skobe and M. Detmar, "Structure, function, and molecular control of the skin lymphatic system," *Journal of Investigative Dermatology Symposium Proceedings*, vol. 5, no. 1, pp. 14–19, 2000.

[23] L. Ranvier, "De quelques traits relatifs à l'histologie et à la physiologie des muscles stries," *Archives de Physiologie Normale et Pathologique*, vol. 6, pp. 1–15, 1874.

[24] F. Marchand, "Über Klasmatozyten, Mastzellen und Phagozyten des Netzes," *Verhandlungen der Deutschen Gesellschaft für Pathologie*, vol. 4, pp. 124–140, 1901.

[25] E. E. Goldman, "Die äußere und innere Sekretion des gesunden und kranken Organismus im Lichte der vitalen Färbung," *Beiträge zur Klinischen Chirurgie*, vol. 64, pp. 192–265, 1909.

[26] A. Maximow, "Der Lymphozyt als gemeinsame Stammzelle der verschiedenen Blutelemente in der embryonalen Entwicklung und im postfetalen Leben der Säugetiere," *Folia Haematologica*, vol. 8, pp. 125–134, 1908.

[27] A. Maximow, "Relation of blood cells to connective tissues and endothelium," *Physiological Reviews*, vol. 4, no. 4, pp. 533–563, 1924.

[28] B. H. Kim, *Great Discovery in Biology and Medicine, Substance of Kyungrak (National Library of Australia)*, Foreign Languages Publishing House, Pyongyang, Democratic Republic of Korea, 1962.

[29] B. H. Kim, "On the Kyungrak system," *Journal of the Academy of Medical Sciences of the Democratic People's Republic of Korea*, vol. 90, pp. 1–35, 1963.

[30] J.-C. Darras, P. De Vernejoul, and P. Albarede, "Nuclear medicine and acupuncture: a study on the migration of radioactive tracers after injection at acupoints," *American Journal of Acupuncture*, vol. 20, no. 3, pp. 245–256, 1992.

[31] J.-C. Darras, P. Albarede, and P. de Vernejoul, "Nuclear medicine investigation of transmission of acupuncture information," *Acupuncture in Medicine*, vol. 11, no. 1, pp. 22–28, 1993.

[32] W.-B. Zhang, Y.-Y. Tian, H. Li et al., "A discovery of low hydraulic resistance channel along meridians," *JAMS Journal of Acupuncture and Meridian Studies*, vol. 1, no. 1, pp. 20–28, 2008.

[33] R. O. Becker, M. Reichmanis, A. A. Marino, and J. A. Spadaro, "Electrophysiological correlates of acupuncture points and meridians," *Psychoenergetic Systems*, vol. 1, pp. 105–112, 1976.

[34] Z. Zhu, "Study on the morphological basis of physiological and biophysical characteristics of acupuncture meridian," *Acupuncture Research (Zhen ci yan jiu; Beijing, China)*, vol. 15, no. 4, pp. 296, 332–334, 1990.

[35] K.-P. Schlebusch, W. Maric-Oehler, and F.-A. Popp, "Biophotonics in the infrared spectral range reveal acupuncture meridian structure of the body," *The Journal of Alternative and Complementary Medicine*, vol. 11, no. 1, pp. 171–173, 2005.

[36] M. Kucia, R. Reca, F. R. Campbell et al., "A population of very small embryonic-like (VSEL) CXCR4$^+$ SSEA-1$^+$Oct-4$^+$ stem cells identified in adult bone marrow," *Leukemia*, vol. 20, no. 5, pp. 857–869, 2006.

[37] S. Biesterfeld, S. Beckers, M. D. C. V. Cadenas, and M. Schramm, "Feulgen staining remains the gold standard for precise DNA image cytometry," *Anticancer Research*, vol. 31, no. 1, pp. 53–58, 2011.

[38] P. Kjellstrand, "Mechanisms of the Feulgen acid hydrolysis," *Journal of Microscopy*, vol. 119, no. 3, pp. 391–396, 1980.

[39] N. A. Hillarp and B. Hokfelt, "Evidence of adrenaline and noradrenaline in separate adrenal medullary cells," *Acta Physiologica Scandinavica*, vol. 30, no. 1, pp. 55–68, 1953.

[40] L. R. Matz and S. L. Skinner, "Staining characteristics of chromaffin granules in human skin," *Nature*, vol. 194, no. 4828, pp. 585–586, 1962.

[41] G. E. Burch and J. H. Phillips Jr., "Chromaffin reacting cells in human digital skin," *Circulation Research*, vol. 6, no. 4, pp. 416–423, 1958.

[42] T. E. Damsgaard, A. B. Olesen, F. B. Sørensen, K. Thestrup-Pedersen, and P. O. Schiøtz, "Mast cells and atopic dermatitis. Stereological quantification of mast cells in atonic dermatitis and normal human skin," *Archives of Dermatological Research*, vol. 289, no. 5, pp. 256–260, 1997.

[43] E. Gurr, *Staining Practical and Theoretical*, Williams & Wilkins, Baltimore, Md, USA, 1962.

[44] H. J. Conn, *H.J. Conn's Biological Stains*, Williams & Wilkins, Baltimore, Md, USA, 1977.

[45] G. J. Murphy and A. D. Leavitt, "A model for studying megakaryocyte development and biology," *Proceedings of the National Academy of Sciences of the United States of America*, vol. 96, no. 6, pp. 3065–3070, 1999.

[46] L. C. de Lima Silveira and V. H. Perry, "A neurofibrillar staining method for retina and skin: a simple modification for improved staining and reliability," *Journal of Neuroscience Methods*, vol. 33, no. 1, pp. 11–21, 1990.

[47] N. Ishizaki, Y. Ishida, and Y. Kawakatsu, "Histological studies on the hypothalamic neurosecretory nucleus. VII. Histological findings of intracellular neurofibrils in the hypothalamic neurosecretory cell: contributions to the comparative histology of the hypothalamo-hyopphysial system. 42nd report," *Archivum Histologicum Japonicum*, vol. 18, no. 3, pp. 429–437, 1959.

[48] I. van Gieson, "Laboratory notes of technical methods for the nervous system," *New York Medical Journal*, vol. 50, pp. 57–60, 1889.

[49] F. H. Verhoeff, "Some new staining methods of wide applicability. Including a rapid differential stain for elastic tissue," *The Journal of the American Medical Association*, vol. 50, pp. 876–877, 1908.

[50] F. L. Carlson and C. Hladik, *Histotechnology: A Self-Instructional Text*, American Society for Clinical Pathology, Hong Kong, 2009.

[51] G. Morel, *Visualization of Nucleic Acids*, CRC Press, 1995.

[52] J. O. Lavarack, "Methyl green and pyronin staining of frozen-dried tissue," *Quarterly Journal of Microscopical Science*, vol. 96, no. 33, pp. 29–33, 1955.

[53] T. B. Feyerabend, H. Hausser, A. Tietz et al., "Loss of histochemical identity in mast cells lacking carboxypeptidase A," *Molecular and Cellular Biology*, vol. 25, no. 14, pp. 6199–6210, 2005.

[54] R. M. Williams and W. W. Webb, "Single granule pH cycling in antigen-induced mast cell secretion," *Journal of Cell Science*, vol. 113, no. 21, pp. 3839–3850, 2000.

[55] M. Gamble and I. Wilson, "The hematoxylins and eosin," in *Theory and Practice of Histological Techniques*, J. D. Bancroft and M. Gamble, Eds., Churchill Livingstone, Edinburgh, UK, 2002.

[56] H. Puchtler, F. Sweat, R. Bates, and J. H. Brown, "On the mechanism of resorcin-fuchsin staining," *The Journal of Histochemistry and Cytochemistry*, vol. 9, no. 5, pp. 553–559, 1961.

[57] Z. Darzynkiewicz, "Differential staining of DNA and RNA in intact cells and isolated cell nuclei with acridine orange," in *Methods in Cell Biology*, D. Zbigniew and A. C. Harry, Eds., chapter 27, pp. 285–298, Academic Press, New York, NY, USA, 1990.

[58] K. S. Fernández and P. A. de Alarcón, "Development of the hematopoietic system and disorders of hematopoiesis that present during infancy and early childhood," *Pediatric Clinics of North America*, vol. 60, no. 6, pp. 1273–1289, 2013.

[59] J. Domen, A. J. Wagers, and I. L. Weissman, "Bone marrow (hematopoietic) stem cells," in *Stem Cell Information [World Wide Web Site]*, National Institutes of Health, U.S. Department of Health and Human Services, Bethesda, Md, USA, 2011, http://stemcells.nih.gov/info/Regenerative_Medicine/pages/2006chapter2.aspx.

[60] C. P. McArthur, "Haematology of the New Zealand freshwater eels *Anguilla australis schmidtii* and *A. dieffenbachii*," *New Zealand Journal of Zoology*, vol. 4, no. 1, pp. 5–20, 1977.

[61] S. Ponsen, N.-A. Narkkong, and W. Angwanich, "Morphological and ultrastructural observations on the blood cells of sand lizards (*Leiolepis belliana* Rubritaeniata) Mertens 1961," *Journal of Animal and Veterinary Advances*, vol. 6, no. 4, pp. 522–527, 2007.

[62] S. Ponsen, N.-A. Narkkong, S. Pamok, and W. Aengwanich, "Comparative hematological values, morphometric and morphological observation of the blood cell in capture and culture Asian Eel, Monopterus albus (Zuiew)," *American Journal of Animal and Veterinary Sciences*, vol. 4, no. 2, pp. 32–36, 2009.

[63] E. L. Alpen, A. K. Davis, and E. M. Jackobsen, "Relative effectiveness of phenylhydrazine treatment and hemorrhage in the production of an erythropoietic factor," *Blood*, vol. 11, no. 10, pp. 937–945, 1956.

[64] C. T. Stone, T. H. Harris, and M. Bodansky, "The treatment of polycythemia vera: report of two cases," *Journal of the American Medical Association*, vol. 101, no. 7, pp. 495–498, 1933.

[65] K. A. Criswell, A. P. Sulkanen, A. F. Hochbaum, and M. R. Bleavins, "Effects of phenylhydrazine or phlebotomy on peripheral blood, bone marrow and erythropoietin in Wistar rats," *Journal of Applied Toxicology*, vol. 20, no. 1, pp. 25–34, 2000.

[66] R. E. Ploemacher and P. L. van Soest, "Morphological investigation on phenylhydrazine induced erythropoiesis in the adult mouse liver," *Cell and Tissue Research*, vol. 178, no. 4, pp. 435–461, 1977.

[67] J. E. Till and E. McCulloch, "A direct measurement of the radiation sensitivity of normal mouse bone marrow cells," *Radiation Research*, vol. 14, pp. 213–222, 1961.

[68] A. J. Becker, E. A. McCulloch, and J. E. Till, "Cytological demonstration of the clonal nature of spleen colonies derived from transplanted mouse marrow cells," *Nature*, vol. 197, no. 4866, pp. 452–454, 1963.

[69] R. G. Edwards, "Stem cells today: B1. Bone marrow stem cells," *Reproductive BioMedicine Online*, vol. 9, no. 5, pp. 541–583, 2004.

[70] A. Can, "Haematopoietic stem cells niches: interrelations between structure and function," *Transfusion and Apheresis Science*, vol. 38, no. 3, pp. 261–268, 2008.

[71] M.-S. Kim, J.-Y. Hong, S. Hong et al., "Bong-Han corpuscles as possible stem cell niches on the organ-surfaces," *Journal of Pharmacopuncture*, vol. 11, no. 1, pp. 5–12, 2008.

[72] B.-C. Lee, K.-H. Bae, G.-J. Jhon, and K.-S. Soh, "Bonghan system as mesenchymal stem cell niches and pathways of macrophages in adipose tissues," *Journal of Acupuncture and Meridian Studies*, vol. 2, no. 1, pp. 79–82, 2009.

[73] E. S. Park, J. H. Lee, W. J. Kim, J. Heo, D. M. Shin, and C. H. Leem, "Expression of stem cell markers in primo vessel of rat," *Evidence-Based Complementary and Alternative Medicine*, vol. 2013, Article ID 438079, 6 pages, 2013.

[74] T. S. Painter, "Studies in mammalian spermatogenesis VI. The chromosomes of the rabbit," *Journal of Morphology*, vol. 43, no. 1, pp. 1–43, 1926.

[75] A. V. Molofsky, R. Pardal, T. Iwashita, I.-K. Park, M. F. Clarke, and S. J. Morrison, "Bmi-1 dependence distinguishes neural stem cell self-renewal from progenitor proliferation," *Nature*, vol. 425, no. 6961, pp. 962–967, 2003.

[76] S. J. Lee, S. H. Park, Y. I. Kim et al., "Adult stem cells from the hyaluronic acid-rich node and duct system differentiate into neuronal cells and repair brain injury," *Stem Cells and Development*, vol. 23, no. 23, pp. 2831–2840, 2014.

[77] D. R. Schultz and W. J. Harrington, "Apoptosis: programmed cell death at a molecular level," *Seminars in Arthritis and Rheumatism*, vol. 32, no. 6, pp. 345–369, 2003.

[78] A. Bergsmedh, A. Szeles, M. Henriksson et al., "Horizontal transfer of oncogenes by uptake of apoptotic bodies," *Proceedings of the National Academy of Sciences of the United States of America*, vol. 98, no. 11, pp. 6407–6411, 2001.

[79] J. Ehnfors, M. Kost-Alimova, N. L. Persson et al., "Horizontal transfer of tumor DNA to endothelial cells in vivo," *Cell Death and Differentiation*, vol. 16, no. 5, pp. 749–757, 2009.

[80] L. Holmgren, A. Szeles, E. Rajnavölgyi et al., "Horizontal transfer of DNA by the uptake of apoptotic bodies," *Blood*, vol. 93, no. 11, pp. 3956–3963, 1999.

[81] W. Scheper and S. Copray, "The molecular mechanism of induced pluripotency: a two-stage switch," *Stem Cell Reviews and Reports*, vol. 5, no. 3, pp. 204–223, 2009.

[82] R. van Wijk, K.-S. Soh, and E. P. A. van Wijk, "Anatomic characterization of acupuncture system and ultra-weak photon emission," *Asian Journal of Physics*, vol. 16, no. 4, pp. 443–474, 2007.

[83] NIN Consensus Development Panel on Acupuncture, "NIH consensus conference. Acupuncture," *The Journal of the American Medical Association*, vol. 280, no. 17, pp. 1518–1524, 1998.

[84] K.-S. Soh, "Bonghan circulatory system as an extension of acupuncture meridians," *Journal of Acupuncture and Meridian Studies*, vol. 2, no. 2, pp. 93–106, 2009.

[85] K. Washington, R. Mosiello, M. Venditto et al., "Presence of Chapman reflex points in hospitalized patients with pneumonia," *Journal of the American Osteopathic Association*, vol. 103, no. 10, pp. 479–483, 2003.

[86] B. J. Chikly, "Manual techniques addressing the lymphatic system: origins and development," *Journal of the American Osteopathic Association*, vol. 105, no. 10, pp. 457–464, 2005.

[87] B.-H. Kim, "Developmental and comparative biological study of primo vascular system," *JAMS Journal of Acupuncture and Meridian Studies*, vol. 5, no. 5, pp. 248–255, 2012.

[88] K. S. Soh, K. A. Kang, and D. K. Harrison, *The Primo Vascular System: Its Role in Cancer and Regeneration*, Springer Science+Business Media LLC, New York, NY, USA, 2012.

Hindawi Publishing Corporation
Evidence-Based Complementary and Alternative Medicine
Volume 2015, Article ID 303769, 6 pages
http://dx.doi.org/10.1155/2015/303769

Review Article

Fascia and Primo Vascular System

Chun Yang,[1,2] Yi-kuan Du,[3] Jian-bin Wu,[3] Jun Wang,[2] Ping Luan,[2] Qin-lao Yang,[1] and Lin Yuan[2,3]

[1]*Key Laboratory of Optoelectronic Devices and Systems of Ministry of Education and Guangdong Province, College of Optoelectronic Engineering, Shenzhen University, Shenzhen 518060, China*
[2]*School of Medicine, Shenzhen University, Shenzhen 518052, China*
[3]*Department of Anatomy, Southern Medical University, Guangzhou 510515, China*

Correspondence should be addressed to Jun Wang; yxywj@szu.edu.cn and Lin Yuan; yuanl@fimmu.com

Received 1 October 2014; Revised 5 December 2014; Accepted 21 January 2015

Academic Editor: Kwang-Sup Soh

The anatomical basis for the concept of acupuncture points/meridians in traditional Chinese medicine (TCM) has not been resolved. This paper reviews the fascia research progress and the relationship among acupuncture points/meridians, primo vascular system (PVS), and fascia. Fascia is as a covering, with common origins of layers of the fascial system despite diverse names for individual parts. Fascia assists gliding and fluid flow and holds memory and is highly innervated. Fascia is intimately involved with nourishment of all cells of the body, including those of disease and cancer. The human body's fascia network may be the physical substrate represented by the meridians of TCM. The PVS is a newly found circulatory system; recent increased interest has led to new research and new discoveries in the anatomical and functional aspects of the PVS. The fasciology theory provides new insights into the physiological effects of acupuncture needling on basic cellular mechanisms including connective tissue mechanotransduction and regeneration. This view represents a theoretical basis and means for applying modern biomedical research to examining TCM principles and therapies, and it favors a holistic approach to diagnosis and treatment.

1. Introduction

Fascia is connective tissue that surrounds and connects every muscle and organ, forming continuity throughout the body. Traditionally, fascia has been thought of as a passive structure. However, it is now evident that fascia is a dynamic tissue with complex vasculature and innervation [1]. A definition of fascia, especially as an integral tissue has been provided here, highlighting the main features of the superficial fascia [2]. Wide anatomic variations and site-specific differences in fascial structure are described, coupled with results of our extensive investigations of fascia anatomy [3]. The anatomy of the fascia network in human body, as demonstrated through the virtual Chinese human (VCH) research and living body imaging studies, is consistent with the traditional view of the meridians, and the efficacy of acupuncture has been shown to rely on interactions with the fascia [4]. Additionally, it appears that the fascia mediates an active mechanical transference role as it provides dynamic connections between and among the muscles and bones. Moreover, the phenomenon of neurogenic inflammation triggered by stimulation of nociceptive receptors [5] in fascia tissues is consistent with the notion that disruption of fascia physiology can have notable consequences on human health. Indeed, it is our view that neurogenic inflammation in fasciae may constitute a form of disruption of meridian energy flow in traditional Chinese medicine (TCM). Since the first report on the primo vascular system (PVS) by Dr. Bong-Han Kim in 1962, there has been significant progress in this research. The PVS is considered as a newly found circulatory system, which is independent of the blood or lymphatic systems. Identification, harvesting, and characterization of the PVS have been a major challenge due to its small size and transparent optical properties. Over the last decade PVS has attracted interest among researchers both

anatomically and histologically. However, it is still unclear what functions primo tissues do.

2. Fascia

Fascia is an uninterrupted viscoelastic tissue which forms a functional 3-dimensional collagen matrix [6] and surrounds and connects every muscle and organ, forming continuity throughout the body [7]. It surrounds and penetrates all structures of the body extending from head to toe, thus making it difficult to isolate and develop its nomenclature. Fascia is considered to be any dense irregular connective tissue sheet in the human body, including aponeuroses, joint capsules, or muscular envelopes such as the endo-, peri-, and epimysium. The epimysium surrounds each muscle and is continuous with tendons that attach muscles to bones. The perimysium divides the muscle into fascicles or muscle fiber bundles. The endomysium is a continuous network of connective tissue that covers individual muscle fibers. Small fascial fibers extend to connect to the cell membrane itself.

Fascia is innervated, mostly by proprioceptive nerves. It is intimately involved with the autonomic nervous system as a sensory, target organ [8]. Both myelinated and unmyelinated fibers in fascia were probably of autonomic origin. The outer layers of the limb deep fascia contained a rich vascular and nerve supply with intrafascial nerve fibers throughout the deep fascia. Some researchers also observed Ruffini and Pacini corpuscles, confirming the earlier findings of Yahia et al. in relation to the lumbodorsal fascia. There were also small nerves oriented perpendicularly and attached to the collagen fibers, which presumed to be stretch receptors. And some small nerves displayed morphological characteristics of autonomic nerves.

Fascia is also capable of transmitting electrical signals throughout the body [9]. Collagen, which is one of the main components of fascia, has been shown to have semiconductive, piezoelectric, and photoconductive properties in vitro. Electronic currents could flow over greater distances. These electronic currents within fascia can be altered by external influences and cause a physiologic response in neighboring structures.

All living cells express some inherent contractility by generating tension within their internal cytoskeleton [10]. Fascia also plays a dynamic role in transmitting mechanical tension and may be able to contract in a smooth muscle like manner [9]. Human lumbar fascia can autonomously contract, hypothesized to be due to the presence of contractile cells within fascia. Fibroblasts, which were contained in fascia, can transform into myofibroblasts, express a gene for alpha-smooth muscle actin, and display contractile behavior. The mechanical forces exerted by these cells regulate cytokine synthesis and production of extracellular matrix components and other processes essential to tissue remodeling [11, 12].

Fascia forms a whole-body continuous matrix that interpenetrates and surrounds all organs, muscles, bones, and nerve fibers. It could be considered as a single organ, a unified whole, connection to every aspect of human physiology [13].

3. Primo Vascular System

The primo vascular system (PVS) was first reported by Bong-Han Kim in the early 1960s, which is a third vascular compartment in addition to the blood and lymphatic systems. The PVS is optically semitransparent, including several subsystems such as Bonghan corpuscles and Bonghan ducts. The structure was also found by Fujiwara's follow-up. Unfortunately, shortly after Kim's reports in 1960s, the PVS research was suddenly discontinued for the method was not disclosed and the experiments were hard to reproduce. In the 2000s, the research was reinitiated. There have been numerous descriptions of the primo vascular system which is comprised of primo nodes (PN) and primo vessels (PV).

Some researchers also have found primo tissues on the surface of the internal organs of various animals such as mice, rats, rabbits, dogs, swine, and cow, including intestine, cardiac vascular vessels, brain [14, 15], adipose tissue [16], inside the blood [17] and lymphatic vessels, epineurium, running along the sciatic nerve, and below the skin. Lee reported on the observation of a human PVS on both the epithelial fascia and inside the blood vessels of the umbilical cord [18]. The PVS has been distinguished from other similar-looking lymphatic vessels and vascular systems by immunostaining [19]. These findings have led them to consider primo vascular system another circulating system [20]. Moreover, Soh claimed that primo nodes and primo vessels were related to acupuncture points and primo vascular system might be an extension of meridians. PVS exists in most mammalian organs, forming an extensive network throughout the entire body. It is considered as the anatomical basis of classical acupuncture meridians.

In order to confirm the structure of PVS, a lot of labs in Korea, China, and USA tried to repeat the labeling methods of PVS provided by Soh. PVS in enterocelia were identified and stained by dropping 0.2% diluted Trypan blue solution. But PVS cannot be found in all the subjects by the staining method. The percentage of celiac PVS emergence was related to a lot of factors such as age and method of anesthesia. This indicated that the PVS may be related to a pathological process. In conclusion, the emergence of PVS could be affected by age and urethane injection methods. So PVS may not be an intrinsic structure of the body and may be a pathological product which is related to the process of inflammation.

As reported, PVS is also associated with tumor. A cancerous environment triggers cancer PVS formation. And it exists not only in and around tumors [21] but also within the tumors. Islam [22] had provided strong evidence of the existence of a tumor-derived PVS in and around the fascia of tumor xenografts. They all appear to be parallel to their associated neurovascular bundles. Tumor-associated PVS harbors a unique population of tumor-derived cells which express high levels of stem cell specific transcription factors. PVS may play an important role as a stem cell "niche." In addition, it was shown that PVS connect the primary and secondary tumors and that cancer cells were transported via the PVS in an active manner [23]. It has been suggested that the PVS might contribute to tumor growth and metastasis

[21]. PVS may also be a unique "niche" for cancer stem cells. The locations of the PVS floating in fluid are not fixed, and those fixed-location PVS like intraorgan PVS are not yet observed. The origin of the primo vessels and nodes associated with xenografted tumor is the host animal, but cells like the histiocytes in the primo node are from the tumor.

In 2000s, Park first started to measure resting and spontaneous potentials in primo node. More researchers have studied PVS electrophysiological characteristics after this study, and they have found bioelectrical signals from primo vessels and lymphatic vessels were different. The small intestine and lymphatic vessels generate an action potential to transfer materials. Neuron spikes are generated when neurons exchange electrical signals. PVS perform different functions in smooth muscles and neurons. The researchers speculate that PVS transfer signals in distinct manners for neurons and do not directly move materials, such as through the small intestine and lymphatic vessels. PVS was considered the substances in acupoints and meridians.

So far, the specific function of PVS in biological processes remains unclear. As reported, the structure of the PVS is distinct from the well-known tissues such as nerves and blood vessels and may be related to acupuncture meridian and the acupuncture points of TCM. The PVs in surface of internal organs did not have an effect in regulating gastric motility induced by acupuncturing at CV12 nor in the facilitation of gastric motility induced by acupuncturing at ST36. The results are valid for the subclass of PVS on the surface of internal organs (OS-PVS). There is a complicated network of five subclasses of PVS, and the most important ones with respect to the intestinal motility are those along blood vessels and nerves as implied in Kim's work. The OS-PVS is deeply related to stem cell like functions and immune functions. It is timely that functional aspects of the PVS are to be studied with respect to both Western and Eastern medicines.

4. Fasciology

According to Professor Lin Yuan, there are close relations of the meridians and acupoints to connective tissues. Under the VCH project, we marked the regions rich in connective tissues on the tomographic images for three-dimensional (3D) reconstruction of the whole-body fascia framework, and the established digital model showed an approximate match with the distribution of the meridian and acupoints. The acupoints were found to locate mainly at the sites with enrichment of certain connective tissues, such as the muscular septa of the limbs, structures with abundant somatic nerve endings, the internal organs with rich sensory nerve distribution, and the visceral mesenteries [24, 25]. All the marked fascia in the body constituted a complete body-shaped framework, and we therefore hypothesized that the fascia network was the anatomical basis of the meridians.

To explore the theoretical support of our hypothesis, Professor Lin Yuan examined developmental biology, the developmental process of an individual embryo, and the evolution of fascia. The fascia network was derived from the residual mesenchyme after it had differentiated into different organs or systems. The extracellular matrix of a single germ layer organism, the mesogloea of a two-germ-layer organism, the mesenchyme of a three-germ-layer organism, and the nonspecific connective tissue of the human body are all homologous structures. The nonspecific connective tissue network in the human body provides cell storage and maintains the stability of the internal environment by cell proliferation, differentiation, repair, and regeneration. We therefore established a new anatomical approach from a dynamic point of view and proposed the two-system theory. In light of this theory, the human body can be divided into two systems. One is the supporting-storing system, consisting of undifferentiated nonspecific connective tissue. The other is the functional system, consisting of various differentiated functional cells. Based on this theory, we can further explore a new research area, fasciology [2]. The term fasciology indicates a biomedical orientation of the TCM theory. According to fasciology, from the axis in the absence of biological life in Darwin's theory of evolution to the Yellow Emperor's understanding of the life axis, we transform the present biomedical research in the two-dimensional coordinates into more complex three-dimensional coordinates.

4.1. Two-System Theory. In the two-system theory, the supporting-storing system consists of undifferentiated cells in unspecialized connective tissues, and the functional system contains diverse differentiated functional cells supported or surrounded by the supporting-storing system. The undifferentiated stem cells in the supporting-storing system constantly differentiate into functional cells. The supporting-storing system throughout the body regulates the functionality and life activities of the differentiated cells and provides a stable environment for their survival. In this context, we put forward a new approach to the division of the discipline anatomy. The anatomical discipline based on the two-system theory is fascial anatomy and studies the human body in light of how organisms survive with a longer life cycle, which is different from regional anatomy study that examines anatomical structures and systematic anatomy that study the functions.

4.2. Fascial Anatomy. Fascial anatomy is a new perspective on anatomy. It classifies body structures into the supporting-storing system and the traditional functional system. This perspective is also applicable to all the living organisms, from a primitive unicellular organism to a higher mammal. It studies the morphological transformation during evolution from simple to complex organisms. It also investigates how an organism maintains a longer life span through the evolution of the supporting-storing system.

Fascia anatomy studies the structure of an organism based on the two-system theory. Fascia anatomy is different from traditional regional anatomy and systematic anatomy. Regional anatomy only studies local human structures and systematic anatomy studies the human body on both a morphological and functional basis. Fascial anatomy incorporates a third parameter, time, to study not only the structures and functions of the body but also the morphological transformation during evolution and embryonic development. It investigates how an organism, such as a primate, can maintain

a longer life span through evolution of the supporting-storing system from the mesoderm. Therefore, fascia anatomy helps scientists better understand the biological essence of an organism by reminding them to study anatomy in a dynamic perspective; that is, all cells and organs maintain their normal structures and functions through the interaction between the supporting-storing system and the functional system.

In other words, fascial anatomy switches anatomical study from the "dead" to the "living." When the supporting-storing system wears out, the body will die. When the wax is depleted, the flame will extinguish, as with the human body.

5. The Relationship between Meridians and Fascia

The theory of meridians and collaterals is a fundamental pillar of TCM, particularly in the areas of acupuncture, moxibustion, and massage, as well as of traditional martial arts such as Tai Chi Chuan. Meridians are essentially strings of acupoints, which may be visualized as passageways through which energy flows throughout the body. The anatomical basis of acupuncture stimulation is the fascia (like intermuscular septum and intermuscular space), which can generate strong biological information upon rotation of the needles [26]. There is only a quantitative, but not qualitative, difference between the acupoints and nonacupoints in the biological information they produce [27]. Similarly, the Chinese herbal medicine regulates the regeneration and activity of the functional cells by improving the microcirculation and permeability of epithelial basement membrane in the fascia.

Fascia has specific cells, ground substance, and fiber types that make it a form of connective tissue proper. A better understanding of fascia at the cellular level gives insight into its functional properties. The cells within fascia include fibrocytes (fibroblasts, myofibroblasts), adipocytes, and various migrating white blood cells [28]. The fascia network of collagen and ground substance is maintained by fibrocytes. Fibrocytes regulate interstitial fluid volume and pressure as well as the extracellular molecular components [6]. It also responds to mechanical stretch through mechanotransduction. Langevin verified the mechanism of mechanotransduction in vivo that applied mechanical stress induces a change in cell morphology. Barnes notes that when performing myofascial release the response is felt in 90–120 s, and therefore any matrix adaptations initiated by a change in mechanical stress apparently take too long to occur to explain the observed immediate benefits of mechanical therapies. Fibrocytes may further transform themselves into myofibroblasts through this mechanical tension, as observed in wound healing [29]. However, myofibroblasts also appear to be a normal component of fascia and importantly they are also observed additionally in epimysium and perimysium. The contractile nature of these cells appears to give them ability to alter tissue tension, through contraction and relaxation, in the short timescales observed in practice.

Steven Finando reconsiders acupuncture, positing that the fascia is the mechanism of action of acupuncture therapy. The fascia has also been conceived as a complex communication network that influences and is influenced by every muscle, organ, blood vessel and nerve. Langevin suggests the fascia to be a metasystem, connecting and influencing all other systems. Incorporating this view would change our core understanding of human physiology. The cytoskeleton of fascia cellular under continuous tension is capable of transmitting mechanical forces through the fascia system. Forces applied to the cytoskeleton can produce biochemical changes on the cellular level by mechanochemical transduction [30]. Guimberteau demonstrates the complex fractal structure of the tissue and how it allows for movement, adaptation, lubrication, and repair. The fascia as our richest sensory organ permeated with four types of sensory receptors. The vascular, nervous, and lymphatic systems all end in the ground substance, providing nutrients to the ground substance as well as information from the periphery. It is both interesting and highly significant to note that acupuncture is based upon the conception of a metasystem that links and influences every aspect of human physiology. The fascia system provides the anatomical basis of that metasystem.

Acupuncture needle manipulation causes mechanical deformation of connective tissue, which in turn results in mechanical stimulation of fibroblasts, with active changes in cell shape and autocrine purinergic signaling [31]. The biomechanical behavior of connective tissue in response to stretching is generally attributed to the molecular composition and organization of its extracellular matrix. It also is becoming apparent that fibroblasts play an active role in regulating connective tissue tension. In response to static stretching of the tissue, fibroblasts expand within minutes by actively remodeling their cytoskeleton. This dynamic change in fibroblast shape contributes to the drop in tissue tension that occurs during viscoelastic relaxation.

The PVS is a novel circulatory system forming a network throughout an animal's body. Bong-Han Kim identified the novel anatomical vessels as meridian primo vessels and proposed that their distribution mirrored acupuncture meridians. According to Dr. Soh's observation, the histological structures of PVS and PN are abundant collagen fibers and elastic fibers. These fibrillar materials are composed of thread-like structures suggestive of collagen and/or elastic fibers. Because of the abundant connective tissue fibers, it could explain why excised vessels and nodes are very elastic in nature and have a tendency to coil spontaneously [32]. The connective tissue is the carrier of the mechanical stimulation induced by acupuncture. According to Professor Kim's conception, all the nuclei of tissue cells are connected with fine terminal subducts, which are connected to the primo vessels for the organs. Acupuncture may regulate organs' function by simulating exterior PVS and PNs through the exterior tissue cells. As reported, fibroblasts and leukocytes might be two kinds of cell types in PVS for both of infected and untreated rats [22]. The suggested functions of the PVS, in general, include a path for neurotransmitter hormones, a circulatory path for primo fluid-containing stem cell like microcells, and proteins related to stem cell differentiation. Evidence also exists for cancer metastasis through the primo vessel. Moreover, PNs and PVS were related to acupuncture points and primo vascular system might be an extension of meridians. Only by establishing the functional connection of

the exterior-interior PVS between the stimulus of acupoints and responses of organs could PVS be a basis for meridians. Thus, a comparison between acupuncture meridians and PVS leaves nothing rigorous but a mist. The data demonstrate that PVS is a novel and distinctive structure, but the criteria of it are still needed to develop. We pay more attention to the function of PVS related to meridians. The study with PVS on the organ surface showed that they are not involved with acupuncture stimulations, and further studies with skin PVS and extra PVS are required to find out the functional relation with acupuncture.

The PVS is thought to originate from fascia connective tissue and be developmentally mesodermal in origin. The PVS is an anatomical structure corresponding to the acupuncture meridians and the acupuncture points of TCM. Meridians have been considered as a part of fascia and the "fasciology" theory used to explain the physiology of acupuncture in general. But the function of the PVS with respect to nerve regeneration and acupuncture is not yet studied. With the deep research of the fasciology and PVS, there will be a bright future of the TCM research.

Conflict of Interests

All authors declare that there is no conflict of interests regarding the publication of this paper.

Authors' Contribution

Chun Yang and Yi-kuan Du contributed to the work equally and should be regarded as co-first authors. Jun Wang and Lin Yuan contributed to the work equally and should be regarded as co-corresponding authors.

References

[1] J. Tesarz, U. Hoheisel, B. Wiedenhöfer, and S. Mense, "Sensory innervation of the thoracolumbar fascia in rats and humans," *Neuroscience*, vol. 194, pp. 302–308, 2011.

[2] C. Yang, J. Dai, and L. Yuan, "Two-system theory and fasciology," *The FASEB Journal*, vol. 26, no. 1, pp. 721–722, 2012.

[3] C. Stecco, C. Tiengo, A. Stecco et al., "Fascia redefined: anatomical features and technical relevance in fascial flap surgery," *Surgical and Radiologic Anatomy*, vol. 35, no. 5, pp. 369–376, 2013.

[4] Y. Bai, J. Wang, J.-P. Wu et al., "Review of evidence suggesting that the fascia network could be the anatomical basis for acupoints and meridians in the human body," *Evidence-Based Complementary and Alternative Medicine*, vol. 2011, Article ID 260510, 6 pages, 2011.

[5] S. Deising, B. Weinkauf, J. Blunk, O. Obreja, M. Schmelz, and R. Rukwied, "NGF-evoked sensitization of muscle fascia nociceptors in humans," *Pain*, vol. 153, no. 8, pp. 1673–1679, 2012.

[6] T. W. Findley, "Fascia research from a clinician/scientist's perspective," *International Journal of Therapeutic Massage & Bodywork*, vol. 4, no. 4, pp. 1–6, 2011.

[7] E. H. Kwong and T. W. Findley, "Fascia—current knowledge and future directions in physiatry: narrative review," *Journal of Rehabilitation Research and Development*, vol. 51, no. 6, pp. 875–884, 2014.

[8] J. Tesarz, U. Hoheisel, B. Wiedenhöfer, and S. Mense, "Sensory innervation of the thoracolumbar fascia in rats and humans," *Neuroscience*, vol. 194, pp. 302–308, 2011.

[9] T. W. Findley and M. Shalwala, "Fascia research congress evidence from the 100 year perspective of Andrew Taylor still," *Journal of Bodywork and Movement Therapies*, vol. 17, no. 3, pp. 356–364, 2013.

[10] R. Schleip, W. Klingler, and F. Lehmann-Horn, "Active fascial contractility: fascia may be able to contract in a smooth muscle-like manner and thereby influence musculoskeletal dynamics," *Medical Hypotheses*, vol. 65, no. 2, pp. 273–277, 2005.

[11] R. D. Abbott, C. Koptiuch, J. C. Iatridis, A. K. Howe, G. J. Badger, and H. M. Langevin, "Stress and matrix-responsive cytoskeletal remodeling in fibroblasts," *Journal of Cellular Physiology*, vol. 228, no. 1, pp. 50–57, 2013.

[12] H. M. Langevin, K. N. Storch, R. R. Snapp et al., "Tissue stretch induces nuclear remodeling in connective tissue fibroblasts," *Histochemistry and Cell Biology*, vol. 133, no. 4, pp. 405–415, 2010.

[13] S. Finando and D. Finando, "Fascia and the mechanism of acupuncture," *Journal of Bodywork and Movement Therapies*, vol. 15, no. 2, pp. 168–176, 2011.

[14] H.-S. Lee, W.-H. Park, A.-R. Je, H.-S. Kweon, and B.-C. Lee, "Evidence for novel structures (primo vessels and primo nodes) floating in the venous sinuses of rat brains," *Neuroscience Letters*, vol. 522, no. 2, pp. 98–102, 2012.

[15] J. Lim, J. H. Jung, S. Lee et al., "Estimating the density of fluorescent nanoparticles in the primo vessels in the fourth ventricle and the spinal cord of a rat," *Journal of Biomedical Optics*, vol. 16, no. 11, Article ID 116010, 2011.

[16] B.-C. Lee, K.-H. Bae, G.-J. Jhon, and K.-S. Soh, "Bonghan system as mesenchymal stem cell niches and pathways of macrophages in adipose tissues," *Journal of Acupuncture and Meridian Studies*, vol. 2, no. 1, pp. 79–82, 2009.

[17] J. S. Yoo, M. S. Kim, V. Ogay, and K.-S. Soh, "In vivo visualization of Bonghan ducts inside blood vessels of mice by using an Alcian blue staining method," *Indian Journal of Experimental Biology*, vol. 46, no. 5, pp. 336–339, 2008.

[18] B. Lee, J. E. Park, H. Choi, S. Choi, and K. Soh, "Primo vascular system in human umbilical cord and placenta," *Journal of Acupuncture and Meridian Studies*, vol. 7, no. 6, pp. 291–297, 2014.

[19] J. S. Yoo, M. Hossein Ayati, H. B. Kim, W.-B. Zhang, and K.-S. Soh, "Characterization of the primo-vascular system in the abdominal cavity of lung cancer mouse model and its differences from the lymphatic system," *PLoS ONE*, vol. 5, no. 4, Article ID e9940, 2010.

[20] M. Hong, S. S. Park, H. Do, G. J. Jhon, M. Suh, and Y. Lee, "Study of the primo-vascular system and location-dependent oxygen levels for a mouse embryo," *Journal of Nanoscience and Nanotechnology*, vol. 12, no. 7, pp. 5168–5172, 2012.

[21] J. S. Yoo, H. B. Kim, N. Won et al., "Evidence for an additional metastatic route: In vivo imaging of cancer cells in the primo-vascular system around tumors and organs," *Molecular Imaging and Biology*, vol. 13, no. 3, pp. 471–480, 2011.

[22] M. A. Islam, S. D. Thomas, S. Slone, H. Alatassi, and D. M. Miller, "Tumor-associated primo vascular system is derived from xenograft, not host," *Experimental and Molecular Pathology*, vol. 94, no. 1, pp. 84–90, 2013.

[23] K. A. Kang, C. Maldonado, G. Perez-Aradia, P. An, and K.-S. Soh, "Primo vascular system and its potential role in cancer

metastasis," *Advances in Experimental Medicine and Biology*, vol. 789, pp. 289–296, 2013.

[24] Y. Huang, L. Yuan, Z. Q. He, and C. L. Wang, "Study on the meridians and acupoints based on fasciaology: an elicitation of the study on digital human being," *Zhongguo Zhen Jiu*, vol. 26, no. 11, pp. 785–788, 2006.

[25] J. Wang, C.-L. Wang, B.-L. Shen, L.-L. Yang, and L. Yuan, "Explanation of essence and substance basis of channels and collaterals with fasciology," *Chinese Acupuncture & Moxibustion*, vol. 27, no. 8, pp. 583–585, 2007.

[26] J. Palhalmi, Y. Bai, and L. Yuan, "Integrative approaches in the research of Fascial network for a better understanding of traditional Chinese medicine mechanisms—summary of the Fascia Congress 2009," *Zhong Xi Yi Jie He XueBao*, vol. 8, no. 2, pp. 199–200, 2010.

[27] X.-M. Jiang, X.-Q. Zhang, and L. Yuan, "Advances in the study on the role of connective tissue in the mechanical signal transduction of acupuncture," *Zhen Ci Yan Jiu*, vol. 34, no. 2, pp. 136–139, 2009.

[28] M. Kumka and J. Bonar, "Fascia: a morphological description and classification system based on a literature review," *The Journal of the Canadian Chiropractic Association*, vol. 56, no. 3, pp. 179–191, 2012.

[29] F. H. Lau and B. Pomahac, "Wound healing in acutely injured fascia," *Wound Repair and Regeneration*, vol. 22, supplement 1, pp. 14–17, 2014.

[30] H. M. Langevin, N. A. Bouffard, J. R. Fox et al., "Fibroblast cytoskeletal remodeling contributes to connective tissue tensiond," *Journal of Cellular Physiology*, vol. 226, no. 5, pp. 1166–1175, 2011.

[31] J. R. Fox, W. Gray, C. Koptiuch, G. J. Badger, and H. M. Langevin, "Anisotropic tissue motion induced by acupuncture needling along Intermuscular connective tissue planes," *The Journal of Alternative and Complementary Medicine*, vol. 20, no. 4, pp. 290–294, 2014.

[32] M. A. Islam, S. D. Thomas, K. J. Sedoris, S. P. Slone, H. Alatassi, and D. M. Miller, "Tumor-associated primo vascular system is derived from xenograft, not host," *Experimental and Molecular Pathology*, vol. 94, no. 1, pp. 84–90, 2013.

Hindawi Publishing Corporation
Evidence-Based Complementary and Alternative Medicine
Volume 2015, Article ID 725989, 8 pages
http://dx.doi.org/10.1155/2015/725989

Research Article

Comparison of Alcian Blue, Trypan Blue, and Toluidine Blue for Visualization of the Primo Vascular System Floating in Lymph Ducts

Da-Un Kim,[1,2] Jae Won Han,[1,2] Sharon Jiyoon Jung,[1] Seung Hwan Lee,[1] Richard Cha,[1,2] Byung-Soo Chang,[3] and Kwang-Sup Soh[1]

[1]*Nano Primo Research Center, Advanced Institute of Convergence Technology, Seoul National University, Suwon 443-270, Republic of Korea*
[2]*College of Physical Education, The University of Suwon, Hwaseong 445-743, Republic of Korea*
[3]*Department of Cosmetology, Hanseo University, Seosan 356-706, Republic of Korea*

Correspondence should be addressed to Richard Cha; wellspring2@naver.com and Byung-Soo Chang; bschang@hanseo.ac.kr

Received 2 July 2014; Accepted 1 September 2014

Academic Editor: Moriya Ohkuma

The primo vascular system (PVS), floating in lymph ducts, was too transparent to be observed by using a stereomicroscope. It was only detectable with the aid of staining dyes, for instance, Alcian blue, which was injected into the lymph nodes. Some dyes were absorbed preferentially by the PVS than the lymph wall. It remains a standing problem to know what dyes are absorbed better by the PVS than the lymph walls. Such information would be useful to unravel the biochemical properties of the PVS that are badly in need for obtaining large amount of PVS specimens. In the current work we tried two other familiar dyes which were used in PVS research before. We found that Trypan blue and toluidine blue did not visualize the PVS. Trypan blue was cleared by the natural washing. Toluidine blue did not stain the PVS, but it did leave stained spots in the lymph wall and its surrounding tissues, and it leaked out of the lymph wall to stain surrounding connective tissues. These completely different behaviors of the three dyes were found for the first time in the current work and provide valuable information to elucidate the mechanism through which some special dyes stained the PVS preferentially compared to the lymphatic wall.

1. Introduction

Long threadlike structures floating in large-caliber lymph ducts were first observed with the aid of staining with the dye Janus green B in the lymph ducts stemming from the lumbar nodes near the caudal vena cava in the abdominal cavity of a rabbit [1]. Since then, various other dyes, such as fluorescent magnetic nanoparticles, Alcian blue [2, 3], and DiI [4], have been used for the same purpose with similar protocols [5, 6]. Subject animals were rabbits [1–5], rats [6], and mice [7]. The target lymph ducts were thoracic ducts [7], as well as the above-mentioned lumbar duct, and the duct around the epigastric blood vessel in the skin [8, 9]. The presence of a lymph-associated primo vascular system (L-PVS) floating in the flow of lymph was first claimed by Kim in the early 1960s [10, 11] and was only recently confirmed by various experimental groups [1–9, 12].

One of the important questions concerns the mechanism through which the dye preferentially stains the L-PVS rather than the lymph wall. In answering this question, knowing which dyes do not stain the L-PVS in a similar process would be helpful. If L-PVS affine and nonaffine dyes are compared, valuable information on the mechanism of the staining can be obtained. The current work reports on the findings for two dyes, Trypan blue and toluidine blue, that did not stain the L-PVS when the same protocol as that for the Alcian blue was used. In the first case, we injected Alcian blue into the inguinal node of one side and Trypan blue into the inguinal

node of the other side. In the second case, toluidine blue and Alcian blue were compared. Trypan blue was chosen for this study because it is effective for staining the primo vascular system (PVS) on the surfaces of internal organs [13], in the brain and the spine [14], and around cancer tissues [15–18]. In the second case, toluidine blue was chosen for this study simply because it is one of the common dyes used in histology and has been used for PVS histology in connection with transmission electron microscopy [19].

Effectively visualizing, observing, and isolating the L-PVS is one of the steps necessary to establish the anatomy and the histology of the L-PVS. The current work is one of various efforts with that purpose. The present situation of PVS research is similar to that of the lymph system about a decade ago. Before the first breakthrough with the identification of the vascular endothelial growth factor VEGF-C as a specific lymphangiogenic growth factor, only a rudimentary understanding of the molecular biology of lymphatics existed due to technical difficulties in identifying lymph vessels within tissues and in isolating pure cultures of lymphatic endothelial cells for detailed characterization [20–22]. A molecular understanding of the PVS, which, in turn, requires a sufficient amount of a specimen for study, is badly needed. The current work is connected indirectly to ways to obtain sufficient specimens of the L-PVS.

The possible medical significance of the PVS was suggested by the observation of abundant immune cells in the PVS with the following population ratios: mast cells (20%), eosinophils (16%), neutrophils (15%), lymphocytes (1%), immature cells (3%), and chromatin cells (0.3%) [12]. These data suggest the roles of the PVS in the immune system and in the well-known lymphatic system. The L-PVS, especially, is interesting because it resides inside lymph ducts, thus indicating a probable interaction between them. As is well known, lymphatics are major paths for metastasis in common cancers, such as breast cancer and colorectal carcinomas, which initially occurs via lymph nodes [23, 24]. Strong evidence exists that the PVS is another path for metastasis in addition to the lymphatic one [15]. Furthermore, a primo node might play a role as a haven for cancer stem cells [18].

2. Materials and Methods

2.1. Animals. Rats (Sprague-Dawley, male, 9 weeks old, 280~300 g) were obtained from DooYeol Biotech (Seoul, Republic of Korea) and housed in a temperature-controlled environment (23°C). Seventeen rats were injected with Trypan blue and twenty-one rats were injected with toluidine blue in the experiments. All animals were exposed to a 12-hour light-dark cycle and were provided food and water *ad libitum*. The procedures involving the animals and their care were in full compliance with current international laws and policies (*Guide for the Care and Use of Laboratory Animals*, National Academy Press, 1996) and were approved by the Institutional Ethics Committee of the Advanced Institute of Convergence Technology (Approval Number: WJIACUC20130212-1-07). The rats were anesthetized by intramuscular injection of a regimen consisting of 1.5 g/kg of urethane and 20 mg/kg of xylazine.

2.2. Staining Dye Preparation. The staining dye 0.2% Alcian blue (A5268, Sigma-Aldrich, St. Louis, MO, USA) solution in boiled phosphate-buffered saline (PBS, pH 7.4) was prepared and was filtered by using a 0.22-μm membrane filter (Merck Millipore, Darmstadt, Germany) with a syringe (BD, Franklin Lakes, NJ, USA). The staining dye Trypan blue solution (25900048R, CORNING Cellgro, Manassas, VA 20109, USA) 0.4% (w/v) in PBS was used. The staining dye with a fiducial volume of 50% toluidine blue working solution was made from the stock solution and 1% sodium chloride (NaCl: 0.05 gm and distilled water: 5 mL). The toluidine blue stock solution was made by melting 0.1 gm of toluidine blue powder (Toluidine blue O, 198161-5G, Sigma-Aldrich, St. Louis, MO, USA) and 10 mL of 70% alcohol.

2.3. In-Vivo Surgical Operation and Visualization of the Primo Vascular System. A 2 cm skin midline incision up and down from the navel along the ventral surface of the abdominal cavity was made, and the skin was retracted towards the rat's spinal column. The inguinal nodes (INs) are bilateral and are situated close to the bifurcation of the superficial epigastric veins. After the left-hand side IN had been exposed, the prepared 0.2% Alcian blue dye was injected into the node at a slow rate. Then, Trypan blue was injected into the right-hand side IN. The order of injections was varied and the left and the right sides were alternated from one experiment to another. The other experiments with Alcian blue and toluidine blue were done using similar procedures.

The main lymph duct to observe was located along the superior epigastric vein and connected the IN to the axillary node (AN); most of the time, it had several branches. Natural circulation of the lymph fluid had to be promoted in order to ensure that the dyeing agent had been thoroughly washed out. Therefore, each rat was covered with paper tissue and kept in the bedding to maintain its body temperature.

Two hours after dye injection, the IN and the lymph duct were exposed to observe the L-PVS. All procedures were performed under a stereomicroscope (SZX12, Olympus, Japan). After the stained L-PVS had been observed, the rats were sacrificed by using an intracardiac injection of urethane (1 mL). The skin, including the lymph ducts, was fixed with a 10% neutral buffered formalin (NBF) solution at 4°C for 24 hours. The lymph ducts, including the L-PVS, were collected from the fixed skin.

For the staining of nuclei with 4′, 6-diamidino-2-phenylindole (DAPI), the specimen was stained with 300-nM DAPI (D1306, Invitrogen, MO, USA) solution for 20 minutes. After the specimen had been washed, it was covered with a mounting solution. The stained specimen was investigated under a phase contrast microscope (Olympus, U-LH100HG, Japan), a microscope with a black and white charge-coupled device (CCD; Nikon, ECLIPSE Ti, Japan), a contrast-enhanced microscope (DM2500, Leika, Germany), and a confocal laser scanning microscope (CLSM; C1 plus, Nikon, Japan).

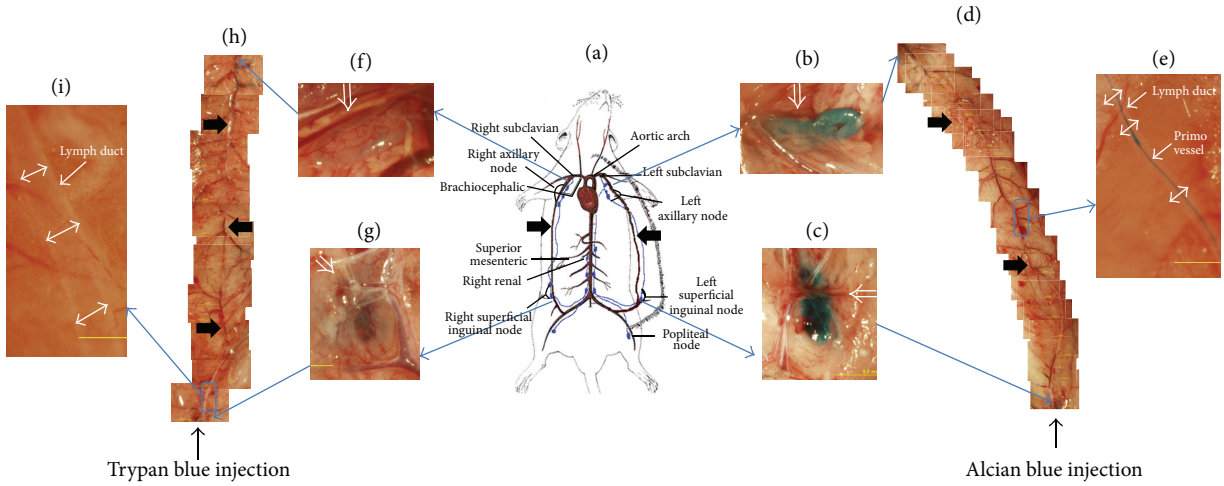

FIGURE 1: Stereomicroscopic images of lymph ducts in which Alcian blue and Trypan blue had been injected. (a) Illustration of the left and the right lymph ducts along the epigastric blood vessels (thick arrows) in skin. (b) Left axillary node (open arrow) which became blue due to the Alcian blue that flowed in the lymph duct. (c) Left inguinal node (open arrow) into which Alcian blue had been injected. (d) Mosaic of images of the left lymph duct along the epigastric blood vessel (thick arrows). (e) Magnified image of the rectangular area in (d). The blue threadlike structure was the primo vessel (arrow), and it was floating in the lymph duct (double arrows). (f) Right axillary node (open arrow) weakly stained by Trypan blue that flowed from the inguinal node through the lymph duct. (g) Right inguinal node (open arrow) into which Trypan blue had been injected. (h) Mosaic images of the right lymph duct from the inguinal node to the axillary node in which Trypan blue flowed. The epigastric blood vessel is indicated with thick arrows. (i) Magnified image of the rectangular area in (h). The lymph duct (double arrows) was washed clean, and the PVS was not stained. More details are presented in Figure 3.

3. Results

The position of the relevant lymph duct in the skin from the inguinal node to the axillary node along the prominent epigastric blood vessel is illustrated in Figure 1(a). As in a previous work with Alcian blue [8], the PVS was observed in this skin lymph duct. In Figure 1(b), the left axillary node was blue due to the Alcian blue which had been injected into the left inguinal node (Figure 1(c)) and had arrived via the lymph duct. A mosaic of the images capturing the whole lymph duct (Figure 1(d)) shows the primo vessel, where one part (Figure 1(e)) was magnified to demonstrate that the primo vessel was stained well by Alcian blue inside the lymph vessel. In comparison, the right axillary node (Figure 1(f)) became weakly blue due to the Trypan blue that had been injected into the right inguinal node (Figure 1(g)) and had flowed via the lymph duct (Figure 1(h)). The magnified mosaic image of the lymph duct (Figure 1(i)) showed that the primo vessel was not stained at all. This showed that Trypan blue in this injection method was not effective for L-PVS visualization.

Compared with Alcian blue and Trypan blue, the dye toluidine blue showed a completely different behavior, as shown in Figure 2. Figure 2(a) is the same illustration of the rat lymph in skin, and the panels from Figures 2(b) to 2(e) are for the right axillary node and the right inguinal node and present a mosaic of images of the lymph duct, along with one magnified image showing the primo vessel in the cleared lymph duct, respectively. Alcian blue showed no differences in its effectiveness in comparison with Trypan blue and toluidine blue. The results with toluidine blue are depicted in Figures 2(f) to 2(i). The left axillary and inguinal nodes were deeply colored due to toluidine blue (Figures 2(f) and 2(g)). The magnified images in Figures 2(h) and 2(i) show that the L-PVS was not stained, but the lymph duct was stained at randomly distributed spots in its wall; furthermore, the dye leaked out to the surrounding tissue.

Figure 3(a) shows the magnified images of the primo vessel inside the lymph duct. Figure 3(b) shows the transparent lymph duct after washing of the preinjected Trypan blue. The L-PVS was not stained at all, so it was not observable. Figure 3(c), an enhanced contrast microscope image of the specimen on a slide glass, shows an extracted lymph duct with the Alcian-blue-stained primo vessel in it. A small part of the primo vessel was drawn out on the left upper part of the lymph duct. This demonstrates the existence of an independent threadlike object inside the lymph duct. Also, the primo vessel is seen to branch where the lymph duct branched.

Figure 4(a) shows another Alcian-blue-stained primo vessel in comparison with the toluidine blue injection case (Figure 4(b)) in which no primo vessel was observed, but in which the lymph duct and the surrounding tissue were weakly stained. In addition, strongly stained spots were sporadically distributed. The dye leaked from the lymph duct. Furthermore, some small blood vessels were strongly stained, and apparently the dye flowed in the blood vessel (Figure 4(c)). This leaking from the lymph duct and flowing in blood vessels of toluidine blue were observed for the first time in this work.

The primo node is an oval-shaped tissue packed with various cells [12]. Figure 5 shows a primo node attached to one primo vessel, during preparation. Indeed, the primo node was packed with various cell nuclei, as seen in Figure 5(b).

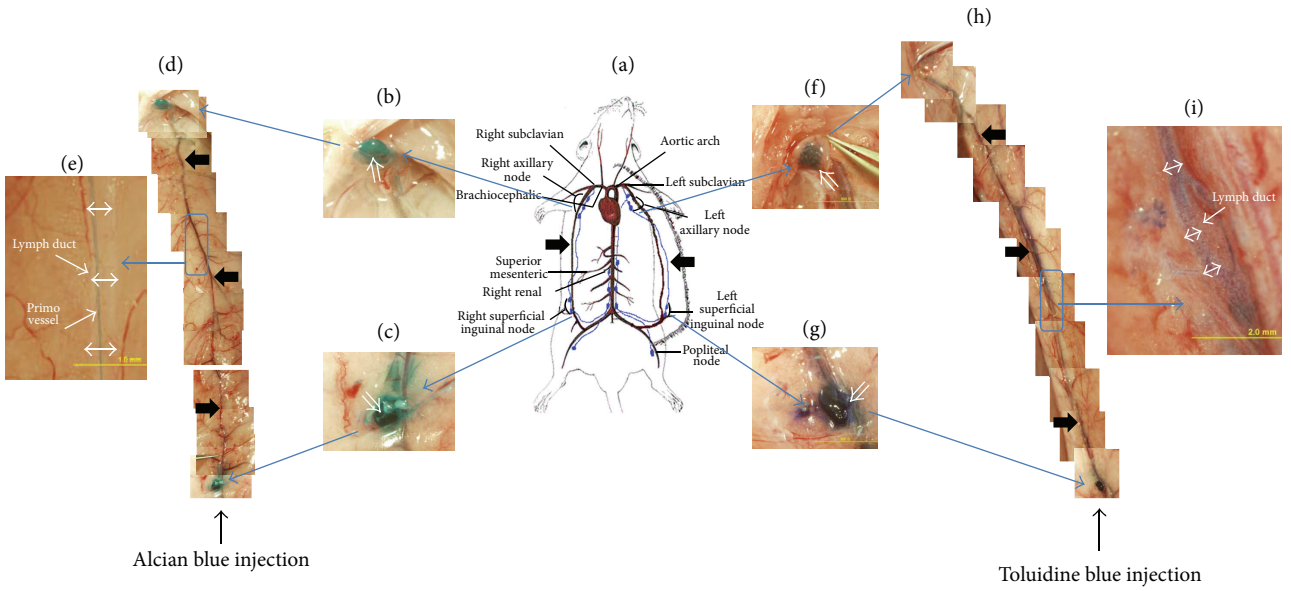

FIGURE 2: Stereomicroscopic images of lymph ducts in which Alcian blue and toluidine blue had been injected. (a) Illustration of the left and the right lymph ducts along the epigastric blood vessels in skin (thick arrows). (b) Right axillary node which became blue due to the Alcian blue that flowed through the lymph duct. (c) Right inguinal node into which Alcian blue had been injected. (d) Mosaic of images of the right lymph duct along the epigastric blood vessel (thick arrows). (e) Magnified image of the rectangular area in (d). The blue threadlike structure was the primo vessel, and it was floating in the lymph duct (double arrows). (f) Left axillary node stained with toluidine blue that flowed from the inguinal node through the lymph duct. (g) Left inguinal node into which toluidine blue had been injected. (h) Combined images of the right lymph duct from the inguinal node to the axillary node in which toluidine blue flowed. (i) Magnified image of the rectangular area in (h). The lymph duct (double arrows) and its surrounding tissue were stained blue, but the PVS was not visible. More details are presented in Figure 4.

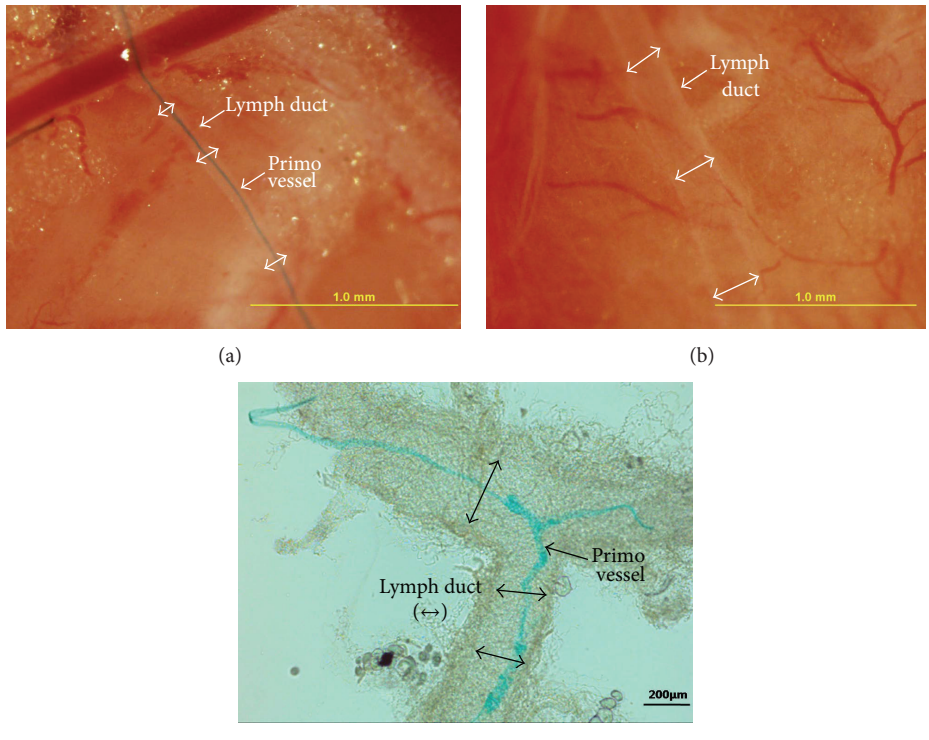

FIGURE 3: Comparison of stereomicroscopic images of the lymph ducts into which Alcian blue and Trypan blue had been injected. (a) A primo vessel emerged in a lymph duct (double arrows) after a two-hour washing of the injected Alcian blue. This image corresponds to Figure 1(e). (b) The lymph duct after a two-hour washing of the injected Trypan blue became clear again without any hint of the presence of the primo vessel. This showed that the L-PVS was selectively stained by the Alcian blue, not by the Trypan blue. (c) Contrast-enhanced microscope image of a branched lymph duct (double arrows) that was extracted and put on a slide. Connective tissues wrapped the lymph duct. The stained L-PVS also branched.

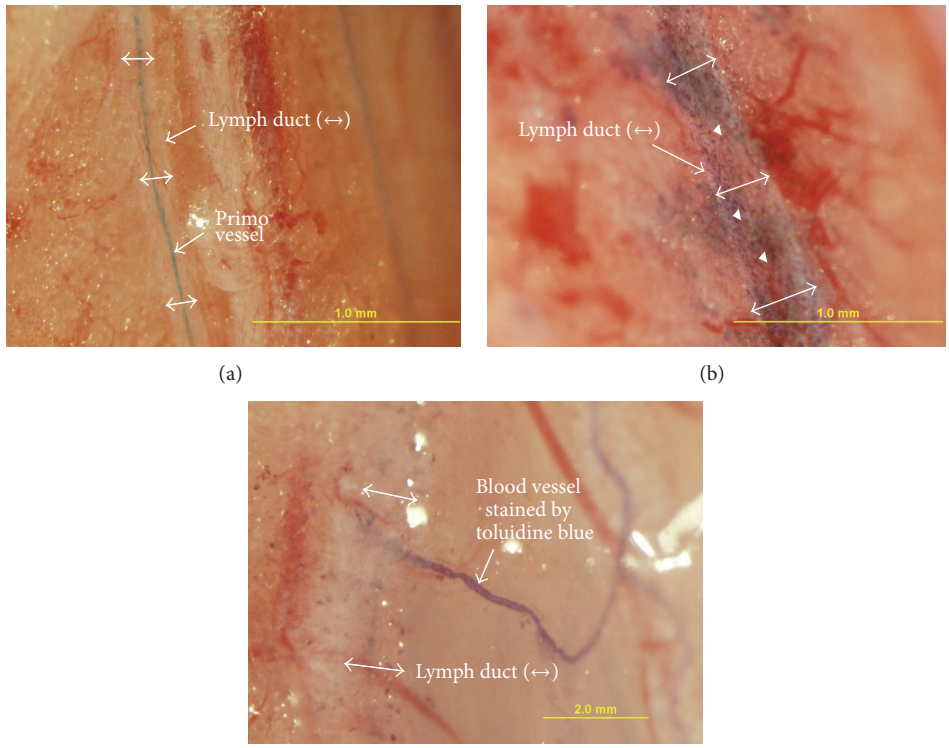

FIGURE 4: Comparison of lymph ducts into which Alcian blue and toluidine blue had been injected. (a) Two branches of lymph ducts (one of them indicated with double arrows) and their L-PVS stained with Alcian blue. (b) Toluidine blue left stained spots in the lymph wall (arrow heads). It also leaked from the wall and stained the surrounding tissues. However, the L-PVS was not stained. (c) A thin blood vessel was deeply stained by using toluidine blue. How it flowed into the blood vessel is not known.

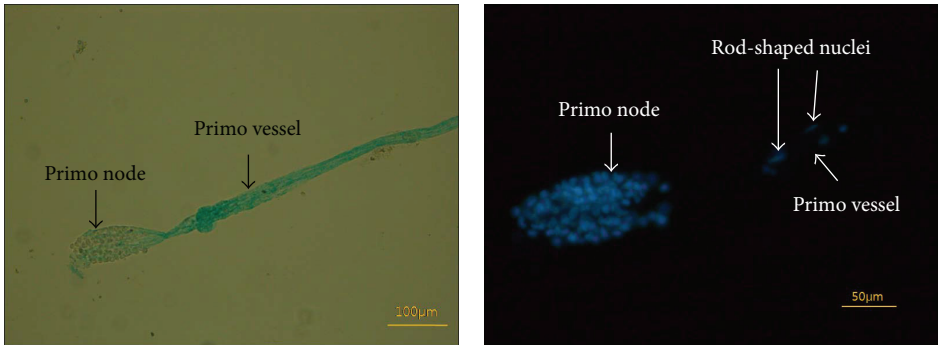

FIGURE 5: Images of a primo node extracted from the lymph duct. (a) A primo node stained by Alcian blue was extracted from a lymph vessel. One of the primo vessels connected to the node was cut off during the extraction process, and only one side was kept. The primo vessel was a bundle of two or more subvessels. (b) DAPI images of the same primo node as in (a), which contained many nuclei. Two rod-shaped nuclei (arrows) can be seen in the primo vessel.

The minimal criterion to confirm the presence of the L-PVS is the observation of a distribution of the rod-shaped nuclei by DAPI staining. Figure 5(b) shows the presence of longitudinally distributed rod-shaped nuclei; more are shown in Figure 6.

Because the distribution of nuclei and their shapes are critical, we present one more specimen with DAPI staining. A phase contrast microscopic image of the extracted primo vessel is shown in Figure 6(a). The DAPI image was taken with a sensitive black and white CCD (Figure 6(b)) and distinguished the part with the rod-shaped nuclei from the part with the round-shaped nuclei of aggregated lymphocytes. The rod-shaped nuclei were located inside the primo vessel, which was confirmed by a series of confocal microscope images of

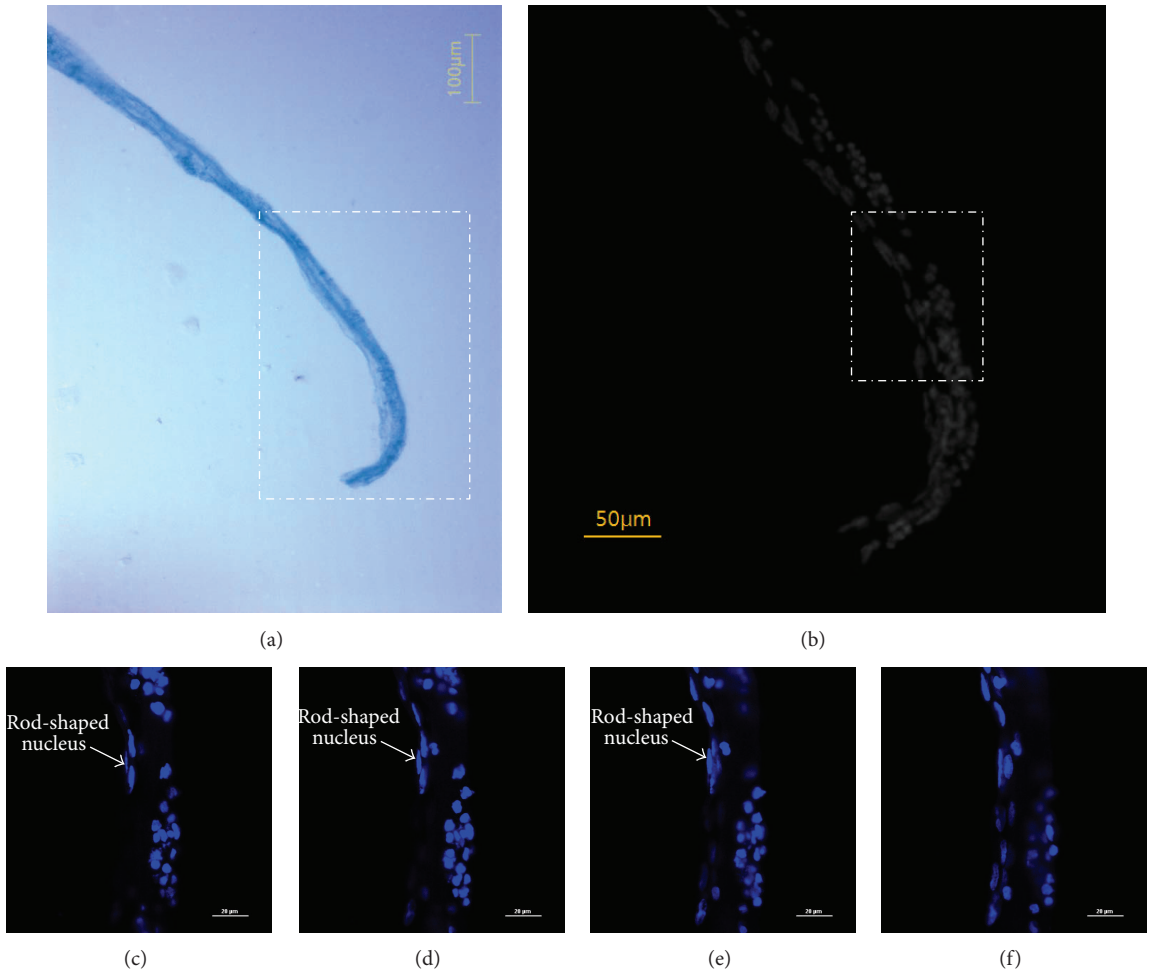

Figure 6: Rod-shaped nuclei in the primo vessel. (a) Phase contrast microscope image of a primo vessel that was extracted from a lymph duct. (b) Fluorescence microscopic image of the boxed area in (a). The boxed area was magnified, and the part with rod-shaped nuclei was the primo vessel. The round-shaped nuclei were aggregated lymphocytes. (c–f) Confocal laser scanning microscope images of the circled area in (b). These panels were consecutive optical sections from top to bottom separated by 2 μm in each step. The same rod-shaped nucleus appeared (panel (c)), looked long (panels (d) and (e)), and then nearly disappeared (panel (f)), which implies that this particular endothelial nucleus was inside the primo vessel and, therefore, had not aggregated from outside.

optical sections (Figures 6(c) to 6(f)). For verification, we chose a particular nucleus (arrow in Figures 6(d) and 6(e)).

4. Discussion

To the present time, several dyes have been used for the visualization of the L-PVS in lymph ducts: Janus green B [1], fluorescent magnetic nanoparticles, Alcian blue [2, 3, 5, 6, 8], and DiI [4]. Among them, Alcian blue has been most extensively used. Even though all these dyes are effective and have different merits, the mechanism through which they stain preferentially the L-PVS has not yet been uncovered. Before we attempted to determine the exact mechanism, we examined the efficacies of two common materials for the visualization of the L-PVS, the results of which should provide more information useful in investigating the mechanism.

Alcian blue, Trypan blue, and toluidine blue showed different behaviors in this experiment. Alcian blue is used for the staining of acidic polysaccharides in histology [25]. It was initially chosen with the expectation that it would stain the hyaluronic acid that is known to be abundant in the primo fluid [11]. Until now, whether the successful application of Alcian blue in many previous experiments [2, 3, 5, 6, 8] was due to its affinity to hyaluronic acid is not yet clear. In the current work, Alcian blue was used as a reference material for the Trypan blue and toluidine blue.

The dye Trypan blue is used in histology for staining connective tissues, such as collagen, muscle, and cornified epithelium [25]. Another common use is to discriminate dead cells from live ones. Trypan blue is also useful for vivistaining of vitreoretinal membranes in ophthalmic surgery [26]. In PVS-visualization work, Trypan blue was first used as a visualizing agent *in vivo* and *in situ*, not as a staining dye of tissue specimens for histological purposes. By using it, we were able to make the following significant contributions: (1) a web-like network of PVS was observed on the omentum

and the visceral peritoneum [13]; (2) the PVS exists around cancer tissues [15–18]; and (3) the PVS exists in the brain and the spine [14]. In the current work, we compared Alcian blue and Trypan blue for their abilities to visualize the L-PVS. Surprisingly, the Trypan blue was not absorbed either by the lymph wall or the L-PVS. We, therefore, conjecture that Trypan blue might have been absorbed by the dead cells of the PVS, which had been exposed to air during the experimental procedure. However, further study is needed before a definite conclusion can be drawn about the mechanism of Trypan-blue absorption by the PVS in previous experiments.

The behavior of the toluidine blue was beyond our expectation in the sense that it leaked out through the lymphatic wall and left randomly-distributed dots in the lymph wall and its surrounding tissues. In addition, the dye flowed in some venules around the lymph duct and strongly stained the vascular wall, but it was not absorbed by the L-PVS. These results were newly found in this experiment. Toluidine blue has often been used in the staining of PVS tissues for light microscopic imaging in transmission electron microscopic studies of PVS tissues [19].

The possible medical significance of the PVS is suggested by the observation of abundant immune cells in the PVS [12]. The data suggest the roles of the PVS in immune systems and as an extrahematopoietic source of immune cells and bone marrow. Other suggested functions of the PVS are a path for metastasis [15] and a haven for cancer stem cells [18], which is worth deeper study.

The present work was limited in that it only compared the efficacies of the three dyes in visualizing the L-PVS and did not uncover the biochemical mechanism for their different behaviors. The understanding of this mechanism is left for a future study. For this purpose it is valuable to know the dyes that were used to stain lymph vessels. For example, Evans blue, and guanylate cyclase that was used to stain dermal lymphatic capillary [27].

In conclusion, Trypan blue and toluidine blue were quite different from Alcian blue in their abilities to visualize the L-PVS. Trypan blue was cleared completely by a two-hour natural washing and did not stain either the lymph wall or the L-PVS. To the contrary, toluidine blue left scattered strongly stained dots in the lymph wall and surrounding tissues after leaking out from the lymph duct. It did not, however, stain the L-PVS at all. Sometimes, it entered some small veins and stained the vessel strongly. These were first observed in this experiment, but this phenomenon, in terms of biochemical processes, is still not understood.

Conflict of Interests

The authors declare that there is no conflict of interests regarding the publication of this paper.

Authors' Contribution

Da-Un Kim and Jae Won Han contributed equally to this paper.

Acknowledgment

This research was supported in part by the Basic Science Research Program through the National Research Foundation of Korea (NRF) funded by the Ministry of Science, ICT & Future Planning (Grant no. 2013R1A1A2008343).

References

[1] B.-C. Lee, J. S. Yoo, K. Y. Baik, K. W. Kim, and K.-S. Soh, "Novel threadlike structures (Bonghan ducts) inside lymphatic vessels of rabbits visualized with a Janus Green B staining method," *Anatomical Record—Part B New Anatomist*, vol. 286, no. 1, pp. 1–7, 2005.

[2] C. Lee, S.-K. Seol, B.-C. Lee, Y.-K. Hong, J.-H. Je, and K.-S. Soh, "Alcian blue staining method to visualize Bonghan threads inside large caliber lymphatic vessels and X-ray microtomography to reveal their microchannels," *Lymphatic Research and Biology*, vol. 4, no. 4, pp. 181–189, 2006.

[3] Y.-I. Noh, M. Rho, Y.-M. Yoo, S. J. Jung, and S.-S. Lee, "Isolation and morphological features of primo vessels in rabbit lymph vessels," *JAMS Journal of Acupuncture and Meridian Studies*, vol. 5, no. 5, pp. 201–205, 2012.

[4] B.-C. Lee and K.-S. Soh, "Contrast-enhancing optical method to observe a Bonghan duct floating inside a lymph vessel of a rabbit," *Lymphology*, vol. 41, no. 4, pp. 178–185, 2008.

[5] S. J. Jung, S. Y. Cho, K.-H. Bae et al., "Protocol for the observation of the primo vascular system in the lymph vessels of rabbits," *JAMS Journal of Acupuncture and Meridian Studies*, vol. 5, no. 5, pp. 234–240, 2012.

[6] S. J. Jung, K.-H. Bae, M.-H. Nam, H. M. Kwon, Y.-K. Song, and K.-S. Soh, "Primo vascular system floating in lymph ducts of rats," *JAMS Journal of Acupuncture and Meridian Studies*, vol. 6, no. 6, pp. 306–318, 2013.

[7] I. H. Choi, H. K. Chung, and Y. K. Hong, "Detection of the primo vessels in the rodent thoracic lymphatic ducts," in *The Primo Vascular System*, K. S. Soh, K. A. Kang, and D. Harrison, Eds., pp. 121–126, Springer, New York, NY, USA, 2011.

[8] S. H. Lee, K.-H. Bae, G. O. Kim et al., "Primo vascular system in the lymph vessel from the inguinal to the axillary nodes," *Evidence-based Complementary and Alternative Medicine*, vol. 2013, Article ID 472704, 6 pages, 2013.

[9] S. J. Jumg, S. H. Lee, K. H. Bae, H. M. Kwon, Y. K. Song, and K. S. Soh, "Visualization of the primo vascular system, a putative cancer metastasis thread afloat in a lymph duct," *Protocol Exchange*, 2013.

[10] B. H. Kim, "On the Kyungrak system," *Journal of the Academy of Medical Sciences of the Democratic People's Republic of Korea*, vol. 90, pp. 1–41, 1963.

[11] B. H. Kim, "The Kyungrak system," *Journal of Jo Sun Medicine*, vol. 108, pp. 1–38, 1965 (Korean).

[12] B. S. Kwon, C. M. Ha, S. Yu, B.-C. Lee, J. Y. Ro, and S. Hwang, "Microscopic nodes and ducts inside lymphatics and on the surface of internal organs are rich in granulocytes and secretory granules," *Cytokine*, vol. 60, no. 2, pp. 587–592, 2012.

[13] B.-C. Lee, K. W. Kim, and K.-S. Soh, "Visualizing the network of bonghan ducts in the omentum and peritoneum by using trypan blue," *JAMS Journal of Acupuncture and Meridian Studies*, vol. 2, no. 1, pp. 66–70, 2009.

[14] J. Dai, B.-C. Lee, P. An et al., "In situ staining of the primo vascular system in the ventricles and subarachnoid space of the

brain by trypan blue injection into the lateral ventricle," *Neural Regeneration Research*, vol. 6, no. 28, pp. 2171–2175, 2011.

[15] J. S. Yoo, M. Hossein Ayati, H. B. Kim, W.-B. Zhang, and K.-S. Soh, "Characterization of the primo-vascular system in the abdominal cavity of lung cancer mouse model and its differences from the lymphatic system," *PLoS ONE*, vol. 5, no. 4, Article ID e9940, 2010.

[16] W. Akers, Y. Liu, G. Sudlow et al., "Identification of primo vascular system in murine tumors and viscera," in *The Primo Vascular System*, pp. 179–183, Springer, New York, NY, USA, 2012.

[17] M. Y. Hong, S. S. Park, H. K. Do, G.-J. Jhon, M. Suh, and Y. Lee, "Primo vascular system of murine melanoma and heterogeneity of tissue oxygenation of the melanoma ," *Journal of Acupuncture and Meridian Studies*, vol. 4, no. 3, pp. 159–163, 2011.

[18] M. A. Islam, S. D. Thomas, S. Slone, H. Alatassi, and D. M. Miller, "Tumor-associated primo vascular system is derived from xenograft, not host," *Experimental and Molecular Pathology*, vol. 94, no. 1, pp. 84–90, 2013.

[19] B.-C. Lee, J. S. Yoo, V. Ogay et al., "Electron microscopic study of novel threadlike structures on the surfaces of mammalian organs," *Microscopy Research and Technique*, vol. 70, no. 1, pp. 34–43, 2007.

[20] M. J. Karkkanien, T. Makinen, and K. Alitalo, "Lymphatic endothelium: a new frontier of metastasis research," *Nature Cell Biology*, vol. 4, pp. E2–E5, 2002.

[21] M. J. Karkkainen and K. Alitalo, "Lymphatic endothelial regulation, lymphoedema, and lymph node metastasis," *Seminars in Cell and Developmental Biology*, vol. 13, no. 1, pp. 9–18, 2002.

[22] L. Jussila and K. Alitalo, "Vascular growth factors and lymphangiogenesis," *Physiological Reviews*, vol. 82, no. 3, pp. 673–700, 2002.

[23] K. Alitalo and P. Carmeliet, "Molecular mechanisms of lymphangiogenesis in health and disease," *Cancer Cell*, vol. 1, no. 3, pp. 219–227, 2002.

[24] G. Oliver and M. Detmar, "The rediscovery of the lymphatic system: old and new insights into the development and biological function of the lymphatic vasculature," *Genes and Development*, vol. 16, no. 7, pp. 773–783, 2002.

[25] G. Clark, *Staining Procedures*, Williams and Wilkins, Baltimore, Md, USA, 4th edition, 1980.

[26] M. Farah, M. Maia, B. Furlani et al., "Current concepts of trypan blue in chromovitrectomy," *Developments in Ophthalmology*, vol. 42, pp. 91–100, 2008.

[27] S. Nishida and M. Ohkuma, "Staining of dermal lymphatic capillary by guanylatecylase," *Lymphology*, vol. 26, no. 4, pp. 195–199, 1993.

Hindawi Publishing Corporation
Evidence-Based Complementary and Alternative Medicine
Volume 2015, Article ID 812354, 8 pages
http://dx.doi.org/10.1155/2015/812354

Research Article

Primo Vascular System: An Endothelial-to-Mesenchymal Potential Transitional Tissue Involved in Gastric Cancer Metastasis

An Ping,[1] Su Zhendong,[2] Qu Rongmei,[3] Dai Jingxing,[3] Chen Wei,[1] Zhou Zhongyin,[1] Luo Hesheng,[1] and Kwang-Sup Soh[4]

[1]*Department of Gastroenterology, Renmin Hospital of Wuhan University, Wuhan 430070, China*
[2]*Department of Biochemistry, Nagoya University Graduate School of Medicine, Nagoya 466-8550, Japan*
[3]*Department of Anatomy, Southern Medical University, Guangzhou 510515, China*
[4]*Nano Primo Research Center, Advanced Institute of Convergence Technology, Seoul National University, Suwon-si 443-270, Republic of Korea*

Correspondence should be addressed to Luo Hesheng; luohswhu@gmail.com and Kwang-Sup Soh; kssoh1@gmail.com

Received 3 October 2014; Revised 19 January 2015; Accepted 21 January 2015

Academic Editor: Kuang C. Lai

Gastric cancer is the fourth commonest cancer in the world and the second leading cause of cancer-related death. Investigation of gastric cancer metastasis is one of the hottest and major focuses in cancer research. Growing evidence manifested that primo vascular system (PVS) is a new kind of circulatory system beyond vascular and lymphatic system. Previous researches revealed that PVS is a specific tissue between endothelium and mesenchyme and is involved in cancer, especially in tumor metastasis and regeneration. In current study, we investigated the role of primo vessels in gastric cancer metastasis and its possible relationship to vascular vessels formation. Our results indicated that primo vessels were involved in gastric cancer metastasis. We observed blood vessel-mediated metastasis, primo vessel-mediated metastasis, and an intermediate state between them. We deduced that primo vessels may be precursors of blood vessels. These results possibly provided a thoroughly new theoretic development in cancer metastasis.

1. Introduction

Gastric cancer is the fourth most common cancer in the world and the second leading cause of cancer-related death despite its declined incidence over the last 50 years [1, 2]. More than 80% of diagnoses occur at the middle to late stage of the disease and metastasis to remote organs frequently is detected [3]. Investigation of gastric cancer metastasis is one of the hottest and major focuses in cancer research. Generally, the metastasis of gastric cancer has three patterns: hematogenous metastasis through vascular vessels, lymphatic metastasis through lymphatic vessels, and implantation metastasis. Recently, growing evidence manifested that primo vascular system (PVS) is a new kind of circulatory system beyond vascular and lymphatic system [4–6]. The functional role of PVS in cancer, especially in tumor metastasis and regeneration, was extensively investigated and recognized by more and more researchers [7–10]. Our previous studies manifested that primo vessels in the mesentery are a specific transitional structure between endothelium and mesenchyme [11]. We deduced that primo vessel cells may be a sort of specific population that had potential capability of transition to endothelial cells or fibroblasts. Therefore, our current study continued to investigate the role of primo vessels in gastric cancer metastasis and its possible relationship to vascular vessels formation.

2. Materials and Methods

2.1. Cell Line and Cell Culture. The MKN-45 cell line, a poorly differentiated human gastric cancer cell line, was obtained from Korean Cell Line Bank. The cells were maintained in RPMI 1640 (GIBCO, CA) supplemented with 10% fetal bovine serum (GIBCO, CA), 1% penicillin/streptomycin, and

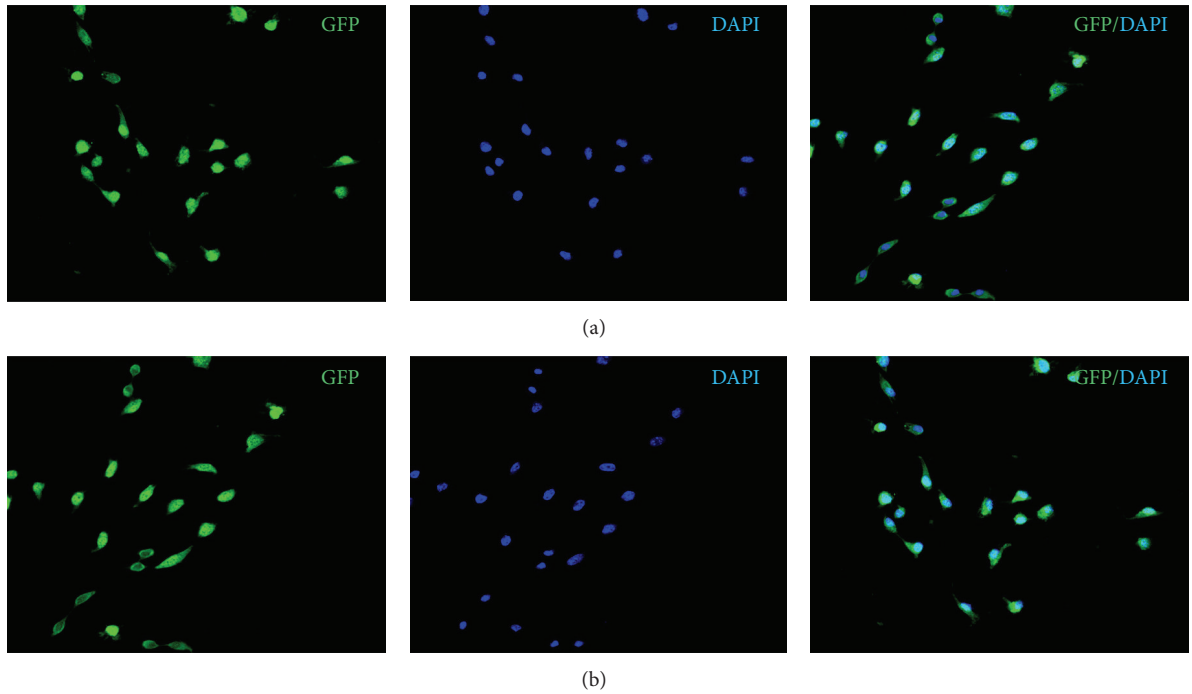

Figure 1: Isolation of stable, high GFP expressed MKN-45-GFP cells. (a) The enhanced GFP4 expression plasmid was transfected MKN-45 cells. The brightest fluorescent cells were sorted and cloned by flow cytometry. Stable high GFP-expression clones were isolated and cultured in the absence of G418 for 10 passages. (b) Stable high GFP-expression MKN-45-GFP cells cultured in the absence of G418 for 20 passages.

1% L-glutamine (Sigma-Aldrich, St. Louis, MO) and cultured in a humidified incubator in an atmosphere of 5% CO2 at 37°C. For GFP gene transduction, the enhanced GFP4 expression plasmids (Clontech, Palo Alto, CA) were transfected into 90% to 95% confluent MKN-45 cells using Lipofectamine 2000 (Invitrogen, CA), according to the instructions of the manufacturer. Transfected MKN-45 cells (MKN-45-GFP) were cultured into a selective medium that contained 200 mg/mL of G418 (GIBCO, CA). The level of G418 was increased to 1000 mg/mL stepwise. The brightest fluorescent cells (above the 95 percentile) were sorted and cloned by flow cytometry. High GFP-expression populations were isolated with cloning cylinders (Bel-Art Products, Pequannock, NJ) and cultured in the absence of G418 for over 10 passages to select for stable expression of GFP.

2.2. Mice. Adult male nude mice (BALB-c-nu/nu, aged 5–7 weeks, weighing 15–20 g, $n = 20$) were obtained from Jung-Ang Laboratory Animal Company (Seoul, Republic of Korea). The animals were maintained in a barrier facility in racks filtered with high-efficiency particulate air filter. All the animal care and studies were approved by the institutional committee on research animal care and were done according to the Korean Policy on Humane Care and Use of Laboratory Animals.

2.3. Orthotopic Implantation in Stomach. MKN-45-GFP cells were collected at the log phase and injected subcutaneously into the mice at 10^7/0.2 mL. Six weeks later, tumors were harvested from the mice under anesthesia (by subcutaneous injection of 0.1 mL of solution of 0.04% Zoletil and 0.06% Rompun) and minced into small pieces ($2 \times 2 \times 2\,mm^3$) in HBSS containing 100 U/mL penicillin and 100 μg/mL streptomycin (Figures 2(a)–2(c)). For implantation, the mouse stomach was gently exteriorized via a left-side upper abdominal incision, and one small tissue pocket was formed in the middle wall of the greater curvature using microscissors. One tumor piece was placed into the pocket and closed with a 6-0 surgical suture (Figures 2(d) and 2(e)). Animals were kept in a sterile environment. All procedures of the operation described above were performed with an X7 magnification microscope (Olympus).

2.4. Intraoperative Imaging. From 6 to 8 weeks after the orthotopic implantation, abdomens of the tumor-bearing mice were incised. Metastatic tumors and primo vascular system were carefully observed under the X7 magnification microscope. Metastatic tumors and primo vessels with classic appearances of free thread-like and semitransparent structure were captured with a CCD camera (Axiophot, Zeiss, Germany). To detect the GFP fluorescence derived from the gastric cancer, a Leica stereo fluorescence microscope LZ12 (Leica Microsystems, Inc., Bannockburn, IL) equipped with a mercury lamp power supply was used. Under the LZ12 microscope, the GFP fluorescence showed sensitive white color. High resolution images of 1024 × 724 pixels were captured. Images were processed for contrast and brightness and analyzed with the use of Image Pro Plus 4.0 software (Media Cybernetics, Silver Springs, MD).

2.5. Phalloidin and DAPI Staining in Tissue Samples. After intraoperative imaging, primo vessels together with

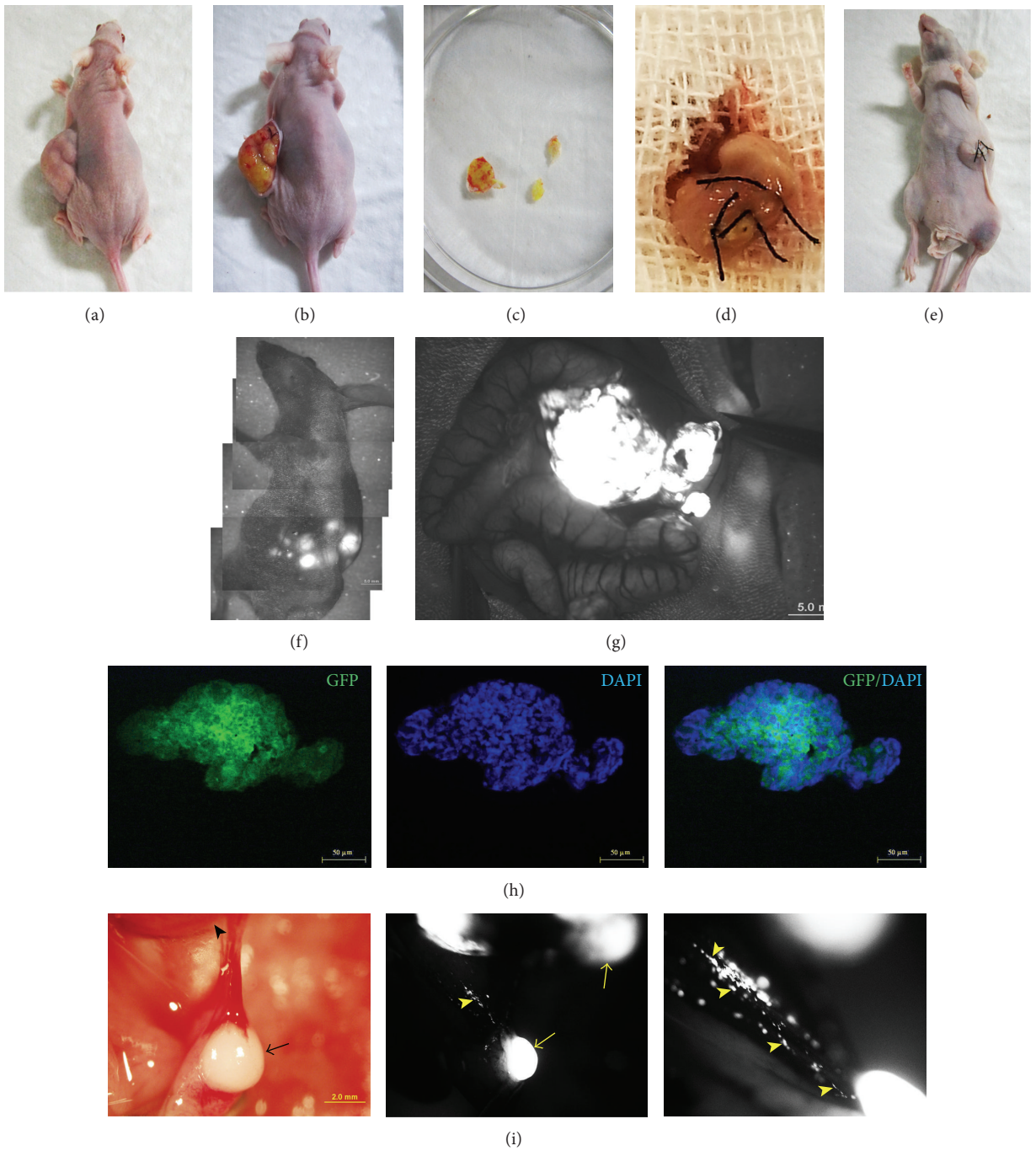

Figure 2: Orthotopic models in vivo and stable high level expression of GFP in gastric cancer metastatic tumors in nude mice. (a) and (b) 5×10^6 MKN-45-GFP cells were inoculated subcutaneously into the left flank of 5–7-week-old anesthetized nude mice. 6 weeks later, subcutaneous tumor grew obviously. (c) Subcutaneous tumor was harvested and incised into small fragments. (d) and (e) Tumor pieces were orthotopically implanted in the gastric wall with surgical suture. (f) and (g) Under the LZ12 microscope, gastric orthotopic tumors expressed strong GFP fluorescence. (h) GFP signals from subcutaneous tumor pieces were tested under fluorescence microscopy. (i) 6 to 8 weeks after the orthotopic implantation, gastric metastasis was investigated. Detection of GFP signal confirmed the metastatic tumors (arrows) and microtumors or gastric cancer cells (arrowheads).

metastatic tumors were taken out carefully. To further identify that the primo vessels were involved in gastric cancer metastasis, phalloidin (Invitrogen, CA) and 4′,6-diamidino-2-phenylindole (DAPI, Invitrogen, CA) staining were performed as described previously [11]. Staining was analyzed independently by two investigators using a fluorescence microscope (BX51, Olympus, Japan).

2.6. H&E Staining of Metastatic Tumors and Primo Vessels. Subsequently, features of primo vessels and related metastatic

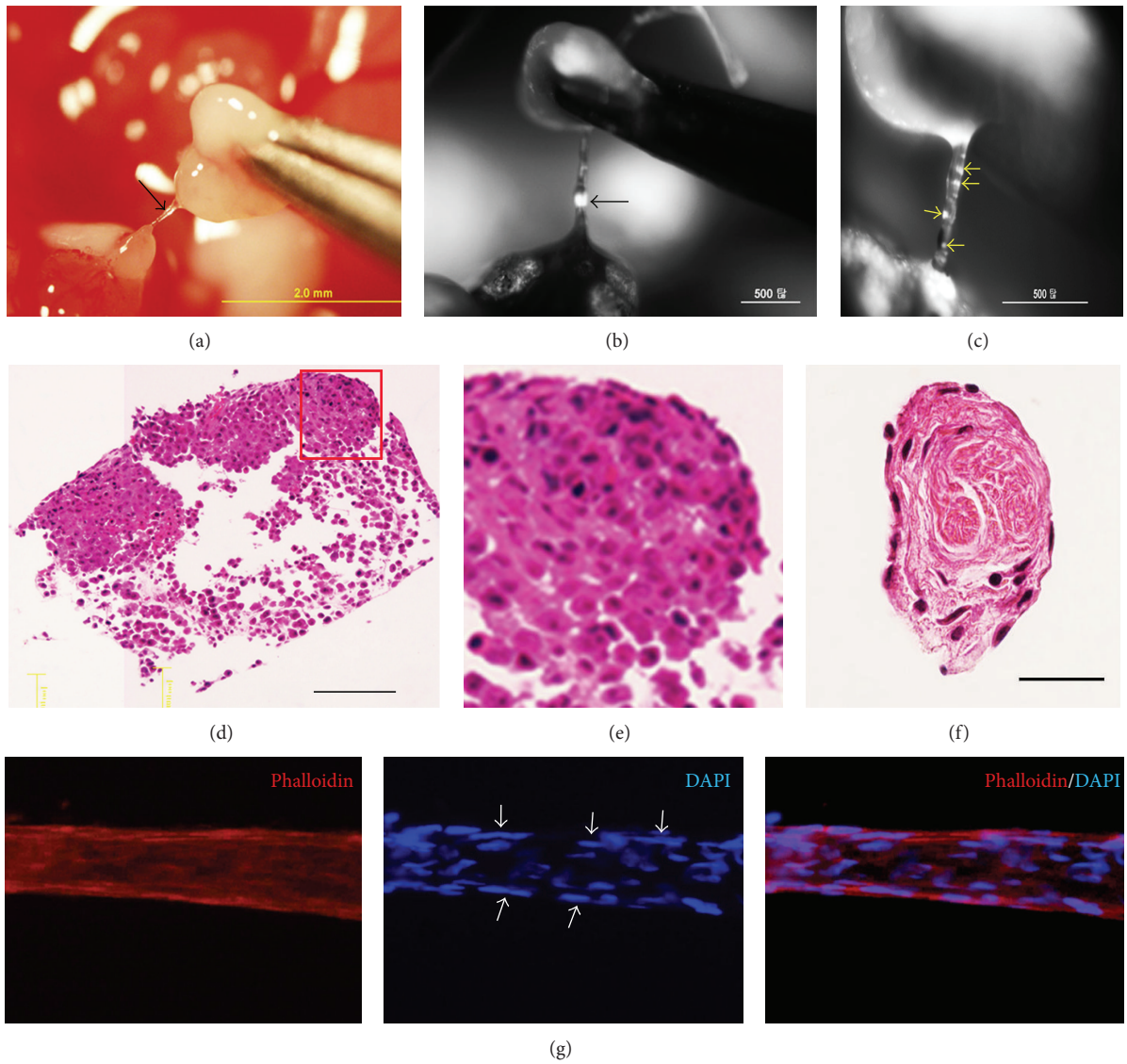

FIGURE 3: Primo vessels were involved in gastric cancer metastasis. (a) A free primo vessel (black arrow) with a thread-like and semitransparent appearance between tumors. (b) Under the LZ12 microscope, a tiny metastatic tumor (black arrow) was observed in the primo vessel. (c) Magnification of (b); more microtumors or gastric cancer cells (yellow arrows) were detected. (d) HE staining for the metastatic tumor mediated by primo vessels. (e) Magnification of framed area of (d) (Bar: 100 μm). (f) Transversal section of the primo vessel embedded was stained by H&E (Bar: 50 μm). No vascular vessels or lymphatic vessels were observed in either metastatic tumors or primo vessels. (g) Primo vessels involved in gastric cancer metastasis showed rod shape nuclei in a linear arrangement (white arrows) and positively expressed phalloidin.

tumors were determined by hematoxylin and eosin (H&E) staining. Briefly, metastatic tumors and primo vessels were fixed in 10% neutral buffered formalin (NBF) (pH 7.6) at 4°C. After dehydration and clearing, all the samples were embedded in paraffin and sectioned using a Vibratome Series 1000 sectioning system (Technical Products International, St. Louis, MO) for further H&E staining.

3. Results and Discussion

3.1. Isolation of Stable, High Level GFP-Expression MKN-45-GFP Cells. In the past, GFP has been used to detect metastatic cells in freshly excised tissue samples [12–14] and for studies of cell motility within primary tumors by in vivo time-lapse confocal microscopy [15]. Studies suggested that the use of GFP-expressing cells could improve in vivo investigations of the metastatic process. Utilization of GFP as a cell label for in vivo experiments requires that cells should be stably transfected and express GFP over a long term. The stable transfected MKN-45-GFP cells used in the present study exhibited a stable and strikingly bright fluorescence (screened by flow cytometry) in the absence of selective agent (G418) after numerous passages (Figure 1). This indicates the suitability and sensitivity of the MKN-45-GFP cells for long term use in vivo.

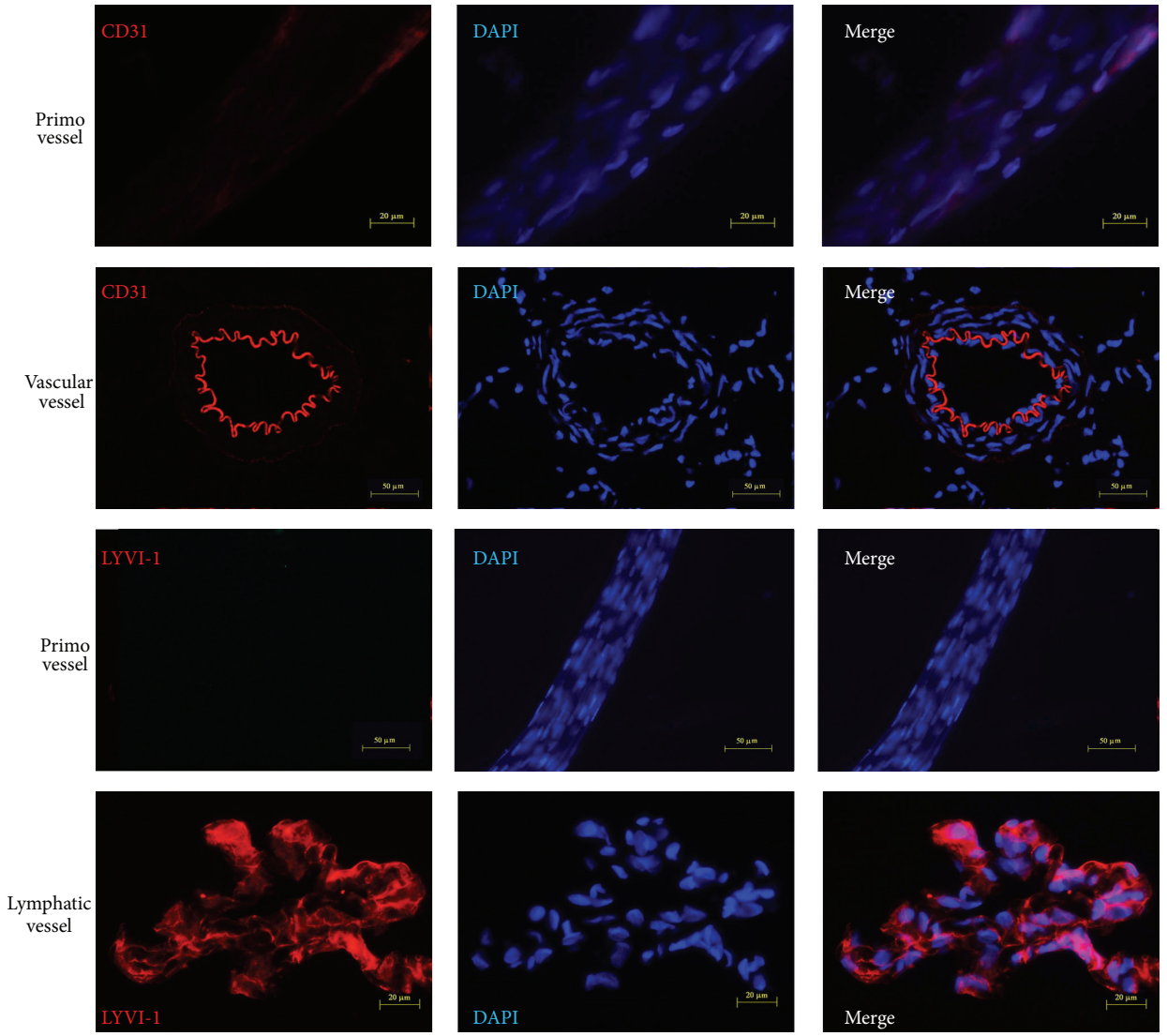

Figure 4: Primo vessels were distinct from vascular vessels and lymphatic vessels. Weak CD31 fluorescence (an endothelium marker) was observed in primo vessels while strong CD31 expression was detected in vascular vessels. Furthermore, primo vessels negatively expressed LYVI-1 (a lymphatic endothelium marker).

3.2. Stable High GFP-Expression in Gastric Metastatic Tumors. After subcutaneous inoculation of MKN-45-GFP cells in nude mice, tumors were harvested. As shown in Figure 2(h), tumor pieces expressed high GFP fluorescence which further indicated the high quality of stably transfected MKN-45-GFP cells. Then, small tumor pieces were orthotopically implanted into the gastric wall. Six–eight weeks later, metastasis in orthotopic implantation mice was investigated. Under the LZ12 microscope, gastric orthotopic tumors expressed strong GFP fluorescence (Figures 2(f) and 2(g)). Furthermore, images also showed that metastatic tumors, especially multiple micrometastatic tumors, were detected clearly (Figure 2(i)). All these observations suggested successful animal models for gastric cancer orthotopic implantation and metastasis investigations.

3.3. Primo Vessels Involved in Gastric Cancer Metastasis. Next, we investigated the role of primo vascular system in gastric cancer metastasis. We discovered that in orthotopic implantation mice, between the orthotopic tumors and the metastatic tumors, there are free thread-like and semitransparent structures that possess the basic features of primo vessels (Figure 3(a)). Under the LZ12 microscope, besides the fact that metastatic tumors with GFP fluorescence were distinctly detected, tiny tumors in primo vessels were clearly observed (Figure 3(b)). Magnified images revealed multiple microtumors in primo vessels (Figure 3(c)). More importantly, in H&E staining, no vascular vessels or lymphatic vessels were observed in metastatic tumors (Figures 3(d) and 3(e)) and primo vessels (Figure 3(f)). Phalloidin and DAPI staining revealed that these primo vessels expressed a linear arrangement of rod shape nuclei and positive phalloidin expression which conformed with the characters of primo vessels (Figure 3(g)). Accordant with our previous studies, the structure of primo vessels was obviously distinct from that of vascular vessels and lymphatic vessels.

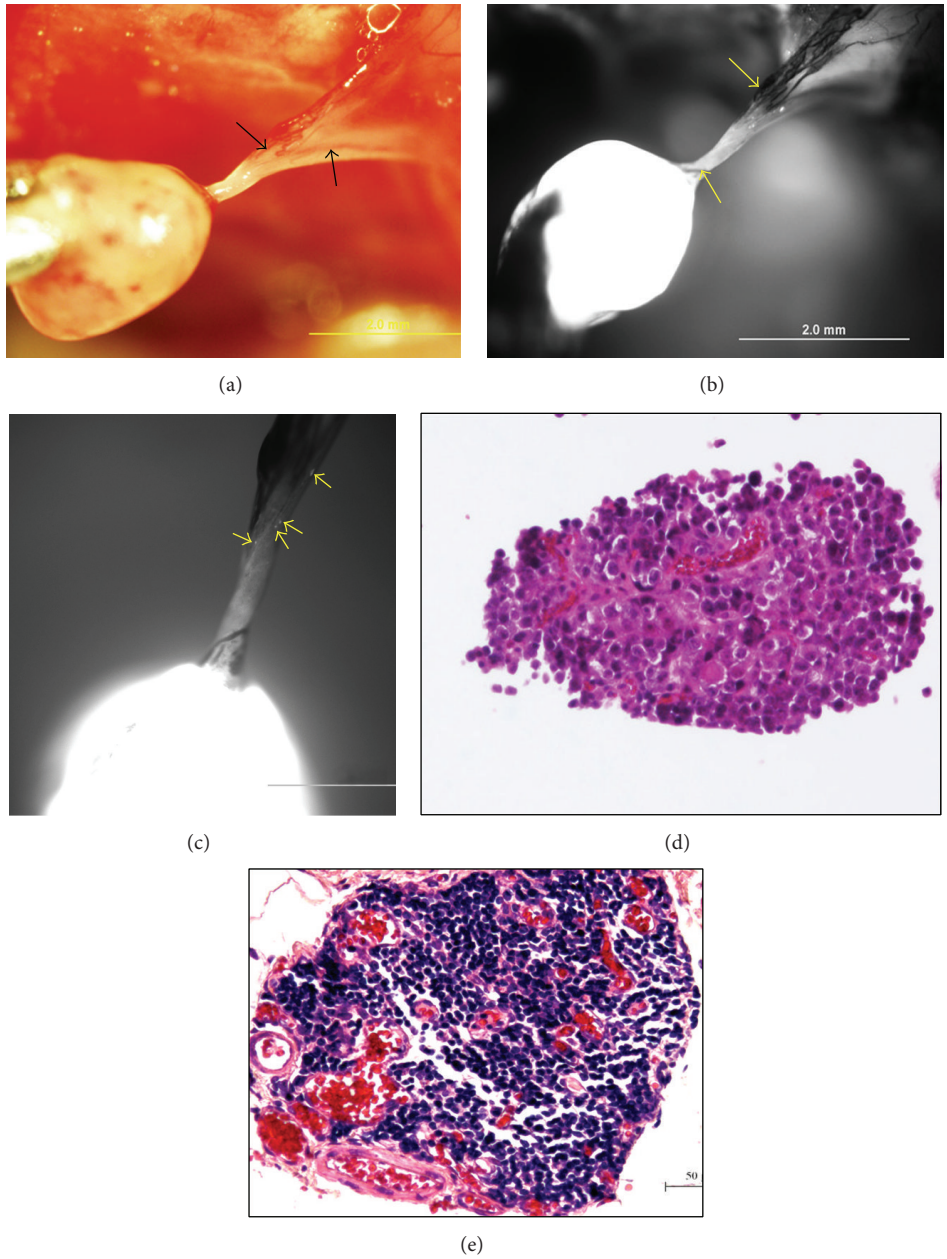

Figure 5: Vascular vessel-mediated metastasis. (a) In vascular vessel-mediated metastasis, metastatic tumors showed orange color and blood vessels were observed (black arrows). (b) Under the LZ12 microscope, metastatic tumor expressed bright GFP fluorescence and vascular vessels were obvious (yellow arrows). (c) Microtumors in the stalk of metastatic tumors were observed. H&E staining revealed blood vessels in the stalk (d) and metastatic tumors (e).

We further studied the biologic features of primo vessels involved in gastric metastasis. Our results indicated that contrast to vascular vessels and lymphatic vessels, primo vessels expressed weak CD31 (a endothelium marker) and negative LYVE-1 (a lymphatic endothelium marker) (Figure 4). These data supported our previous opinion that primo vessels belong to a type of endothelial-to-mesenchymal transitional tissues [11] and suggested them as a new metastatic pathway in gastric metastasis. This is another new finding and proof that revealed the role of primo vascular system in cancer metastasis.

Compared with metastasis mediated by vascular vessels, we observed an interesting phenomenon that the brightness of GFP-tagged metastatic tumors was much different between primo vessel-mediated metastasis and vascular vessel-mediated ones. In vascular vessel-mediated metastasis, tumors appeared yellow color (Figure 5(a)) and expressed much brighter GFP fluorescence (Figure 5(b)) while primo vessel-mediated metastatic tumors showed whiter color (Figure 2(a)) but weaker GFP signal (Figure 3(b)). In high magnified images, microtumors in the stalk of metastatic tumors also were observed (Figure 5(c)). H&E staining

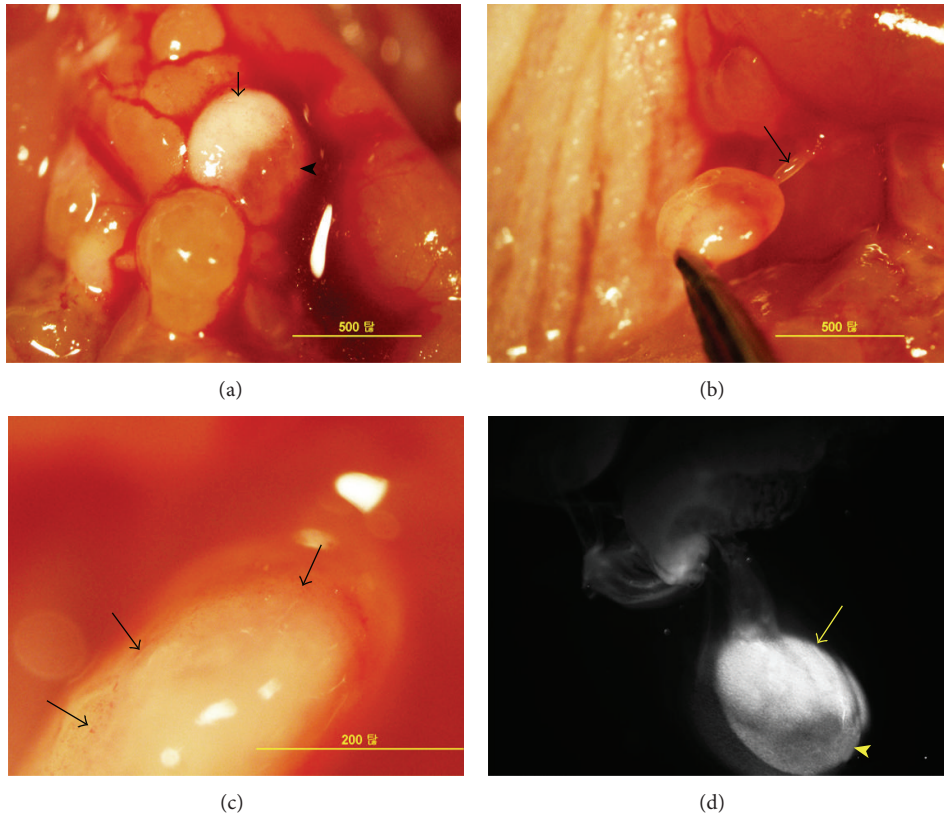

(a) (b) (c) (d)

Figure 6: Intermediate state of metastasis between primo vessel-mediated metastasis and vascular vessel-mediated metastasis. (a) Intermediate metastatic tumors between primo vessel-mediated metastasis and blood vessel-mediated metastasis were detected. Half of the tumor showed white color (black arrow) and the other part showed orange color (black arrowhead). (b) Lifting the metastatic tumor in (a); a free, semitransparent, and thread-like structure was detected (black arrow). (c) Magnification of metastatic tumor; red blood vessels and capillaries were obvious (black arrow). (d) Under the LZ12 microscope, high GFP fluorescence was expressed in the proximal part of metastatic tumor (yellow arrow) while lower GFP fluorescence was expressed in the distal part (yellow arrowhead).

confirmed vascular vessels in the stalks and metastatic tumors in vascular vessel-mediated metastasis (Figures 5(d) and 5(e)). Interestingly, intermediate metastatic tumors between these two states were detected. As shown in Figure 6, half of the tumor showed white color and the other part showed orange color. Because the cancer cells employed in our experiment were transfected by GFP plasmids, we deduced that the different color indicated different amount of cancer cells in metastasis tumors. Further fluorescence detection revealed the different GFP signals between these two parts (Figure 6(d)).

Our previous study has revealed that primo vessel cells belong to a population between endothelium and mesenchyme [11]. Together with our current observations of the three states in gastric cancer metastasis, we hypothesized that primo vessels may be the precursor for vascular vessels. These results possibly provided a thoroughly new theoretic development in cancer metastasis. Much more work should be done to further reveal the relationship between primo vessels and vascular vessels. We will continue our studies in disclosing the role of primo vascular system in cancer metastasis.

4. Conclusions

In conclusion, our research demonstrated that primo vessels are involved in gastric cancer metastasis and may be a potential precursor of vascular vessels. These results possibly provided a thoroughly new theoretic development in cancer metastasis.

Conflict of Interests

The authors declare that there is no conflict of interests regarding the publication of this paper.

Acknowledgments

This work was supported in part by a grant from National Natural Science Foundation of China (81302131) and Natural Science Foundation of Hubei Province, China (2012FKB04432).

References

[1] J.-Y. Deng and H. Liang, "Clinical significance of lymph node metastasis in gastric cancer," *World Journal of Gastroenterology*, vol. 20, no. 14, pp. 3967–3975, 2014.

[2] X. Jin, Z. Zhu, and Y. Shi, "Metastasis mechanism and gene/protein expression in gastric cancer with distant organs metastasis," *Bulletin du Cancer*, vol. 101, no. 1, pp. E1–E12, 2014.

[3] Y. Kodera, K. Fujitani, N. Fukushima et al., "Surgical resection of hepatic metastasis from gastric cancer: a review and new recommendation in the Japanese gastric cancer treatment guidelines," *Gastric Cancer*, vol. 17, no. 2, pp. 206–212, 2014.

[4] R. R. Markwald, T. P. Fitzharris, and F. J. Manasek, "Structural development of endocardial cushions," *The American Journal of Anatomy*, vol. 148, no. 1, pp. 85–119, 1977.

[5] M. Stefanov, M. Potroz, J. Kim, J. Lim, R. Cha, and M. H. Nam, "The primo vascular system as a new anatomical system," *Journal of Acupuncture and Meridian Studies*, vol. 6, no. 6, pp. 331–338, 2013.

[6] P. An, J. Dai, Z. Su et al., "Putative primo-vascular system in mesentery of rats," *Journal of Acupuncture and Meridian Studies*, vol. 3, no. 4, pp. 232–240, 2010.

[7] J. S. Yoo, M. H. Ayati, H. B. Kim, W.-B. Zhang, and K.-S. Soh, "Characterization of the primo-vascular system in the abdominal cavity of lung cancer mouse model and its differences from the lymphatic system," *PLoS ONE*, vol. 5, no. 4, Article ID e9940, 2010.

[8] K. A. Kang, C. Maldonado, G. Perez-Aradia, P. An, and K.-S. Soh, "Primo vascular system and its potential role in cancer metastasis," *Advances in Experimental Medicine and Biology*, vol. 789, pp. 289–296, 2013.

[9] H. G. Kim, "Formative research on the primo vascular system and acceptance by the Korean scientific community: the gap between creative basic science and practical convergence technology," *Journal of Acupuncture and Meridian Studies*, vol. 6, no. 6, pp. 319–330, 2013.

[10] B. C. Lee, W. J. Akers, X. Jing, M. I. Perez, and Y. Ryu, "Primo vascular system: past, present, and future," *Evidence-Based Complementary and Alternative Medicine*, vol. 2013, Article ID 240168, 2 pages, 2013.

[11] A. Ping, S. Zhendong, D. Jingxing, and et al, "Discovery of endothelium and mesenchymal properties of primo vessels in the mesentery," *Evidence-Based Complementary and Alternative Medicine*, vol. 2013, Article ID 205951, 10 pages, 2013.

[12] T. Chishima, Y. Miyagi, X. Wang et al., "Visualization of the metastatic process by green fluorescent protein expression," *Anticancer Research*, vol. 17, no. 4, pp. 2377–2384, 1997.

[13] M. Yang, S. Hasegawa, P. Jiang et al., "Widespread skeletal metastatic potential of human lung cancer revealed by green fluorescent protein expression," *Cancer Research*, vol. 58, no. 19, pp. 4217–4221, 1998.

[14] T.-T. Yang, P. Sinai, G. Green et al., "Improved fluorescence and dual color detection with enhanced blue and green variants of the green fluorescent protein," *The Journal of Biological Chemistry*, vol. 273, no. 14, pp. 8212–8216, 1998.

[15] M. Kneen, J. Farinas, Y. Li, and A. S. Verkman, "Green fluorescent protein as a noninvasive intracellular pH indicator," *Biophysical Journal*, vol. 74, no. 3, pp. 1591–1599, 1998.